

THE INTERNATIONAL JOURNAL OF CERAMICS

CERAMICS

international

GENERAL INDEX - Vols. 1-11

VOL.
11
1985



Editors-in-Chief

P. BOCH
France

W.D. KINGERY
USA

H. HAUSNER
Berlin

E.K. KOEHLER †
USSR

M. KOIZUMI
Japan

R. PAMPUCH
Poland

YEN-TUNG-SHENG
China

CERAMICS international

EDITORIAL BOARD

General Editor

P. VINCENZINI
National Research Council,
Research Institute for Ceramics
Technology, Via Granarolo 6,
48018 Faenza, Italy

Editors in Chief

P. BOCH
Ecole Nationale Supérieure
de Ceramique Industrielle,
47-73 Rue Albert Thomas,
87065-Limoges Cedex, France

W.D. KINGERY
Massachusetts Institute
of Technology, Ceramic Division,
4090 77 Massachusetts Avenue,
Cambridge, Massachusetts
02139, U.S.A.

H. HAUSNER
Institut für Nichtmetallische
Werkstoffe,
Technische Universität Berlin,
Englische Strasse 20,
1000 Berlin 12, Germany

E.K. KOEHLER
Institut Chimii Silikatov,
Ak. Nauk U.S.S.R.,
Nabereznaia Makarova 2,
Leningrad B-164, USSR

M. KOIZUMI
The Institute of Scientific
and Industrial Research,
Osaka University, Yamadakami,
Siuta, Osaka 565, Japan

R. PAMPUCH
Cracow Academy
of Mining and Metallurgy
Institute of Materials Science,
30-095 Al. Mickiewicza,
30 Cracow, Poland

YEN-TUNG SHENG
Shanghai Institute of Ceramics,
Academia Sinica,
865 Chang ning Rd., Shanghai,
People's Republic of China

Editorial Board

V.L. BALKIEVITCH
Moskovskii Technologicheskii
Institut D.I. - Mendeleyev -
Muusskaya Ploschad 9,
Moskva, USSR

M. BILLY
Laboratoire de Ceramique
Nouvelles, Université de Limoges,
123 Avenue Albert Thomas
87060 - Limoges Cedex, France

R.C. BRADT
Department of Materials Science and
Engineering, Roberts Hall, FB-10
University of Washington
Seattle, Washington 98195, USA

R. BROOK
Houldsworth School
of Applied Science,
Department of Ceramics,
University of Leeds,
Leeds LS2 9JT, England

R.W. DAVIDGE
AERE,
Materials Development Division,
Building 552, Didcot,
Oxfordshire OX11 ORA,
England

S. DE AZA
Instituto de Ceramica y Vidrio,
Carretera de Valencia,
Km. 24,300, Arganda del Rey,
Madrid, Spain

F.P. GLASSER
Department of Chemistry,
University of Aberdeen,
Meston Walk,
Old Aberdeen AB9 2UE,
Scotland

R.S. GORDON
Department of Materials Science
and Engineering, The University of
Utah, Salt Lake City, Utah
84112, U.S.A.

GUO JING-KUN
Shanghai Institute of Ceramics
865 Chang ning Rd., Shanghai,
People's Republic of China

K. HABERKO
Cracow Academy of Mining
and Metallurgy, Institute of
Materials Science,
Al. Mickiewicza 30,
Cracow, Poland

D.P.H. HASSELMAN
Department of Materials
Engineering, Virginia Polytechnic
Institute, Blacksburg,
Virginia 24061, U.S.A.

L.L. HENCH
Department of Materials Science
and Engineering, University of
Florida, Gainesville, Florida
32611, U.S.A.

A.H. HEUER
Department of Metallurgy and
Material Science,
Case Western Reserve University,
Cleveland, Ohio 44106, U.S.A.

A. KATO
Department of
Applied Chemistry,
Faculty of Engineering,
Kyushu University, Higashiku,
Fukuoka-shi 821, Japan

D. KOLAR
Institute Joseph Stefan,
Jamova 39, Ljubljana,
Yugoslavia

L. MICHALOWSKY
Bergakademie Freiberg
Sektion Verfahrens-
und Silikattechnik
9200 Freiberg Akademiestraße 6
DDR

F.F. LANGE
Rockell International Science
Center, 1049 Camino Dos Rios,
Thousand Oaks, California,
U.S.A.

M.G. McLAREN
Rutgers University, Department
of Ceramics, P.O. Box 909
Piscataway, N.J. 08854,
New Jersey 08903, U.S.A.

E.R. McCARTNEY
Department of Ceramic
Engineering, The University
of New South Wales P.O. Box 1,
Kensington, N.S.W., Australia

W. KOMATSU
Department of Industrial
and Engineering Chemistry,
Jikutoku Technical University,
1030 Shimo-ogino, Atsugi-shi,
Kanagawa-ken, 243-02, Japan

A. MOCELLIN
Ecole Polytechnique Fédérale
de Lausanne, 34 chemin
de Bellerive, CH-1007 Lausanne,
Switzerland

F. NADACHOWSKI
Akademia Gorniczo-Hutnicza,
Al. Mickiewicza 30/059,
Crakow, Poland

J.S. NADEAU
Department of Metallurgy,
University of British Columbia,
Vancouver 8, B.C., Canada

P.S. NICHOLSON
Mc Master University,
Department of Metallurgy
and Materials Science,
1280 Main Street West Hamilton,
Ontario, Canada, L8S4L7 Canada

K. OKAZAKI
Department of Electrical
Engineering, National Defense
Academy, Hashirimizu,
Yokosuka, Japan

H. PALMOUR III
Department of Engineering
Research, North Carolina State
University, 2707 Mayview Road,
North Carolina 27607, U.S.A.

S. PIZZINI
Dipartimento di Chimica Fisica ed
Elettrochimica, Università di Milano
Via Golgi 19, Milano (Italy)

J.A. PASK
Department of Materials Science
and Engineering, University
of California, Berkeley,
California 94720, U.S.A.

M. PAULUS
Laboratoire d'Etude et de
Syntèse des Microstructures,
E.S.P.C.I., 10 Rue Vanquelin,
75231 Paris Cedex 05, France

G. PETZOW
Pulvermetallurgisches
Laboratorium,
Max-Planck-Institut für
Werkstoffwissenschaften,
Bunsauer Strasse 175,
7000 Stuttgart 80, West Germany

D.W. READY
Department of Ceramic
Engineering, The Ohio State
University, 177 Watts Hall,
2041 College Road, Columbus,
Ohio 43210, U.S.A.

K.D. REEVE
Ceramics Section, AAEC
Research Establishment,
Private Mail Bag, Sutherland,
N.S.W. 2232, Australia

P. REYNEN
Institut für Gesteinshuttenkunde,
R.W.T.H., 51 Aachen
Maurestrasse 5, West Germany

T. SATA
Kumamoto Institute of Technology
Department of Industrial Chemistry
Ikeda - 4, Kumamoto 860, Japan

V. SATAVA
Institute of Chemical
Technology, Suchbátorova 5,
16628 Prague 6, Czechoslovakia

R. SERSALE
Istituto di Chimica Applicata,
Università di Napoli, Piazzale
Tecchio, 80125 Fuorigrotta,
Napoli, Italy

S. SHIRASAKI
National Institute for Research
in Inorganic Materials,
Sakura-Mura, Niihari-Gun,
Ibaraki 300-31, Japan

K.K. STRELLOV
Vtuzgorodok Polytechnic
of the Urals, S.M. Kirova
Institute, Sverdlovsk 2, USSR

I. STAMENKOVIC
Boris Kidric Institute, Lab. 280
P.O. Box 522, 11001 Beograd,
Yugoslavia

Prof. E.C. SUBARRAO
TATA Research Development
and Designe Centre,
1, Mangaldas Road,
Pune 411001, India

R.E. TRESSLER
Department of Materials Science
and Engineering,
The Pennsylvania State
University, University Park,
PA 16802, U.S.A.

J.A. VARELA
Universidade Estadual Paulista
Departamento de Fisico-Química
Caixa Postal 174
14800 Araraquara - S.P., Brasil

T. YAMAGUCHI
Department of Applied
Chemistry, Keio University,
Hiyoshi, Yokohama-Shi, Japan

O.J. WHITTEMORE
Department of Materials Science and
Engineering, Roberts Hall, FB-10
University of Washington
Seattle, Washington 98195, USA

Ex Officio

A.M. ANTONY (France) - N.N. AULT (USA) - S.B. AUSTERMAN (USA) - R.E. CARTER (USA) - T. EMILIANI (Italy) - V.D. FRECHETTE (USA) - N. ICHINOSE (Japan) - D.L. JOHNSON (USA) - V. LACH (Czechoslovakia) - O.P. MCCHEDLOV-PETROSSYAN (USSR) - D.N. POLOBOYARINOV * (USSR) - G.V. SAMSONOV * (USSR) - R.L. TAKUR (India) - F.D. TAMAS (Hungary) - H. YANAGIDA (Japan) - G.W. BRINDLEY * (USA) - P. POPPER (U.K.) - D. ALVAREZ-ESTRADA (Spain).

CERAMICS INTERNATIONAL

Vol. I-XI

TABLE OF CONTENTS

Vol. I, January/December, 1975

123 YOKO SUYAMA and AKIO KATO
Reactivity of Ultrafine-TiO₂ (Anatase) Powders with BaCO₃ 5
» P. DURAN
Phase Relationships in the Systems HfO₂-La₂O₃ and HfO₂-Nd₂O₃ 10
» R. PAMPUCH, Z. LIBRANT and J. PIEKARCZYK
Texture and Sinterability of MgO Powders 14
» D.E. CLARK, G.J. SCOTT and L.L. HENCH
Quantitative Use of Guiner X-ray Cameras in Solid State Reaction Kinetics 19
» A. PASSERONE, E. BIAGINI and V. LORENZELLI
Wetting of Barium Hexaferrite by Molten Metals 23
» M. HABERKO and K. HABERKO
Effect of Glaze on Strength of High-Tension Porcelain 28
124 R.L. BERTOLOTTI
Dependence of Fracture Strength on Strain-Rate in Polycrystalline Alumina 33
» G. BIFFI, G. ORTELLI and P. VINCENZINI
Ceramic Glazes Opacified with CaTiSiO₅ 34
» K.D. REEVE
Ceramics as Nuclear Reactor Fuels 59
» C.F. BILSBY and D.A. MOORE
Twining in Monoclinic Europium Sesquioxide 72
» R.W. DAVIDGE
The Mechanical Properties and Design Data for Engineering Ceramics 75
» R. PAMPUCH, H. TOMASZEWSKI and K. HABERKO
Hot-Pressing of Active Magnesia 81
» D. BERUTO, L. BARCO and G. BELLERI
On the Stability of Refractory Materials Under Industrial Vacuum Conditions: Al₂O₃, BeO, CaO, Cr₂O₃, MgO, SiO₂, TiO₂ Systems 87
» B.B. GHATE, D.P.H. HASSELMAN and R.M. SPRIGGS
Kinetics of Pressure-Sintering and Grain-Growth of Ultrafine Mullite Powder 105
» K. HABERKO, A. CIESLA and A. PRON
Sintering Behaviour of Yttria-Stabilized Zirconia Powders Prepared from Gels 111
125 S. MROWEC and K. SLOCZYNSKA
Oxidation of Ferrochromium Powder in Periclase or Magnesiocromite 117
» YOKO SUYAMA and AKIO KATO
A Comment on the Chemical Equilibrium in the BaCO₃-TiO₂ System 123

125 M.J. BANNISTER and W.G. GARRETT
Production of Stabilized Zirconia for Use as a Solid-State Electrolyte 127
» VU TIEN, L.F. CABANNES and A.M. ANTHONY
Joining of Lanthanum Chromite and Zirconia Ceramics 134
» H.G. EMBLEM
Some Uses of Alkyl Silicates in Refractory Technology 136

Vol. II, January/December, 1976

125 W.O. WILLIAMSON
Bubbles in Ceramic Systems 3
» E. LUCCHINI and G. SLOCCARI
Subsolidus Equilibria in the Pseudoternary System CaO-SrO-Fe₂O₃ 13
» L.M. LOPATO
Highly Refractory Oxide Systems Containing Oxides of Rare-Earth Elements 18
126 G. FAGHERAZZI
Magnetic and Microstructural Properties of SiO₂-Modified γ -Fe₂O₃ Prepared in a Fluid Bed Furnace 33
» W. PIATKOWSKY
SEM and Electron Microprobe Observations of Some Phenomena Occurring in Magnesia-Chrome Refractories 38
» T. EMILIANI and G. BIFFI
Once Pressed Single Fired Glazed Floor Tiles 42
» F. NADACHOWSKI
Refractories Based on Lime: Development and Perspectives 55
» C. BERTHELET, W.D. KINGERY and J.B. VANDERSANDE
Magnesium Aluminate Spinel Precipitation in MgO 62
» M. KOIZUMI, K. KODAIRA, Y. ISHITOBI, M. SHIMADA and F. KANAMARU
Fabrication of Translucent Ceramics by Isostatic Hot-Pressing 67
127 N.A.L. MANSOUR
Crystallite Growth and Changes of Some Related Characteristics of Magnesia Obtained by Thermal Decomposition of Basic Carbonate 72
» T. YAMAGUCHI, S.H. CHO, M. HAKOMORI and H. KUNO
Effects of Raw Materials and Mixing Methods on the Solid State Reactions Involved in Fabrication of Electronic Ceramics 76

127	V.L. BALKEVICH and C.M. FLIDLIDER Hot-Pressing of Some Piezoelectric Ceramics in the PZT System	81	130	A.M. ANTHONY, K. DEMBINSKI, J.L. DU- NAND, L. DUPONT and R. MOTTU The Adaptation to Space Applications of a 2000°C Furnace in an Oxidizing Atmosphere	29
»	M. HOCH and K.M. NAIR Densification Characteristics of Ultrafine Powders	88	»	P. REYNEN and M. FAIZULLAH Synthetic Raw Materials from Bentonite and Con- centrated Salt Solutions	33
»	V.P. VARLAMOV, L.A. KROICHUCK and A.A. TOPORKOVA A New Method for Estimating the Drying Sensi- tivity of Clays	98	»	R. PAMPUCH and L. STOBIERSKI Morphology of Silicon Carbide Formed by Chemi- cal Vapour Deposition	43
»	S.W. FREIMAN Effect of Environment on Fracture of Ceramics	111	»	K. NAGATA, H. SCHMITT, K. STATHAKIS and H.E. MÜSER Vacuum Sintering of Transparent Piezo-Ceramics	53
»	A.K. KUZNETSOV, P.A. TIKHONOV, M.V. KRAVCHINSKAYA and E.K. KOEHLER Subsolidus Equilibria and Kinetics of Decomposi- tion of Solid Solutions in the $\text{HfO}_2(\text{ZrO}_2)\text{-MgO}$ Sy- stems	119	»	E. KOSTIĆ and I. MOMČILOVIĆ Reaction Sintered MgAl_2O_4 Bodies from Different Batch Compositions	57
128	S.C. SINGHAL Thermodynamic Analysis of the High-Temperature Stability of Silicon Nitride and Silicon Carbide	123	131	A.M. VOGELS, R. DERIE and M. GHODSI Study of the Behaviour of Zinc Oxide in Direct-on Enamels	61
»	A. NEGRO, M. MURAT and F. SASSI Thermal Crystallization of Cordierite Glass Powder with Platinum as a Nucleating Agent	131	»	H. MOERTEL Porcelain for Fast Firing	65
»	K.S.E. FORSSBERG Mechanical and Thermal Properties of Boehmite Bonded Alumina Bodies	135	»	G. ASTI, P. CAVALLOTTI and R. ROBERTI Metal-Barium Hexaferrite Composites as Perma- nent Magnets	70
»	J. GUSMAN Ceramic Composite Materials Based on Refractory Oxides with Nitride and Oxynitride Bonds	141	»	A. BELLOSI and P. VINCENZINI Crystallite Growth of a Sodium Beta-Alumina Pow- der Determined by X-Ray Line Broadening	78
»	MASAYUKI NAGAI and HIROAKI YA- NAGIDA Semiconducting Barium Titanate Films by a Mod- ified Doctor Blade Method	145	»	G. SLOCCARI, E. LUCCHINI and G. ASTI The Subsystem $\text{BaO} \cdot 6\text{Fe}_2\text{O}_3 \cdot \text{CaO} \cdot 4\text{Fe}_2\text{O}_3 \cdot \text{SrO} \cdot 6\text{Fe}_2\text{O}_3$	79
»	R.W. DAVIDGE The Technology and Properties of Fibre Reinforced Ceramic Composites	163	»	F.P. GLASSER and J. MARR The Synthesis, Composition and Properties of Pel- lyite: $\text{Ba}_2\text{Ca}(\text{Mg},\text{Fe}^{2+},\text{Zn},\text{Co})_2\text{Si}_6\text{O}_{17}$	89
129	N. ICHINOSE, T. TAKAHASHI, Y. YA- MASHITA and H. IWASAKI $\text{PbTiO}_3\text{-PbZrO}_3\text{-In(Li}_{3/5}\text{W}_{2/5})\text{O}_3$ Piezoelectric Ce- ramics for Surface Wave Filters	170	»	S. PEJOVNIK, D. SUŠNIK and D. KOLAR Densification of TiO_2 by Hot Pressing	92
»	L.J. BOWEN, R.J. WESTON, T.G. CARRU- THERS and R.J. BROOK Mechanisms of Densification During the Pressure Sintering of α -silicon nitride	173	»	C.E. HOGE and J.A. PASK Thermodynamic and Geometric Considerations of Solid State Sintering	95
»	J. PIEKARZYK and R. PAMPUCH Microscopic Study of Pore Structure	177	132	N. ICHINOSE, T. MIZUTANI, H. HIRAKI and H. OOKUMA Microwave Dielectric Materials in the System $(\text{Sr}_{1-x}\text{Ca}_x)(\text{Li}_{1/4}\text{Nb}_{3/4})_{1-y}\text{Ti}_y\text{O}_3$	100
»	M. GAŠIĆ and F. SIGULINSKI Investigation on Formation and Behaviour of the Phosphate Bonding in Electrofused MgO	184	»	J.A. COATH and B. WILSHIRE Deformation Processes During High Temperature Creep of Lime, Magnesia and Doloma	103
»	G. PERUGINI Analysis of Dynamic Fusion Phenomena of Ceramic and Metallic Powders Injected into a Argon Plasma- Jet	190	»	J. ESPINOSA DE LOS MONTEROS, M.A. DEL RIO, R. MARTINEZ CACERES, D. ALVAREZ- ESTRADA and V. ALEIXANDRE Sericite Clay as a Raw Material for the Fabrication of Whiteware Bodies	109

Vol. III, January/December, 1977

129	M.R. NOTIS Advances in Ceramic hot Forming and Pressing: Theory and Practice	3	»	C.A.M. VAN DER BROEK Introduction of Various Grades of Raw Materials in Ferrite Magnet Production	115
»	G. SLOCCARI and E. LUCCHINI Subsolidus Phase Relationships in the System $\text{BaO}\text{-CaO}\text{-Fe}_2\text{O}_3$	10	»	P.E.C. FRANKEN, H. VAN DOREVEN and J.A.T. VERHOEVEN The Grain Boundary Compositions of MnZn Ferri- tes with CaO , SiO_2 and TiO_2 Additions	122
130	F. NADACHOWSKI, T. RYMON-LIPINSKI and M. JANIEC Some Reactions Occurring in Lime Refractories Containing Calcium Chloride	13	»	Y. ISHITOBI, M. SHIMADA, M. KOIZUMI and R. HAYAMI Grain Growth in Pressure-Sintered Al_2O_3 Ceramics	123
»	J.B. AINSCOUGH, D.A. MOORE and S.C. OSBORN Europia Ceramics for Use as Fast Reactor Neutron Absorbers	18	»	J. RANACHOWSKI and W. WŁOSINSKI Calculation of Diffusion Coefficients of Manganese in Debased Alumina	124
»	I. STAMENKOVIĆ and F. SIGULINSKI The Influence of Starting Material Characteristics on the Properties of High-Porosity Forsterite Bricks	25	»	T. YAMAGUCHI and H. SUTOH Effect of Cation Substitution on the Eutectoid De- composition of CuFe_2O_4	133
			»	P. DURÁN Phase Relationships in the Hafnia-Gadolina System	137
			»	Y. SUYAMA, T. MIZOBE and A. KATO ZrO_2 Powders Produced by Vapor Phase Reaction	141

133	G.N. BABINI, A. BELLOSI and P. VINCENZINI Densification Kinetics of Vacuum Hot-Pressed Sodium Beta-Aluminas	135	N.S. BELOSTOTSKAYYA and L. Ja. SHAPIRO The Effect of Grog Type on the Quality of Surface of Sanitary Ware Made of Faience Grog
		147	» G.E. YOUNGBLOOD and R.S. GORDON Texture-Conductivity Relationships in Polycrystalline Lithia-Stabilized β -Alumina
»	S. BASINSKA-PAMPUCH and T. GIBAS Observations on Some Plasma-Sprayed Metal Carbides	152	» G. VISOMBLIN and D. TCHOUBAR Premetallizing of High Alumina Ceramics
»	A.G. DOBROVOLSKIY Development of Slip Moulding Methods	159	» R.G. ANTHONY and E.R. McCARTNEY Hydrothermal Reactions in the Systems $\text{CaCO}_3\text{-SiO}_2$ and $\text{MgCO}_3\text{-SiO}_2$
»	J. RANACHOWSKI, M. STEPNIOWSKI and W. WLOSINSKI Interfacial Phases in a Metal-to-Aluminum Oxide Ceramic Seal	165	» B. HARDIMAN, K.V. KIEHL, C.P. REEVES and R.R. ZEYFANG Lead Titanate Zirconate-Based Pyroelectric Ceramics
»	I. STAMENKOVIĆ, V. SIMIĆIĆ, F. SIGULINSKI, P. MARTINOVIC and R. STEFANOVIĆ Properties of $\text{Al}_2\text{O}_3\text{-SiO}_2$ Heat Insulating Refractories	168	136 G.A. GOGOTSI, Ya. L. GROUSHEVSKY and K.K. STRELOV

Vol. IV, January/December, 1978

133	G. PERUGINI Ceramic Self-Sealing Coatings for High-Temperature Surfaces	3	Voltammetric Techniques in Ceramic Analysis. The Status of the Art	125
»	M.V. KRAVCHINSKAYA, A.K. KUZNETSOV, P.A. TIKHONOV and E.K. KOEHLER Phase Diagrams of the Systems $\text{HfO}_2\text{-Pr}_2\text{O}_3$ and $\text{Dy}_2\text{O}_3\text{-Pr}_2\text{O}_3$	14	D.P.H. HASSELMAN Figures-of-Merit for the Thermal Stress Resistance of High-Temperature Brittle Materials: a Review	147
134	J.D. HODGE and R.S. GORDON Grain Growth and Creep in Polycrystalline Magnesium Oxide Fabricated with and without a LiF Additive	17	E.M.H. SALLAM and A.C.D. CHAKLADER Sintering Characteristics of Porcelain	151
»	V. LONGO and L. PODDA The Phase Diagram of the System $\text{ZrO}_2\text{-CaO-MgO}$ Between 1200° and 1700°C	21	J. SCHLICHTING High Temperature Oxidation of Disilicides in the System $\text{MoSi}_2\text{-TiSi}_2$	162
»	N.A.L. MANSOUR Variation of Some Physical Properties with Calcination and Annealing Temperature of Magnesia Obtained by Thermal Decomposition of Basic Magnesium Carbonate	24	S. SHIMADA, K. KODAIRA, T. MATSUSHITA, K. ICHIJO and R. MAEDA Effect of CdO Additive on Sintering of LiNbO_3	167
»	V. LACH Microstructural Changes During the Firing of Wall Tile and Sanitaryware	28	E.A. EL-RAFEI High Quality Chrome-Bearing Basic Refractories from Brine Magnesia	172
»	D.P.H. HASSELMAN and G. ZIEGLER On the Effect of Crack Growth on the Scatter of Strength of Brittle Materials	38	V.B. GLUSHKOVA, F. HANIC and L.V. SAZONOVA Lattice Parameters of Cubic Solid Solutions in the Systems $\text{uR}_2\text{O}_3\text{-(1-u)MO}_2$	176
»	JELENA BRUN LANGENSIEPEN and F.A. HUMMEL Compatibility Relations in the System $\text{Al}_2\text{O}_3\text{-P}_2\text{O}_5\text{-WO}_3$	39	Vol. V, January/December, 1979	
»	S. MROWEC On the Defect Structure in Nonstoichiometric Metal Oxides	47	137 G. ALBANESE and A. DERIU Magnetic Properties of Al, Ga, Sc, In Substituted Barium Ferrites: A Comparative Analysis	3
»	J.T. KLOMP and R.H. LINDENHOVIUS Microstructural and Physical Properties of $\text{Al}_2\text{O}_3\text{-Fe}$ Cermets	59	» A.F. HENRIKSEN and W.D. KINGERY The Solid Solubility of Sc_2O_3 , Al_2O_3 , Cr_2O_3 , SiO_2 and ZrO_2 in MgO	11
»	J.A. COATH and B. WILSHIRE The Influence of Variations in Composition on the Creep Behaviour of Doloma	66	» A. PASSERONE, R. SANGIORGI and G. VALBUSA Surface Tension and Density of Molten Glasses in the System $\text{La}_2\text{O}_3\text{-Na}_2\text{Si}_2\text{O}_5$	18
135	J.G.J. PEELEN, B.V. REJDA and K. DE GROOT Preparation and Properties of Sintered Hydroxylapatite	71	» K. KURIBAYASHI and T. SATA Electrical Conductivity of Polycrystalline $3\text{Y}_2\text{O}_3\text{-WO}_3$ at High Temperatures	23
»	M. HANDKE and W. PTAK Ir and Raman Studies of the Stabilization of $\beta\text{-Ca}_2\text{SiO}_4$	75	» M. ZBOROWSKA, M. GRYLICKI and J. ZBOROWSKI The Corrosion Resistance of Strontium Zirconate Ceramics to Coal Ash Constituents and Potassium Seed of MHD-Generators	28
»	L. GIARDA, G. BOTTONI, D. CANDOLFO, A. CECCHETTI and F. MASOLI Ceramic and Magnetic Properties of Strontium Hexaferrite Powders Prepared by a Fluidized Bed Technique	79	» H. SCHNEIDER and A. MAJDIĆ Kinetics and Mechanism of the Solid-State High-Temperature Transformation of Andalusite (Al_2SiO_5) Into 3/2-Mullite ($3\text{Al}_2\text{O}_3\text{-2SiO}_2$) and Silica (SiO_2)	31
			» W. RICHARD OTT Kinetics and Mechanism of the Reaction Between Sodium Carbonate and Silica	37

VOL.
11
1985

138	T.A. WHEAT, E.M.H. SALLAM and A.C.D. CHAKLADER Synthesis of Mullite by a Freeze-Dry Process	42	G. BAGNASCO, P. PERNICE and P. GIORDANO ORSINI The Corrosion of Tin Oxide Semiconducting Glasses	161
»	S.A. ABDEL-HADY, N.A. AHMED, A.R. EL-DIB and M.S. FARAG Effect of Calcination Temperature on Lattice Defects in Impure Magnesium Oxide	45	» G. DE PORTU and P. VINCENZINI Young's Modulus-Porosity Relationship for Alumina Substrates	165
»	O. MARUYAMA and W. KOMATSU Observations on the Grain-Boundary of Al_2O_3 Bicrystals	51	» H. TAKASHIMA Some Observations on Opacification in K_2O -Containing Borosilicate Glasses	167
»	A.F. HENRIKSEN and W.D. KINGERY Effects of Strain Energy on Precipitate Morphology in MgO	56		
»	SU-JIL PYUN Fabrication of Stabilized ZrO_2 by Hot Petroleum Drying Method	61		
»	A.V. VIRKAR, T.D. KETCHAM and R.S. GORDON Hot Pressing of Lithia-Stabilized β -Alumina	66	141 J.J. STIGLICH, Jr., D.G. BHAT and R.A. HOLZL High Temperature Structural Ceramic Materials Manufactured by the CNTD Process	3
»	J.G.J. PEELEN Transparent Hot-Pressed Alumina - I: Hot Pressing of Alumina	70	» TERENCE G. LANGDON Deformation Mechanism Maps for Applications at High Temperatures	11
139	R. PAMPUCH Mechanisms of Hot Pressing of Magnesium Oxide Powders	76	» R.C. GARVIE, R.H.J. HANNINK and C. URBANI Fracture Mechanics Study of a Transformation Toughened Zirconia Alloy in the CaO-ZrO_2 System	19
»	Y. SUYAMA, M. TANAKA and A. KATO Submicron $\text{TiO}_2\text{-ZrO}_2$ Powders Produced by Vapor Phase Reaction of $\text{TiCl}_4\text{-ZrCl}_4\text{-O}_2$ System	84	» G. ZIEGLER and J. HEINRICH Effect of Porosity on the Thermal Shock Behaviour of Reaction-Sintered Silicon Nitride	25
»	A. BELLOSI and P. VINCENZINI Grain Growth During Sintering of Alumina Substrates	89	» G.A. GOGOTSI Thermal Stress Behaviour of Yttria, Scandia and AlN Ceramics	31
»	G. BANDYOPADHYAY, J.T. DUSEK and T.M. GALVIN Development of Porous Sintered-Ceramic Separators for Application in a Li-Al/LiCl-KCl/FeS Battery	95	» MIAO HO-CHO, CHOW CHIA-BAO, LIU YUAN-HO, CHIANG TSO-CHAO, LIU KUO-LIANG and TANG CHEN-HUEI Studies on the Application of Hot-Pressed Silicon Nitride Ceramics as Cutting-Tools	36
»	G. SCHNEIDER, L.J. GAUCKLER and G. PETZOW Phase Equilibria in the Si, Al, Be/C, N System	101	142 J.RZECHULA and M. GRYLICKI Some Phenomena Occurring in Basalt Glass Fibres at High Temperatures	39
»	K.A. SCHWETZ, M. HOERLE and J. BAUER Contribution to the System Europium-Boron-Carbon	105	» G. GRATHWOHL and F. THÜMMLER Interaction between Creep, Oxidation and Micro-porosity in Reaction-Bonded Silicon Nitride	43
»	A. GIACHELLO and P. POPPER Post-Sintering of Reaction-Bonded Silicon Nitride	110	» H. KNOCH and G.E. GAZZA On the α to β Phase Transformation and Grain Growth During Hot-Pressing of Si_3N_4 Containing MgO	51
140	J.G.J. PEELEN Transparent Hot-Pressed Alumina - II: Transparent Versus Translucent Alumina	115	» YOSHIKAZU NAKAMURA, SUDHIR S. CHANDRATREYA and RICHARD M. FULRATH Expansion During the Reaction Sintering of PZT	57
»	G. WROBLEWSKA Effect of Titanate Additions on Sintering Temperature of Al_2O_3	120	» H. SCHNEIDER and A. MAJDIC Kinetics of the Thermal Decomposition of Kyanite	61
»	C. FIORI, G. FUSAROLI, A. KRAJEWSKI and P. VINCENZINI On the Fracture Strength of Tape-Casted Alumina Substrates	124	» C. COMA DÍAZ, J.M. GONZÁLES PEÑA and D. ALVAREZ-ESTRADA Electron Microscopy of Some Wollastonite Based Porcelains	67
»	G. ZIEGLER and D.P.H. HASSELMAN Effect of Data Scatter on Apparent Thermal Stress Failure Mode of Brittle Ceramics	126	» P.C. KAPUR Thermal Insulations from Rice Husk Ash, an Agricultural Waste	75
»	T. MITAMURA, E. HALL, W.D. KINGERY and J.B. VANDERSANDE Grain Boundary Segregation of Iron in Polycrystalline Magnesium Oxide Observed by STEM	131	143 A. KWIATKOWSKI, K. RESZKA and A. SZYMANSKI Preparation of Corundum and Steatite Ceramics by the Freeze-Drying Method	79
»	O. HUNTER, Jr., R.W. SCHEIDECKER and SETSUO TOJO Characterization of Metastable Tetragonal Hafnia	137	» NORMAN L.P. LOW Formation and Properties of Glass-Mica Composite Materials	85
»	K. KEIZER, M.J. WERKERK and A.J. BURG-GRAAF Preparation and Properties of New Oxygen Ion Conductors for the Use at Low Temperatures	143	» G.N. BABINI, A. BELLOSI and P. VINCENZINI Hot Pressing of Silicon Nitride with Ceria Additions	91
»	K. HABERKO Characteristics and Sintering Behaviour of Zirconia Ultrafine Powders	148		
»	J.D. HONG, M.H. HON and R.F. DAVIS Self-Diffusion in Alpha and Beta Silicon Carbide	155		

143	M. ZBOROWSKA, M. GRYLICKI and J. ZBOROWSKI The Preparation and Properties of Strontium Zirconate Ceramics for Channels of Open-Cycle MHD Generators	99	145	E. CRIADO, J.S. MOYA and S. DE AZA Alkalines Vapour Attack on a High Alumina Refractory	19
»	O. YAMAGUCHI, K. TOMINAGA and K. SHIMIZU Formation and Transformation of Alkoxy-Derived BaB ₂ O ₄	103	»	TAHANY EL ADLY, DOREYA M. IBRAHIM and MOHAMED T. HUSSEIN Effect of the Main Whiteware Components on the Dissociation of Barite	22
»	S. KANEKO, H.N. TRAN, Y. KUBO and F. IMOTO Phase Equilibria in the SiO ₂ -TiO ₂ Binary and the Effect of TiO ₂ on the α - β Transformation in Cristobalite	106	»	TAHANY EL ADLY, DOREYA M. IBRAHIM and MOHAMED T. HUSSEIN Barite as a Main Constituent in Whiteware Composition	26
»	M.A. FADEL, I.A.F. WAFA and D.S. AL-ALOUSI New Approaches to Porcelain Dosimeters for Measuring Fast Neutron Fluxes	109	»	O.S. GRUM-GRZHIMAILO Optical Properties of Low-Temperature B ₂ O ₃ -and ZrO ₂ -Opacified Glazes	31
»	N.A. HAROUN Effect of MgO and NiO on the Sintering of Slip Cast Alumina	113	»	P. BÁLINT, B. SZÓKE, Z. JUHÁSZ and T. SKVORECZ Equilibrium Moisture Diagrams for the Drying of Clays	35
144	S. STRIJBOS Phenomena at the Powder-Wall Boundary During Die Compaction of a Fine Oxide Powder	119	»	N.A. HAROUN and M.A.A. EL-MASRY Bloating of Slip Cast MgO	38
»	D.E. CLARK and S.M. CLARK Characterization of Metallized Ceramic Interfaces	123	146	F. CERVANTES LEE, J. MARR and F.P. GLASSER Compounds in the Na ₂ O-Y ₂ O ₃ -SiO ₂ System	43
»	G. DE PORTU and P. VINCENZINI Young's Modulus of Silicon Nitride Hot Pressed with Ceria Additions	129	»	M. VARDELLE and J.L. BESSON γ -Alumina Obtained by Arc Plasma Spraying: a Study of the Optimization of Spraying Conditions	48
»	W. PIATKOWSKI and B. RÓZANOWSKI Hot Forming of Dolomite Briquettes	133	»	J.M. KOWALSKI and H.L. TULLER Ceramic Electrodes for Photoelectrolytic Decomposition of Water	55
»	T. RYMON - LIPINSKI An Alternative Technology for Making Carbon Containing Basic Refractories	137	»	IBRAHIM NASR, F.M. ABDEL-KADER and H.K. EMBABI Properties of Some High Alumina Refractories Obtained from Different Alumina Sources	60
»	P.S. KISLY, M.A. KUZENKOVA, L.I. PRIKHOD'KO and V.K. KAZAKOV Refractory and Electric Insulating Materials Based on Non-Metallic Nitrides	141	»	ZHONG XIANGCHONG and LI GUANGPING Sintering Characteristics of Chinese Bauxites	65
»	M. SHIBATA, N. KINOMURA and M. KOIZUMI High-Pressure Sintering of Silicon Nitride	146	»	D.M. IBRAHIM, E.H. SALLAM, A.A. KHALIL and S.M.H. NAGA Nepheline Syenite-Talc Low Temperature Vitrified Bodies	69
»	M.B. TRIGG and E.R. McCARTNEY The Reactions of Silicon Nitride with Vanadium Oxides	147	»	OSAMU YAMAGUCHI, SHIGEHARU YAMAMOTO and KIYOSHI SHIMIZU Kinetics of the Formation of Alkoxy-Derived MgO ₂ TiO ₂ and MgO-TiO ₂	73
»	I.A. BONDAR', M.G. DEGEN, L.P. MEZENTSEVA and L.N. KOROLEVA Formation and Growth Processes of rare Earth Niobates and Phosphates	148	»	V.A. LAVRENKO, S. JONAS and R. PAMPUCH Petrographic and X-Ray Identification of Phases Formed by Oxidation of Silicon Carbide	75
»	G.N. BABINI, A. BELLOSI and P. VINCENZINI Precipitation of CeO ₂ Crystals in a Glassy Oxide Phase Formed During Oxidation of CeO ₂ -Doped Hot Pressed Silicon Nitride	150	»	G.N. BABINI, A. BELLOSI and P. VINCENZINI Oxidation of Silicon Nitride Hot Pressed with CeO ₂ and SiO ₂ Additions	78
147	MICHIIRO NISHIOKA, S.S. CHIANG, RICHARD M. FULRATH and JOSEPH A. PASK Influence of Mixing Medium on Sintering and Coupling Coefficient of PZT Ceramics	87	»	MICHIIRO NISHIOKA, S.S. CHIANG, RICHARD M. FULRATH and JOSEPH A. PASK Influence of Mixing Medium on Sintering and Coupling Coefficient of PZT Ceramics	87
»	R.M. SMART and F.P. GLASSER The Subsolidus Phase Equilibria and Melting Temperatures of MgO-Al ₂ O ₃ -SiO ₂ Compositions	90	»	KUO CHU-KUN and LI SHAN-TIN Electro-Mechanical Degradation of Polycrystalline Beta-Alumina	98
»	V. LONGO, D. MINICHELLI and F. RICCIARDIELLO Crystallographic Characteristics of the Solid Solution SrCeO ₃ -BaCeO ₃	102	»	V. LONGO, D. MINICHELLI and F. RICCIARDIELLO Crystallographic Characteristics of the Solid Solution SrCeO ₃ -BaCeO ₃	102
»	M. KOMAC The Investigation of High-Temperature Strength of SiC Based Refractories	103	»	R. RÖTTENBACHER, H.J. OEL and G. TOMANDL Ferroelectric Ferromagnetics	106
»	TUNG-SHENG YEN Progress of Ceramic Research in the Shanghai Institute of Ceramics, Academia Sinica	111	»	TUNG-SHENG YEN Progress of Ceramic Research in the Shanghai Institute of Ceramics, Academia Sinica	111

Vol. VII, January/December, 1981

145	T. SASAMOTO, W.R. CANNON and H.K. BOWEN Phase Relationships, Electrical Conductivities and Vaporization Rates in the System La(Fe _{0.5} Cr _{0.5})O ₃ -Sr(Fe _{0.5} Cr _{0.5})O ₃ -SrZrO ₃ in Air	3
»	SEUNG-AM CHO, RAYMOND FOOKE and CHARLES A. GARRIS Efficiency of Ceramic Absorber Coatings for Solar-Thermal Conversion	8
»	M. BILLY, P. BOCH, C. DUMAZEAU, J.C. GLANDUS and P. GOURSAT Preparation and Properties of New Silicon Oxynitride Based Ceramics	13

147	H. SCHNEIDER and K. WOHLLEBEN Microchemical Composition and Cell Dimensions of Mullites from Refractory-Grade South American Bauxites	130	A.I. KINGON, P.J. TERBLANCHÉ and J.B. CLARK Effect of Reactant Dispersion on Formation of PZT Solid Solutions	108
»	F. ABBATTISTA and M. LUCCO BORLERA Reduction of LaMnO_3 , Structural Features of Phases $\text{La}_8\text{Mn}_8\text{O}_{23}$ and $\text{La}_4\text{Mn}_4\text{O}_{11}$	137	» H. TOMASZEWSKI, L. KULIG, J. TORUŃ, H. KOZŁOWSKA and M. WÓJCIK SEM, TEM and EPMA Study of Intergranular Phases in Alumina Ceramics	115
148	D. TREHEUX, J. DUBOIS and G. FANTOZZI Bulk and Grain Boundary Diffusion of ^{14}C in Tungsten Hemicarbide	142	» K.H. HÄRDTL Electrical and Mechanical Losses in Ferroelectric Ceramics	121
			» J.F. DeNATALE, D.K. McELFRESH and D.G. HOWITT Preliminary Observations on the Microstructure of Nuclear Waste Glasses	128
			» S.F. HULBERT, L.L. HENCH, D. FORBERS and L.S. BOWMAN History of Bioceramics	131
			» HIROSCHI HASEGAWA, MASAHIKO SHIMADA and MITSUE KOIZUMI Preparation of Glass-Ceramics $\text{Pb}_2\text{Ge}_{3-x}\text{Si}_x\text{O}_{11}$ ($0 \leq x \leq 1.75$)	141
			» J.D. FRIDEZ, C. CARRY and A. MOCELLIN Acoustic Activity in a Quartz Containing Porcelain Subjected to Low Rate Thermal Changes	144
			151 AMAR P.S. RANA, OSAMU AIKO and JOSEPH A. PASK Sintering of $\alpha\text{-Al}_2\text{O}_3$ / Quartz, and $\alpha\text{-Al}_2\text{O}_3$ / Cri- stobalite Related to Mullite Formation	151
			» T. EPICIER and G. ORANGE Electron Microscopy Study of the Microstructure of a Hot-Pressed Silicon Nitride	154

Vol. VIII, January/December, 1982

148	E. GÖRLICH The Structure of SiO_2 - Current Views	3	150 A.I. KINGON, P.J. TERBLANCHÉ and J.B. CLARK Effect of Reactant Dispersion on Formation of PZT Solid Solutions	108
»	Y. SUYAMA and A. KATO Characterization and Sintering of Mg-Al Spinel Prepared by Spray-pyrolysis Technique	17	» H. TOMASZEWSKI, L. KULIG, J. TORUŃ, H. KOZŁOWSKA and M. WÓJCIK SEM, TEM and EPMA Study of Intergranular Phases in Alumina Ceramics	115
»	G.A. GOGOTSI and Ja.L. GROUSHEVSKY Statistical Studies of the Strength of Inelastic Ceramics	22	» K.H. HÄRDTL Electrical and Mechanical Losses in Ferroelectric Ceramics	121
»	S.P. CHAUDHURI Crystallization of Glass of the System $\text{K}_2\text{O}(\text{Na}_2\text{O})$ - Al_2O_3 - SiO_2	27	» J.F. DeNATALE, D.K. McELFRESH and D.G. HOWITT Preliminary Observations on the Microstructure of Nuclear Waste Glasses	128
»	P. BOCH, J.C. GLANDUS, J. JARRIGE, J.P. LE-COMPTÉ and J. MEXMAIN Sintering, Oxidation and Mechanical Properties of Hot Pressed Aluminium Nitride	34	» S.F. HULBERT, L.L. HENCH, D. FORBERS and L.S. BOWMAN History of Bioceramics	131
»	K.S. MAZDIYASNI Powder Synthesis from Metal-Organic Precursors	42	» HIROSCHI HASEGAWA, MASAHIKO SHIMADA and MITSUE KOIZUMI Preparation of Glass-Ceramics $\text{Pb}_2\text{Ge}_{3-x}\text{Si}_x\text{O}_{11}$ ($0 \leq x \leq 1.75$)	141
149	Y. NURISHI and J.A. PASK Sintering of $\alpha\text{-Al}_2\text{O}_3$ -Amorphous Silica Compacts	57	» J.D. FRIDEZ, C. CARRY and A. MOCELLIN Acoustic Activity in a Quartz Containing Porcelain Subjected to Low Rate Thermal Changes	144
»	H. TOMASZEWSKI Effect of Cr_2O_3 Additions on the Sintering and Mechanical Properties of Al_2O_3	60	151 AMAR P.S. RANA, OSAMU AIKO and JOSEPH A. PASK Sintering of $\alpha\text{-Al}_2\text{O}_3$ / Quartz, and $\alpha\text{-Al}_2\text{O}_3$ / Cri- stobalite Related to Mullite Formation	151
»	D. GOZZI and R. GIGLI A Mathematical Model for Calculation of n, p-Type Conductivity Surfaces of Solid Oxide Electrolytes: an Application to 15 m/o CSZ	65	» T. EPICIER and G. ORANGE Electron Microscopy Study of the Microstructure of a Hot-Pressed Silicon Nitride	154
»	M.V. KRAVCHINSKAYA, P.A. TIKHONOV and E.K. KOEHLER Eutectoid Decomposition Processes of Solid Solutions in the HfO_2 - $\text{PrO}_{1.5}$ and HfO_2 - MgO Systems and Their Influence on the Physico-Chemical Properties of Refractory Materials	70		
»	H. TAKASHIMA Behaviour of Cr^{3+} and Fe^{3+} Ions in the Gahnite Crystallized from Zinc Opaque Glazes	74		
»	F. CAMBIER, C. LEBLUD and M.R. ANSEAU Reaction Sintering of MgO - TiO_2 Mixtures	77		
»	H. SCHNEIDER, A. MAJDIĆ and H.D. WERNER Effect of Explosive Shock Waves on Mullite Powders	79		
»	I.A. BONDAR Rare-Earth Silicates	83		
»	E.A. COLBOURN and W.C. MACKRODT The Influence of Impurities on the Migration Energy of Cation Vacancies in MgO	90		
150	TETSUO YAMADA, ATSUSHI TANAKA, MASAHIKO SHIMADA and MITSUE KOIZUMI Densification of α - and β - Si_3N_4 under Pressure	93		
»	M. LEJEUNE and J.P. BOILLOT Formation Mechanism and Ceramic Process of the Ferroelectric Perovskites: $\text{Pb}(\text{Mg}_{1/3}\text{Nb}_{2/3})\text{O}_3$ and $\text{Pb}(\text{Fe}_{1/2}\text{Nb}_{1/2})\text{O}_3$	99		
»	XUE JUNGAN Recent Developments of Cement Chemistry in China	104		

Vol. IX, January/December, 1983

60	151 J.C. BOKROS Carbon in Medical Devices	3		
65	» K. HABERKO and R. PAMPUCH Influence of Yttria Content on Phase Composition and Mechanical Properties of Y-PSZ	8		
70	» T. KIMURA and T. YAMAGUCHI Fused Salt Synthesis of $\text{Bi}_4\text{Ti}_3\text{O}_{12}$	13		
74	» OSAMU YAMAGUCHI, TATURO KANAZAWA, MASAMI YOKOIGAWA and KIYOSHI SHIMIZU Formation of Alkoxy-Derived $3\text{Al}_2\text{O}_3 \cdot 2\text{GeO}_2$	18		
77	» D. BERUTO, G. SPINOLO, L. BARCO, U. ANSELMI TAMBURINI and G. BELLERI On the Nature of the Crystallographic Disorder in Submicrometer Particles of $\text{Ca}(\text{OH})_2$ Produced by Vapour Phase Hydration	22		
79	152 J. ZBOROWSKI The Properties of Magnesia Powders for the Hot Welding Process	26		
83	» N. MIZUTANI, A.J. GARRATT-REED and W.D. KINGERY Grain Boundary Segregation of Iron, Chromium and Scandium in Polycrystalline Magnesium Oxide	31		
90	» F. ABBATTISTA and M. VALLINO Remarks on the La_2O_3 - Li_2O Binary System Between 750° and 1000°C	35		
93	» SHEN YANGYUN and R.J. BROOK Preparation and Strength of Forsterite-Zirconia Ceramic Composites	39		
99	» P.A. VITYAZ, I.L. FYODOROVA, I.N. YERMOLENKO and T.M. ULYANOVA Synthesis of Alumina and Zirconia Fibers	46		
104	» S.K. BHATTACHARYA and A.C.D. CHAKLADER Densification of Silicon Nitride Powder with Various Additives	49		

152	D. DERUTO, G. BELLERI, L. BARCO and V. LONGO Interactions of LiBr with Calcite and Calcium Oxide Powders	53	J. DUSZA, Ľ. PARILÁK, J. DIBLÍK and M. ŠLEŠÁR Elastic and Plastic Behaviour of WC - Co Composites	144
153	M.D. RASMUSSEN, G.W. JORDAN, M. AKINC, O. HUNTER, Jr. and M.F. BERARD Influence of Precipitation Procedure on Sinterability of Y_2O_3 Prepared from Hydroxide Precursor	59	» N.N. KRUGLITSKI Optimizing the Deformation Properties of Ceramic Pastes by Evaluating Relevant Physical and Chemical Mechanisms	146
»	S. HISHITA, I. MUTOH, K. KOUMOTO and H. YANAGIDA Inhibition Mechanism of the Anatase-Rutile Phase Transformation by Rare Earth Oxides	61	Vol. X, January/December, 1984	
»	EMANUEL I. COOPER and DAVID H. KOHN The Use of Molten Magnesium Chloride in the Preparation of Crystallite Ceramic Powders	68	155 E.K. HOEHLER The Structure and Properties of Refractory Zirconia Ceramics - I. Fundamental Investigations	3
»	OSAMU YAMAGUCHI, HIROTO SASAKI, KOJI SUGIURA and KIYOSHI SHIMIZU Formation and Transformation of $SrGeO_3$	75	» Z.K. HUANG, P. GREIL and G. PETZOW Formation of Silicon Oxinitride from Si_3N_4 and SiO_2 in the Presence of Al_2O_3	14
»	V.A. LAVRENKO and A.F. ALEXEEV Oxidation of Sintered Aluminium Nitride	80	» G. WÖTTING and G. ZIEGLER Influence of Powder Properties and Processing Conditions on Microstructure and Mechanical Properties of Sintered Si_3N_4	18
»	N. CLAUSSEN, G. LINDEMANN and G. PETZOW Rapid Solidification in the Al_2O_3 - ZrO_2 System	83	156 M.M.P. LOW and P. FAZIO Preparation and Properties of Binary and Ternary Composite Solids in the Clay-Mica-Glass System	23
»	G.W. JORDAN and M.F. BERARD Production of Highly-Sinterable Rare-Earth Oxide Powders by Controlled Humidity Dewatering of Precursors	87	» M. VALLINO Kinetic Study of the Crystallization of Amorphous-Derived $CaO \cdot 2Al_2O_3$	30
»	M. MARRAHA, J.-C. HEUGHEBAERT and G. BONEL Formation of a New Solid β Tricalcium Orthophosphate Structure, from Reaction Between Hydroxyapatite and Ammonium Sulfate	93	» M.M. ABOU-SEKKINA and BD-EL-RAOUF F. TAWFIK Counter Current Compensation of Double Doped $Pb(Zr_{1-x}, Ti_x)O_3$ Piezoelectric Ceramics	33
154	N.N. KRUGLISKI and V.YA. KRUGLITSKAYA Complete Rheological Curves for Clay Dispersions and Pastes and Their Associated Energetics	97	» A. KATO, H. MIZUMOTO and Y. FUKUSHIGE A Comment on the Equilibrium of $Si_3N_4 + 3C \rightleftharpoons 3SiC + 2N_2$	37
»	MORSY M. ABOU SEKKINA, M.K. EL-NIMR and E.W. ABD ALLAH Temperature Dependence of Electrical Resistivity and Dielectric Characteristics of Poled and $BaZrO_3$ Modified $BaTiO_3$ Ceramics	100	» V.V. MINCHENKO and S.F. MISCHENKO Structure Formation in Heated Clay Dispersions	39
»	P. REYNEN, A. FIRATLI, D. Von MALLINCKRODT and H. BOEß A High Temperature Ternary Phase in the System MgO - Al_2O_3 - ZrO_2	104	» S. MIZUTA, M. PARISH and H.K. BOWEN Dispersion of $BaTiO_3$ Powders (Part I)	43
»	JOSEPH A. PASK Stable and Metastable Phase Equilibria and Reactions in the SiO_2 - αAl_2O_3 System	107	» R. ANGERS and M. BEAUVY Hot-Pressing of Boron Carbide	49
»	H.C. CHANDAN, L. HERMANSSON, H. ABE and R.C. BRADT Elevated Temperature Instrumented Charpy Impact of a Sintered Silicon Carbide	114	» K. KODAIRA, S. TERAMOTO, S. SHIMADA and T. MATSUSHITA Pressure Sintering of Al_2O_3 - MgO Mixtures Under 10 Kbars	56
»	M. LEJEUNE and J.P. BOILOT Influence of Ceramic Processing on Dielectric Properties of Perovskite Type Compound: $Pb(Mg_{1/3}Nb_{2/3})O_3$	119	» N.M.P. LOW, P. FAZIO and P. GUISTE Development of Light-Weight Insulating Clay Products from the Clay-Sawdust-Glass System	59
»	S.C. HU and L.C. DE JONGHE Pre-Eutectic Densification in MgF_2 - CaF_2	123	157 E.K. KOEHLER The Structure and Properties of Refractory Zirconia Ceramics - II. Applied Investigations	66
»	F. PERNOT, P. BALDET, F. BONNEL, J. ZARZYCKI and P. RABISCHONG Development of Phosphate Glass-Ceramics for Bone Implants	127	» M. PARISH and H.K. BOWEN Narrow Size Distribution Powders From Commercial Ceramic Powders	75
»	JIŘÍ BULANDR and JAROSLAV DUDEK Mechanical Processing of Bentonites	132	» N.N. KRUGLITSKY, B.M. DATSENKO and B.I. MOROZ The Influence of Raw Materials Composition on the Properties of Fired Clay Products	78
155	YU. BORISOV and A.L. BORISOVA Interface Interaction and Structural Transformation in Particles of Ceramic and Cermet Composite Powders in Flame Spraying	138	» S. MIZUTA, M. PARISH and H.K. BOWEN Dispersion of $BaTiO_3$ Powders (Part II)	83
»	M.S. BIBILASHVILI, O.S. GRUM-GRZHEMAILO and N.S. BELOSTOTSKAYA Raw Materials for the Production of Pigments in the System ZrO_2 - SiO_2 - Fe_2O_3	142	» E.H. SALLAM, S.M. NAGA and D.M. IBRAHIM Mode of Talc Addition and its Effect on the Properties of Ceramic Bodies	87
			» M. HASSANEIN, WAFA I. ABDEL-FATTAH, K. NAKHLA and F.A. NOUR Some Color Aspects of Parian Bodies	93
			» M.D. RASMUSSEN, M. AKINC and M.F. BERARD Effect of Precursor Freeze-Drying Conditions on the Sinterability of Hydroxide-Derived Y_2O_3 Powders	99

157	C. SARAGOVI-BADLER and C. PUGLISI Mössbauer Studies of the Corrosion Reactions in Arc-Furnace Refractories - Part I	105	159	Y.H. KIM, J.P. MERCURIO and C. GAULT Synthesis, Formation Mechanisms and Polymorphism of Iron and/or Alkali-Substituted Cordierites	27
158	C. PUGLISI, F. LABENSKY and C. SARAGOVI-BADLER Mössbauer Studies of the Corrosion Reactions in Arc-Furnace Refractories - Part II	111	»	C.S. HOGG A Comparison of Plaster Casting and Pressure Casting of Sanitaryware with Particular Reference to Clay Properties	32
»	S.J. PARK, K. HIROTA and H. YAMAMURA Densification of Nonadditive SnO_2 by Hot Isostatic Pressing	116	160	J.A. COSTELLO and R.E. TRESSLER Oxygen Penetration Into Silicon Carbide Ceramics During Oxidation	39
»	P. CHAGNON and P. FAUCHAIS Thermal Spraying of Ceramics	119	»	A. CABALLERO, F.J. VALLE, S. DE AZA and S. CASTILLO Constitution of Calcined Refractory-Grade Bauxites: An Interpretation	45
»	M. GAVOGLIO and D. BERUTO Influence of the CO_2 Back Flux on the Reaction Mechanism of BaTiO_3 Formation from High TiO_2 Content in $\text{TiO}_2\text{-BaCO}_3$ Mixtures	132	»	M.D. RASMUSSEN, M. AKINC and O. HUNTER, Jr. Processing of Yttria Powders Derived from Hydroxide Precursors	51
»	U. SEIFERT-KRAUS and H. SCHNEIDER Cation Distribution Between Cristobalite, Tridymite, and Coexisting Glass Phase in Used Silica Bricks	135	»	V.B. GLUSHKOVA and M.V. KRAVCHINSKAYA HfO_2 -Based Refractory Compounds and Solid Solutions	56
»	S.T. SONG, H.Y. PAN, Z. WANG and B. YANG Synthesis, Properties and Application of High Conductive LaCrO_3 -Based Ceramic Materials	143	»	J. ZBOROWSKI Microstructural Changes in Hot-Pressed Salt-Lime Bodies During Heating	66
»	P. MIRANZO and J.S. MOYA Elastic-Plastic Indentation in Ceramics: a Fracture Toughness Determination Method	147	»	S. TANASE, Y. MIYAZAKI, M. YANAGIDA and T. KODAMA Corrosion Study on Ceramics for Conductance Measurements of Molten Carbonates	71
159	P. ESCRIBANO, C. GUILLEM and J. ALARCON Solid-State Reaction of Cr_2O_3 and SnO_2	153	»	T. YAMAMOTO, H. IGARASHI and K. OKAZAKI Mechanical Properties of (Pb, Ca) TiO_3 Family Ceramics with Zero Planar Coupling Factor	75
159	E.K. KOEHLER The Structure and Properties of Refractory Zirconia Ceramics - III. Studies of Technical Properties of Materials and Technological Elaborations	3	»	V.B. GLUSHKOVA and V.A. KRZHIZHANOVSKAYA HfO_2 -Based Refractory Compounds and Solid Solutions	80
»	M. HAVIAR, Z. PANEK and P. SÁJGALÍK The Use of Electrical Conductivity Measurements to Study Sintering Mechanisms	13	161	J.J. LANNUTTI and D.E. CLARK Sol-Gel Derived Alumina Substrates	91
»	H. YAMAMURA, A. WATANABE, S. SHIRASAKI, Y. MORIYOSHI and M. TANADA Preparation of Barium Titanate by Oxalate Method in Ethanol Solution	17	»	J.M. RINCON and F. CAPEL Microindentation Behaviour K_{IC} Factor Determination and Microstructure Analyses of Some $\text{Li}_2\text{O}\text{-SiO}_2$ Glass-Ceramic Materials	97
»	H. YAMAMURA, M. TANADA, H. HANEDA, S. SHIRASAKI and Y. MORIYOSHI Preparation of PLZT by Oxalate Method in Ethanol Solution	23	»	H. WARACHIM, J. RZECHULA and A. PIELAK Magnesium-Cobalt (II)-Aluminium Spinels for Pigments	103
			»	O. YAMAGUCHI, K. MATUI and K. SHIMIZU Formation of YAlO_3 with Garnet Structure	107

CERAMICS INTERNATIONAL

Vol. I-XI

AUTHORS INDEX

Abbattista, F.	7 (1981) 137	Berard, M.F.	9 (1983) 142	Cecchetti, A.	4 (1978) 79
Abd Allah, E.W.	9 (1983) 35	Berthelet, G.	9 (1983) 59	Cervantes Lee, F.	7 (1981) 43
Abdel-Fattah, W.I.	9 (1983) 100	Bertolotti, R.L.	9 (1983) 87	Chagnon, P.	10 (1984) 119
Abdel-Hady, S.A.	10 (1984) 93	Beruto, D.	10 (1984) 99	Chaklader, A.C.D.	4 (1978) 151
Abdel-Kader, F.M.	5 (1979) 45	Besson, J.L.	2 (1976) 62	Chandan, H.C.	5 (1979) 42
Abe, H.	7 (1981) 60	Bhat, D.G. Jr.	1 (1975) 33	Chandratreya, S.S.	9 (1983) 49
Abou Sekkina, M.M.	9 (1983) 100	Bhattacharya, S.K.	1 (1975) 87	Chaudhuri, S.P.	9 (1983) 114
Ahmed, N.A.	10 (1984) 33	Biagini, E.	9 (1983) 22	Chiang, S.S.	6 (1980) 57
Aiko, O.	5 (1979) 45	Bibilashvili, M.S.	9 (1983) 53	Chiang Tso-Chao	8 (1982) 27
Ainscough, J.B.	8 (1982) 151	Biffi, G.	10 (1984) 132	Chow Chia-Bao	7 (1981) 87
Akinc, M.	3 (1977) 18	Billy, M.	7 (1981) 48	Ciesla, A.	6 (1980) 36
Al-Alousi, D.S.	9 (1983) 59	Bilsby, C.F.	6 (1980) 3	Clark, D.E.	2 (1976) 76
Alarcon, J.	10 (1984) 99	Boch, P.	9 (1983) 49	Cho, S.H.	6 (1980) 36
Albanese, G.	6 (1980) 109	Boeß, H.	1 (1975) 23	Coath, J.A.	1 (1975) 111
Alexandre, V.	5 (1979) 3	Boilot, J.P.	9 (1983) 142	Clark, J.B.	1 (1975) 19
Alexeev, A.F.	3 (1977) 109	Bokros, J.C.	1 (1975) 34	Clark, S.M.	6 (1980) 123
Angers, R.	9 (1983) 80	Bondar', I.A.	2 (1976) 42	Claussen, N.	9 (1983) 83
Anseau, M.R.	10 (1984) 49	Bonet, G.	9 (1983) 104	Coath, J.A.	3 (1977) 103
Anselmi Tamburini, U.	8 (1982) 77	Bonnel, F.	8 (1982) 99	Colbourn, E.A.	4 (1978) 66
Anthony, A.M.	9 (1983) 22	Borisov, Yu.	9 (1983) 119	Coma Diaz, C.	8 (1982) 90
Anthony, R.G.	1 (1975) 134	Borisova, A.L.	9 (1983) 3	Cooper, E.I.	6 (1980) 67
Asti, G.	3 (1977) 29	Bottoni, G.	6 (1980) 148	Costello, J.A.	9 (1983) 68
Babini, G.N.	4 (1978) 104	Bowen, H.K.	8 (1982) 83	Criado, E.	11 (1985) 39
Bagnasco, G.	3 (1977) 70	Bonel, G.	9 (1983) 93	Datsenko, B.M.	7 (1981) 19
Baldet, P.	3 (1977) 79	Bonnel, F.	9 (1983) 127	Davidge, R.W.	10 (1984) 78
Bálint, P.	9 (1983) 127	Borisov, Yu.	9 (1983) 138	De Groot, K.	1 (1975) 75
Balkevich, V.L.	7 (1981) 35	Borisova, A.L.	9 (1983) 138	De Jonghe, L.C.	2 (1976) 163
Bandyopadhyay, G.	2 (1976) 81	Bottoni, G.	4 (1978) 79	Del Rio, M.A.	5 (1979) 155
Bannister, M.J.	5 (1979) 95	Bowen, L.J.	7 (1981) 3	Davis, R.F.	7 (1981) 45
Barco, L.	1 (1975) 127	Bowman, L.S.	10 (1984) 43	Degen, M.G.	6 (1980) 148
Basinska-Pampuch, S.	1 (1975) 87	Bradt, R.C.	10 (1984) 75	De Groot, K.	4 (1978) 71
Bauer, J.	9 (1983) 22	Brook, R.J.	10 (1984) 83	De Jonghe, L.C.	9 (1983) 123
Beauvy, M.	9 (1983) 53	Buland, J.	2 (1976) 173	De Natale, J.F.	3 (1977) 109
Belleri, G.	10 (1984) 49	Buldini, P.L.	8 (1982) 131	De Portu, G.	3 (1982) 29
Bellosi, A.	1 (1975) 87	Burggraaf, A.J.	9 (1983) 114	Dobrovolskiy, A.G.	8 (1982) 128
Belostotskaya, N.S.	9 (1983) 22	Caballero, A.	2 (1976) 173	Dobrovolskiy, A.G.	5 (1979) 165
	9 (1983) 53	Cabannes, L.F.	4 (1978) 125	Deric, R.	6 (1980) 129
	10 (1984) 49	Cambier, F.	5 (1979) 143	Deriu, A.	3 (1977) 61
	3 (1977) 78	Candolfo, D.	11 (1985) 45	Diblk, J.	5 (1979) 3
	3 (1977) 147	Cannon, W.R.	1 (1975) 134	Dobrovol'skiy, A.G.	9 (1983) 144
	5 (1979) 89	Capel, F.	8 (1982) 77	Dubois, J.	3 (1977) 159
	6 (1980) 91	Carruthers, T.G.	4 (1978) 79	Dudek, J.	7 (1981) 142
	6 (1980) 150	Carry, C.	7 (1981) 3	Dumazeau, C.	9 (1983) 132
	7 (1981) 78	Castillo, S.	11 (1985) 97	Dunand, J.L.	7 (1981) 13
	4 (1978) 81	Cavallotti, P.	2 (1976) 173	Dupont, L.	3 (1977) 29
			8 (1982) 144	Durán, P.	1 (1975) 10
			11 (1985) 45	Dusek, J.T.	3 (1977) 137
			3 (1977) 70	Dusza, J.	5 (1979) 95
					9 (1983) 144

El Adly, T.	7 (1981) 22	Groushevsky, Ya.L.	4 (1978) 113	Iwasaki, H.	2 (1976) 170
El-Dib, A.R.	7 (1981) 26	Grum-Grzhimailo, O.S.	8 (1982) 22	Janiec, M.	3 (1977) 13
El-Masry, M.A.A.	5 (1979) 45	Grylicki, M.	7 (1981) 31	Jarrige, J.	8 (1982) 34
El-Nimr, M.K.	7 (1981) 38	Guillem, C.	9 (1983) 142	Jonas, S.	7 (1981) 75
El-Rafei, E.A.	9 (1983) 100	Guite, P.	5 (1979) 28	Jordan, G.W.	9 (1983) 59
Embabi, H.K.	4 (1978) 172	Gusman, J.	6 (1980) 39	Juhász, Z.	9 (1983) 87
Emblem, H.G.	7 (1981) 60	Haberko, K.	6 (1980) 99	Kanamaru, F.	7 (1981) 35
Emiliani, T.	1 (1975) 136	Hakomori, M.	10 (1984) 153	Kanazawa, T.	2 (1976) 67
Epicier, T.	2 (1976) 42	Hall, E.L.	10 (1984) 59	Kaneko, S.	9 (1983) 18
Escribano, P.	8 (1982) 154	Handke, M.	2 (1976) 141	Kapur, P.C.	6 (1980) 106
Espinosa, J.	10 (1984) 153	Haneda, H.	1 (1975) 28	Kato, A.	6 (1980) 75
Estrada, D.A.	3 (1977) 109	Hanick, F.	1 (1975) 81	Kazakov, V.K.	1 (1975) 5
	3 (1977) 109	Hannink, R.H.J.	1 (1975) 111	Keizer, K.	1 (1975) 123
	6 (1980) 67	Hareoun, N.A.	5 (1979) 148	Ketcham, T.D.	3 (1977) 141
Fadel, M.A.	6 (1980) 109	Hasegawa, H.	9 (1983) 8	Khalil, A.A.	5 (1979) 84
Fagherazzi, G.	2 (1976) 33	Hassanein, M.	1 (1975) 28	Kiehl, K.V.	8 (1982) 17
Faizullah, M.	3 (1977) 33	Hasselman, D.P.H.	2 (1976) 76	Kim, Y.H.	10 (1984) 37
Fantozzi, G.	7 (1981) 142	Hoch, M.	5 (1979) 131	Kimura, T.	6 (1980) 141
Farag, M.S.	5 (1979) 45	Hiraki, H.	4 (1978) 75	Kingery, W.D.	5 (1979) 143
Fauchais, P.	10 (1984) 119	Hirota, K.	11 (1985) 23	Keizer, K.	5 (1979) 66
Fazio, P.	10 (1984) 23	Hishita, S.	4 (1978) 176	Ketcham, T.D.	7 (1981) 69
	10 (1984) 59	Hodges, C.E.	6 (1980) 19	Khalil, A.A.	4 (1978) 108
Fiori, C.	5 (1979) 124	Hogge, C.E.	4 (1978) 108	Kiehl, K.V.	11 (1985) 27
Firatli, A.	9 (1983) 104	Holzl, R.A.	8 (1982) 121	Kimura, T.	9 (1983) 13
Flidliker, C.M.	2 (1976) 81	Huang, Z.K.	6 (1980) 113	Kingery, W.D.	2 (1976) 62
Fookes, R.	7 (1981) 8	Hughes, D.F.	7 (1981) 38		5 (1979) 11
Forbers, D.	8 (1982) 131	Hulbert, S.F.	8 (1982) 141		5 (1979) 56
Forssberg, K.S.E.	2 (1976) 135	Hummel, F.A.	10 (1984) 93		5 (1979) 131
Franken, P.E.C.	3 (1977) 122	Hunter, O. Jr.	1 (1975) 105		5 (1979) 131
Freiman, S.W.	2 (1976) 111	Ibrahim, D.M.	4 (1978) 38		9 (1983) 31
Fridez, J.D.	8 (1982) 144	Ichijo, K.	4 (1978) 147		9 (1982) 108
Fukushige, Y.	10 (1984) 37	Ichinose, N.	5 (1979) 126		6 (1980) 146
Fulrath, R.M.	6 (1980) 57	Igarashi, H.	11 (1985) 13		6 (1980) 141
	7 (1981) 87	Imoto, F.	3 (1977) 123		4 (1978) 59
Fusaroli, G.	5 (1979) 124	Ishitobi, Y.	6 (1980) 25		6 (1980) 51
Fyodorova, I.L.	9 (1983) 46	Hench, L.L.	1 (1975) 19		2 (1976) 67
			8 (1982) 131		4 (1978) 167
Galvin, T.M.	5 (1979) 95	Henriksen, A.F.	5 (1979) 11		10 (1984) 56
Garratt-Reed, A.J.	9 (1983) 31	Hermannsson, L.	5 (1979) 56		11 (1985) 71
Garrett, W.G.	1 (1975) 127	Heughebaert, J.-C.	9 (1983) 114		2 (1976) 119
Garris, C.A.	7 (1981) 8	Hiraki, H.	9 (1983) 93		4 (1978) 14
Garvie, R.C.	6 (1980) 19	Hirota, K.	3 (1977) 100		8 (1982) 70
Gašić, M.	2 (1976) 184	Hishita, S.	10 (1984) 116		10 (1984) 3
Gauckler, L.J.	5 (1979) 101	Hoch, M.	9 (1983) 61		10 (1984) 66
Gault, C.	11 (1985) 27	Hodge, J.D.	2 (1976) 88		11 (1985) 3
Gavoglio, M.	10 (1984) 132	Hoerle, M.	4 (1978) 17		Kohn, D.H.
Gazza, G.E.	6 (1980) 51	Hogge, C.E.	5 (1979) 105		9 (1983) 68
Ghate, B.B.	1 (1975) 105	Hogg, C.S.	3 (1977) 95		Koizumi, M.
Ghodsi, M.	3 (1977) 61	Holzl, R.A.	11 (1985) 32		2 (1976) 67
Giachello, A.	5 (1979) 110	Hon, M.H.	6 (1980) 3		3 (1977) 123
Giarda, L.	4 (1978) 79	Hong, J.D.	5 (1979) 155		6 (1980) 146
Gibas, T.	3 (1977) 152	Huang, Z.K.	5 (1979) 155		8 (1982) 93
Gigli, R.	8 (1982) 65	Hulbert, S.F.	5 (1979) 155		8 (1982) 141
Giordano Orsini, P.	5 (1979) 161	Ibrahim, D.M.	8 (1982) 128		Kolar, D.
Glandus, J.C.	7 (1981) 13	Huang, Z.K.	9 (1983) 123		3 (1977) 92
	8 (1982) 34	Hummel, F.A.	10 (1984) 14		Komac, M.
Glasser, F.P.	3 (1977) 89	Hunter, O. Jr.	8 (1982) 131		7 (1981) 103
	7 (1981) 43	Ibrahim, D.M.	4 (1978) 39		Komatsu, W.
	7 (1981) 90	Ichijo, K.	5 (1979) 137		5 (1979) 51
Glushkova, V.B.	4 (1978) 176	Ichinose, N.	9 (1983) 59		6 (1980) 148
	11 (1985) 56	Igarashi, H.	11 (1985) 51		Koroleva, L.N.
	11 (1985) 80	Imoto, F.	7 (1981) 22		8 (1982) 57
Gogotsi, G.A.	4 (1978) 113	Ishitobi, Y.	7 (1981) 26		Koumoto, K.
	6 (1980) 31	Hussein, M.T.	7 (1981) 22		7 (1981) 55
	8 (1982) 22	Ibrahim, D.M.	7 (1981) 26		Kowalski, J.M.
González Peña, J.M. ^a	6 (1980) 67		7 (1981) 26		Kozłowska, H.
Gordon, R.S.	4 (1978) 17		7 (1981) 69		8 (1982) 115
	4 (1978) 93		10 (1984) 87		5 (1979) 124
	5 (1979) 66		4 (1978) 167		2 (1976) 119
Görlich, E.	8 (1982) 3		2 (1976) 170		4 (1978) 14
Goursat, P.	7 (1981) 13		3 (1977) 100		8 (1982) 70
Gozzi, D.	8 (1982) 65		11 (1985) 75		11 (1985) 56
Grathwohl, G.	6 (1980) 43		6 (1980) 106		2 (1976) 98
Greil, P.	10 (1984) 14		2 (1976) 67		Krulitskaya, V.Ya.
			3 (1977) 123		9 (1983) 97
					Kruglitsky, N.N.
					9 (1983) 97
					9 (1983) 146
					10 (1984) 78
					Krzhizhanovskaya, V.A.
					11 (1985) 80
					6 (1980) 106
					8 (1982) 115
					2 (1976) 76
					2 (1976) 76
					7 (1981) 98

Kurabayashi, K.	5 (1979) 23	Mocellin, A.	8 (1982) 144	Piekarczyk, J.	1 (1975) 14
Kuzenkova, M.A.	6 (1980) 141	Moertel, H.	3 (1977) 65		2 (1976) 177
Kuznetsov, A.K.	2 (1976) 119	Momčilović, I.	3 (1977) 57	Pielak, A.	11 (1985) 103
	4 (1978) 14	Moore, D.A.	1 (1975) 72	Podda, L.	4 (1978) 21
Kwiatkowski, A.	6 (1980) 79	Moriyoshi, Y.	3 (1977) 18	Popper, P.	5 (1979) 110
Labenski, F.	10 (1984) 111		11 (1985) 17	Prihod'ko, L.I.	6 (1980) 141
Lach, V.	4 (1978) 28	Moroz, B.I.	11 (1985) 23	Pron, A.	1 (1975) 111
Langdon, T.G.	6 (1980) 11	Mottu, R.	10 (1984) 78	Ptak, W.	4 (1978) 75
Langensiepen, J.B.	4 (1978) 39	Moya, J.S.	3 (1977) 29	Puglisi, C.	10 (1984) 105
Lannutti, J.J.	11 (1985) 91		7 (1981) 19		10 (1984) 111
Lavrenko, V.A.	7 (1981) 75	Mrowec, S.	10 (1984) 147	Rabischong, P.	9 (1983) 127
	9 (1983) 80	Murat, M.	1 (1975) 117	Rana, A.P.S.	8 (1982) 151
Leblud, C.	8 (1982) 77	Murray, M.J.	4 (1978) 47	Ranachowski, J.	3 (1977) 124
Lecompte, J.P.	8 (1982) 34	Müser, H.E.	2 (1976) 131	Rasmussen, M.D.	3 (1977) 165
Lejeune, M.	8 (1982) 99	Mutoh, I.	4 (1978) 119		9 (1983) 59
	9 (1983) 119		3 (1977) 53		10 (1984) 99
Li Guangping	7 (1981) 65		9 (1983) 61		11 (1985) 51
Li Shan-Tin	7 (1981) 98	Nadachowski, F.		Reeve, K.D.	1 (1975) 59
Librant, Z.	1 (1975) 14		2 (1976) 55	Reeves, C.P.	4 (1978) 108
Lindemann, G.	9 (1983) 83	Naga, S.M.	3 (1977) 13	Rejda, B.V.	4 (1978) 71
Lindenholz, R.H.	4 (1978) 59	Naga, S.M.H.	10 (1984) 87	Reszka, K.	6 (1980) 79
Liu Kuo-Liang	6 (1980) 36	Nagai, M.	7 (1981) 69	Reynen, P.	3 (1977) 33
Liu Yuan-Ho	6 (1980) 36	Nagata, K.	2 (1976) 145	Ricciardiello, F.	9 (1983) 104
Liversidge, R.M.	4 (1978) 119	Nair, K.M.	3 (1977) 53	Rincon, J.M.	7 (1981) 102
Longo, V.	4 (1978) 21	Nakamura, Y.	2 (1976) 88	Roberti, R.	11 (1985) 97
	7 (1981) 102	Nakhla, K.	6 (1980) 57	Röttenbacher, R.	3 (1977) 70
Lopato, L.M.	2 (1976) 18	Nasr, I.	10 (1984) 93	Rózanowski, B.	7 (1981) 106
Lorenzelli, V.	1 (1975) 23	Nishioka, M.	7 (1981) 60	Rymon-Lipinski, T.	6 (1980) 133
Low, N.L.P.	6 (1980) 85	Notis, M.R.	2 (1976) 131	Rzechula, J.	3 (1977) 13
	10 (1984) 23	Nour, F.A.	7 (1981) 87	Sájgalik, P.	6 (1980) 137
	10 (1984) 59	Nurishi, Y.	3 (1977) 3	Sallam, E.H.	11 (1985) 103
Lucchini, E.	2 (1976) 13		10 (1984) 93		11 (1985) 13
	3 (1977) 10	Oel, H.J.	8 (1982) 57		7 (1981) 69
	3 (1977) 79	Okazaki, K.	7 (1981) 106		10 (1984) 87
Lucco Borlera, M.	7 (1981) 137	Ookuma, H.	11 (1985) 75	Sallam, E.M.H.	4 (1978) 151
Mackrodt, W.C.	8 (1982) 90	Orange, G.	3 (1977) 100		5 (1979) 42
Maeda, R.	4 (1978) 167	Ortelli, G.	8 (1982) 154	Sangiorgi, R.	5 (1979) 18
Majdić, A.	5 (1979) 31	Osborn, S.C.	1 (1975) 34	Saragovi-Badler, C.	10 (1984) 105
	6 (1980) 61	Ott, W.R.	3 (1977) 18	Sasaki, H.	10 (1984) 111
	8 (1982) 79	Pampuch, R.	5 (1979) 37	Sasamoto, T.	9 (1983) 75
Mansour, N.A.L.	2 (1976) 72		1 (1975) 14	Sassi, F.	7 (1981) 3
	4 (1978) 24		1 (1975) 81	Sata, T.	2 (1976) 131
Marr, J.	3 (1977) 89		2 (1976) 177	Sazonova, L.V.	5 (1979) 23
	7 (1981) 43		3 (1977) 43	Scheidecker, R.W.	4 (1978) 176
Marraha, M.	9 (1983) 93		5 (1979) 76	Schlichting, J.	5 (1979) 137
Martinez Caceres, R.	3 (1977) 109	Pan, H.Y.	7 (1981) 75	Schmitt, H.	4 (1978) 162
Martinović, P.	3 (1977) 168	Pánek, Z.	9 (1983) 8	Schneider, G.	3 (1977) 53
Maruyama, O.	5 (1979) 51	Parilák, L.	10 (1984) 143	Schneider, H.	5 (1979) 101
Masoli, F.	4 (1978) 79	Parish, M.	11 (1985) 13		5 (1979) 31
Matsushita, T.	4 (1978) 167		9 (1983) 144		6 (1980) 61
	10 (1984) 56		10 (1984) 43		7 (1981) 130
Matui, K.	11 (1985) 107	Park, S.J.	10 (1984) 75		8 (1982) 79
Mazdiyasni, K.S.	8 (1982) 42	Pask, J.A.	10 (1984) 83		10 (1983) 135
McCartney, E.R.	4 (1978) 104		10 (1984) 116	Schwetz, K.A.	5 (1979) 105
	6 (1980) 147		3 (1977) 95	Scott, G.J.	1 (1975) 19
McElfresh, D.K.	8 (1982) 128		7 (1981) 87	Seifert-Kraus, U.	10 (1984) 135
Mercurio, J.P.	11 (1985) 27		8 (1982) 57	Setsuo Tojo	5 (1979) 137
Mexmain, J.	8 (1982) 34	Passerone, A.	8 (1982) 151	Seung-Am Cho	7 (1981) 8
Mezentseva, L.P.	6 (1980) 148		9 (1983) 107	Shapiro, L. Ja	4 (1978) 81
Miao Ho-Cho	6 (1980) 36	Peelen, J.G.J.	1 (1975) 23	Shen Yangyun	9 (1983) 39
Minchenko, V.V.	10 (1984) 39		5 (1979) 18	Shibata, M.	6 (1980) 146
Minichelli, D.	7 (1981) 102		4 (1978) 71	Shimada, M.	2 (1976) 67
Miranzo, P.	10 (1984) 147	Pejovnik, S.	5 (1979) 70		3 (1977) 123
Mischenko, S.F.	10 (1984) 39	Pernice, P.	5 (1979) 115		8 (1982) 93
Mitamura, T.	5 (1979) 131	Pernot, F.	3 (1977) 92	Shimada, S.	8 (1982) 141
Miyazaki, Y.	11 (1985) 71	Perugini, G.	5 (1979) 161		4 (1978) 167
Mizobe, T.	3 (1977) 141		9 (1983) 127	Shimizu, K.	10 (1984) 56
Mizumoto, H.	10 (1984) 37	Petzow, G.	2 (1976) 190		6 (1980) 103
Mizuta, S.	10 (1984) 43		4 (1978) 3		7 (1981) 73
	10 (1984) 83		5 (1979) 101		9 (1983) 18
Mizutani, N.	9 (1983) 31	Piatkowsky, W.	9 (1983) 83		9 (1983) 75
Mizutani, T.	3 (1977) 100		10 (1984) 14	Shirasaki, S.	11 (1985) 107
			2 (1976) 38		11 (1985) 23
			6 (1980) 133		

Sigulinski, F.	2 (1976) 184	Tomandl, G.	7 (1981) 106	Werner, H.D.	8 (1982) 79
	3 (1977) 25	Tomaszewski, H.	1 (1975) 81	Weston, R.J.	2 (1976) 173
	3 (1977) 168		8 (1982) 60	Wheat, T.A.	5 (1979) 42
Simičić, V.	3 (1977) 168	Tominaga, K.	8 (1982) 115	Williamson, W.O.	2 (1976) 3
Singhal, S.C.	2 (1976) 123	Toporkova, A.A.	6 (1980) 103	Wilshire, B.	3 (1977) 103
Skvorecz, T.	7 (1981) 35		2 (1976) 98		4 (1978) 66
Šlesár, M.	9 (1983) 144	Toruň, J.	8 (1982) 115	Włosinski, W.	3 (1977) 124
Slocardi, G.	2 (1976) 13	Tran, H.N.	6 (1980) 106		3 (1977) 165
	3 (1977) 10	Treheux, D.	7 (1981) 142	Wohlleben, K.	7 (1981) 130
	3 (1977) 79	Tressler, R.E.	11 (1985) 39	Wójcik, M.	8 (1982) 115
Sloczynska, K.	1 (1975) 117	Trigg, M.B.	6 (1980) 147	Wötting, G.	10 (1984) 18
Smart, R.M.	7 (1981) 90	Tuller, H.L.	7 (1981) 55	Wroblewska, G.	5 (1979) 120
Song, S.T.	10 (1984) 143	Tung-Sheng Yen	7 (1981) 111		
Spinolo, G.	9 (1983) 22			Xue Jungan	8 (1982) 104
Spriggs, R.M.	1 (1975) 105				
Stamenković, I.	3 (1977) 25	Ulyanova, T.M.	9 (1983) 46	Yamada, T.	8 (1982) 93
	3 (1977) 168	Urbani, C.	6 (1980) 19	Yamaguchi, O.	6 (1980) 103
Stathakis, K.	3 (1977) 53				7 (1981) 73
Stefanović, R.	3 (1977) 168				9 (1983) 18
Stepniewski, M.	3 (1977) 165	Valbusa, G.	5 (1979) 18		9 (1983) 75
Stiglich, J.J.Jr.	6 (1980) 3	Valle, F.J.	11 (1985) 45		11 (1985) 107
Stobierski, L.	3 (1977) 43	Vallino, M.	9 (1983) 35	Yamaguchi, T.	2 (1976) 76
Strelcov, K.K.	4 (1978) 113		10 (1984) 30		3 (1977) 133
Strijbos, S.	6 (1980) 119	Van Den Broek, C.A.M.	3 (1977) 115		9 (1983) 13
Sugiura, K.	9 (1983) 75	Vandersande, J.B.	2 (1976) 62		7 (1981) 73
Su-ll Pyun	5 (1979) 61	Van Doreven, H.	5 (1979) 131	Yamamoto, S.	11 (1985) 75
Sušnik, D.	3 (1977) 92	Vardelle, M.	3 (1977) 122	Yamamoto, T.	10 (1984) 116
Sutoh, H.	3 (1977) 133	Varlamov, V.P.	7 (1981) 48	Yamamura, H.	11 (1985) 17
Suyama, Y.	1 (1975) 5	Verhoeven, J.A.T.	2 (1976) 98		11 (1985) 23
	1 (1975) 123	Verkerk, M.J.	3 (1977) 122	Yamashita, Y.	2 (1976) 170
	3 (1977) 141	Vincenzini, P.	5 (1979) 143	Yanagida, H.	2 (1976) 145
	5 (1979) 84		1 (1975) 34		9 (1983) 61
	8 (1982) 17		3 (1977) 78	Yanagida, M.	11 (1985) 71
Szóke, B.	7 (1981) 35		3 (1977) 147	Yang, B.	10 (1984) 143
Szymanski, A.	6 (1980) 79		5 (1979) 89	Yermolenko, I.N.	9 (1983) 46
			5 (1979) 124	Yokoigawa, M.	9 (1983) 18
Takahashi, T.	2 (1976) 170		5 (1979) 165	Youngblood, G.E.	4 (1978) 93
Takashima, H.	5 (1979) 167		6 (1980) 91		19
	8 (1982) 74		6 (1980) 129		
Tanada, M.	11 (1985) 17		6 (1980) 150	Zarzycki, J.	9 (1983) 127
	11 (1985) 23		7 (1981) 78	Zborowska, M.	5 (1979) 28
Tanaka, A.	8 (1982) 93	Virkar, A.V.	5 (1979) 66		6 (1980) 99
Tanaka, M.	5 (1979) 84	Visomblin, G.	4 (1978) 99	Zborowski, J.	5 (1979) 28
Tanase, S.	11 (1985) 71	Vityaz, P.A.	9 (1983) 46		6 (1980) 99
Tang Chen-Huei	6 (1980) 36	Vogels, A.M.	3 (1977) 61		9 (1983) 26
Tawfik B-E-R.F.	10 (1984) 33	Von Mallinckrodt, D.	9 (1983) 104		11 (1985) 66
Tchoubar, D.	4 (1978) 99	Vu Tien	1 (1975) 134	Zeyfang, R.R.	4 (1978) 108
Teramoto, S.	10 (1984) 56			Zhong Xiangchong	7 (1981) 65
Terblanché, P.J.	8 (1982) 108			Ziegler, G.	4 (1978) 38
Thümmler, F.	6 (1980) 43	Wafa, I.A.F.	6 (1980) 109		5 (1979) 126
Tikhonov, P.A.	2 (1976) 119	Wang, Z.	10 (1984) 143		6 (1980) 25
	4 (1978) 14	Warachim, H.	11 (1985) 103		10 (1984) 18
	8 (1982) 70	Watanabe, A.	11 (1985) 17		

CERAMICS INTERNATIONAL

Vol. I-XI

ABSTRACTS OF PAPERS

Vol. I, January/December, 1975

REACTIVITY OF ULTRAFINE-TiO₂ (ANATASE) POWDERS WITH BaCO₃

Yoko Suyama and Akio Kato

The solid-state reaction between anatase-TiO₂ powders with various particle-size distributions and BaCO₃, was investigated by means of TGA in O₂ and in CO₂. The reactivity of TiO₂ powders increased remarkably as the particle size grew smaller than 0.2 μ m. TG curves in CO₂ differed from those in O₂. In CO₂, a high reactivity was observed at around 620°C and the reactivity increased as the size of TiO₂-particles decreased. The beginning and completion temperatures of the reaction in CO₂ were higher by about 100°C than those in O₂. The difference of TG curves between the two atmospheres was interpreted in terms of a layered interface model. The particle-size distribution curve of the BaTiO₃ powder produced was parallel to that of the starting TiO₂ powder.

PHASE RELATIONSHIPS IN THE SYSTEMS HfO₂-La₂O₃ AND HfO₂-Nd₂O₃

P. Duran

Phase relationships were studied in the systems HfO₂-La₂O₃ and HfO₂-Nd₂O₃ at temperatures between 1,300°C to 2,300°C. The formation of the pyrochlore structure compounds La₂Hf₂O₇ ($a = 10.779 \text{ \AA}$) and Nd₂Hf₂O₇ ($a = 10.629 \text{ \AA}$) was found. Limits were established for the range of the single-phase and two phase regions of the solid solutions based on HfO₂, La₂Hf₂O₇, Nd₂Hf₂O₇, La₂O₃ and Nd₂O₃. Based on experimental evidence obtained by X-ray diffraction and using precision lattice parameters, phase diagrams for the systems hafnianthana and hafnia-neodimia are suggested.

TEXTURE AND SINTERABILITY OF MgO POWDERS

R. Pampuch, Z. Librant and J. Piekarzyk

Characterization of MgO powders obtained by thermal decomposition of spectrally-pure magnesium hydroxide, magnesium-ammonium carbonate, and magnesium oxalate at 350°-1000°C, in terms of the crystallite size, lattice microstrains, and texture. The composition of the systems was checked by X-ray diffraction and IR-spectrography. The behaviour during heating and the final microstructure of sintered ceramic bodies have been shown to be a function of the initial texture of the powders which is due to the different mechanism of decomposition of the particular starting compounds. The results, supported by parallel observations of

behaviour on heating of MgO derived from a well-oriented natural brucite, agree with the analysis of the initial stages of sintering published by Pampuch and later by Exner, Petzow, and Wellner.

QUANTITATIVE USE OF GUINIER X-RAY CAMERAS IN SOLID STATE REACTION KINETICS

D.E. Clark, G.J. Scott and L.L. Hench

Monochromated Guinier-deWolff and Guinier-Lenne x-ray powder cameras and a scanning microdensitometer have been combined into a data system for the study of solid state reaction kinetics. Application of the room-temperature and high temperature cameras to both interface-controlled and diffusion-controlled kinetics is discussed. A graphical analysis method is presented.

WETTING OF BARIUM HEXAFERRITE BY MOLTEN METALS

A. Passerone, E. Biagini and V. Lorenzelli

The interaction between molten metals and the sintered magnetic oxide BaFe₁₂O₁₉ has been studied in order to determine its wettability. Pure copper, silver and silver-zinc alloys, insofar as they are oxygen-active are the metals considered. The pure metals do not wet the ferrite. Introduction of zinc into silver results in a strong interaction between liquid and the ferrite thus giving a marked decrease of the contact angle. Coating the ferrite with an intermediate surface-active metal which forms a solid solution with the molten metal results in complete spreading if the temperature, time of contact and thickness of the deposited metal are adequately controlled.

EFFECT OF GLAZE ON STRENGTH OF HIGH-TENSION PORCELAIN

M. Haberko and K. Haberko

Seventy glazes of different compositions were applied to high alumina porcelain body. Reaction between a glaze and the body was studied. Three types of an intermediate zone were found. Phases crystallizing at the glaze-body contact were determined. In overlying glaze layers cristobalite and quartz grains were observed. No correlation was found between the type and thickness of the intermediate layer and tensile strength of the glazed test samples, but a strong correlation existed between cristobalite and quartz content in a glaze layer and the tensile strength of the glazed test samples.

DEPENDENCE OF FRACTURE STRENGTH ON STRAIN-RATE IN POLYCRYSTALLINE ALUMINA

R.L. Bertolotti

Short Communication.

CERAMIC GLAZES OPACIFIED WITH CaTiSiO_5

G. Biffi, G. Ortelli and P. Vincenzini

Short Communication.

CERAMICS AS NUCLEAR REACTOR FUELS

K.D. Reeve

Ceramics are widely accepted as nuclear reactor fuel materials, for both metal clad ceramic and all-ceramic fuel designs. Metal clad UO_2 is used commercially in large tonnages in five different power reactor designs. UO_2 pellets are made by familiar ceramic techniques but in a reactor they undergo complex thermal and chemical changes which must be thoroughly understood. Metal clad uranium-plutonium dioxide is used in present day fast breeder reactors, but may eventually be replaced by uranium-plutonium carbide or nitride. All-ceramic fuels, which are necessary for reactors operating above about 750°C , must incorporate one or more fission product retentive ceramic coatings. BeO -coated BeO matrix dispersion fuels and silicate glaze coated $\text{UO}_2\text{-SiO}_2$ have been studied for specialised applications, but the only commercial high temperature fuel is based on graphite in which small fuel particles, each coated with vapour deposited carbon and silicon carbide, are dispersed. Ceramists have much to contribute to many aspects of fuel science and technology.

TWINNING IN MONOCLINIC EUROPiUM SESQUIOXIDE

C.F. Bilsby and D.A. Moore

Fine lamellar structures and larger growth twins have been observed in dense sintered europia. Transmission electron microscopy has been used to demonstrate that these lamellae are also growth twins in the monoclinic Eu_2O_3 crystals of composition plane (313) and (313), and twinning axis [101], and evidence for twinning on the (111) and (111) planes with the same twinning axis is presented. Cubic Eu_2O_3 detected by X-ray diffraction in trace quantities in the sintered Eu_2O_3 was not detected by electron microscopy.

THE MECHANICAL PROPERTIES AND DESIGN DATA FOR ENGINEERING CERAMICS

R.W. Davidge

This paper summarises some recent developments in understanding the mechanical properties of ceramics from a materials science viewpoint, and in the generation of design data for ceramics of direct applicability to engineering applications. General recommendations for future research are made.

HOT-PRESSING OF ACTIVE MAGNESIA

R. Pampuch, H. Tomaszewski and K. Haberko

Isothermal hot-pressing of powders of active MgO formed by thermal decomposition of $\text{Mg}(\text{OH})_2$ at temperatures of $500\text{-}700^\circ\text{C}$ and pressures of $2000\text{-}2800 \text{ kg/cm}^2$ yields transparent polycrystalline MgO having densities close to theoretical.

A detailed characterization of the MgO powders before, during, and after hot-pressing and by an analysis of creep kinetics allowed to indicate the probable dominant mechanisms leading to densification. In systems consisting of crystallites having a strained lattice, densification during hot-pressing at 500°C appears to be due to a point-defect diffusion mechanism; this is possible at such low temperatures because vacancies become mobile in ionic crystals at 0.25 T_m , i.e. at 770°K (500°C) in MgO , and their concentration is considerably increased in strained (stressed) crystallites in comparison with unstrained crystallites. Such a mechanism does not appear to occur in systems consisting of unstrained crystallites, either on hot-pressing at 500°C or at 700°C where crystallite boundary sliding by dislocation glide/climb is more probable. A rearrangement of crystallites due to crystallite boundary sliding, by dislocation glide/climb, as well as the lubricating action of traces of water may also contribute to the densification of the systems studied. Fragmentation does not contribute to the enhanced densification at the low temperatures of hot-pressing utilized in the present work.

ON THE STABILITY OF REFRACtORY MATERIALS UNDER INDUSTRIAL VACUUM CONDITIONS: Al_2O_3 , BeO , CaO , Cr_2O_3 , MgO , SiO_2 , TiO_2 SYSTEMS

D. Beruto, L. Barco and G. Belleri

The volatility and stability of refractory oxides, such as Al_2O_3 , BeO , CaO , Cr_2O_3 , MgO , SiO_2 and TiO_2 , towards oxygen has been studied using data of standard free energy for the vaporization processes and the kinetic theory of gases. The analysis has been made removing the congruence condition and examining the system's behaviour in the monovariant region. The results appear to be a useful tool in choosing the experimental strategy for getting simultaneous information on both volatility and stability towards oxygen. Some of the experimental data available in the literature on mixtures of oxides have been compared with ours, and the good qualitative agreement obtained will probably allow the application of our approach also to commercial refractories.

KINETICS OF PRESSURE-SINTERING AND GRAIN-GROWTH OF ULTRA-FINE MULLITE POWDER

B.B. Ghate, D.P.H. Hasselman and R.M. Spriggs

The kinetics of densification of high-purity, fine-grained mullite were studied by vacuum hot-pressing between 1470° and 1620°C and 1000 to 6000 psi. Mullite could be readily pressure sintered to 0.988 relative density and to $< 1.5 \mu\text{m}$ grain size. After the rapid initial stage consisting of large scale particle rearrangement, fragmentation and probably large scale grain boundary sliding, densification followed first order kinetics. Based on the stress exponents ($n = 2.0$ to 1.3), diffusional creep processes and non-Newtonian grain boundary sliding were thought to be the controlling mechanisms of densification beyond ~ 0.85 relative density. The activation energy for pressure sintering was found to be $163 \pm 22 \text{ Kcal/mole}$, whereas the activation energy for grain-growth was $182 \pm 45 \text{ Kcal/mole}$. These high activation energies coupled with values for the diffusion coefficients of sintering representative of Si^{+4} suggest that the diffusion of the silicon ion was the rate controlling process during densification as well as grain growth.

SINTERING BEHAVIOUR OF YTTRIA-STABILIZED ZIRCONIA POWDERS PREPARED FROM GELS

K. Haberko, A. Ciesla and A. Pron

An aqueous solution of ZrCl_4 and YCl_3 was hydrolyzed with NH_4OH to obtain atomically homogenous coprecipitates. The coprecipitation process was quantitative if the pH of the

suspension was ≥ 9 . On heating, the coprecipitates form $\text{ZrO}_2\text{-Y}_2\text{O}_3$ cubic solid solutions at very low temperatures (400°C for the ZrO_2 -6 mole % Y_2O_3 composition). Powders obtained by calcination of the coprecipitates were extremely active: shrinkage began on heating to 450°C \pm 550°C, depending on the initial calcination temperature, and densification to a body of 95% theoretical density and maximum grain size of about 4 μm was achieved by sintering at 1500°C. The influence of agglomerates in the starting powder on densification and the microstructure of the sintered body are also considered.

OXIDATION OF FERROCHROMIUM POWDER IN PERICLASE OR MAGNESIOTRICRIMITE

S. Mrowec and K. Słoczyńska

TG, X-ray diffractometry, optical microscopy and X-ray microanalysis have been used for kinetics studies on the oxidation mechanism of ferrochromium powder in the surrounding of magnesiotrichrime or periclase. It is shown that the transport of the reactants is the rate determining step of the oxidation process, and that diffusion of oxygen in the gas phase is the predominant factor in the initial stage, whereas lattice diffusion becomes the rate determining step in the latter stages. When the metal is dispersed in a non-metallic phase it has been found that the oxidation rate is faster and very sensitive to the nature of the dispersing medium. In oxidation processes considerable acceleration has been found when the dispersing medium reacts with the oxidation products.

A COMMENT ON THE CHEMICAL EQUILIBRIUM IN THE $\text{BaCO}_3\text{-TiO}_2$ SYSTEM

Yoko Suyama and Akio Kato

An equilibrium study was done on the following reactions: $\text{BaCO}_3 + \text{TiO}_2$ (anatase) $\Rightarrow \text{BaTiO}_3 + \text{CO}_2$ [1]; $\text{BaCO}_3 + \text{TiO}_2$ (rutile) $\Rightarrow \text{BaTiO}_3 + \text{CO}_2$ [2]; $\text{BaCO}_3 + \text{BaTiO}_3 \Rightarrow \text{Ba}_2\text{TiO}_4 + \text{CO}_2$ [3]. The following reaction temperatures under 1 atmosphere of CO_2 were found: $530^\circ \pm 5^\circ\text{C}$ [1], $650^\circ \pm 5^\circ\text{C}$ [2] and $1145^\circ \pm 3^\circ\text{C}$ [3]. These temperatures are higher by 90° to 240°C than those calculated from thermochemical tables. The discrepancies can be explained by assuming -296.5 ± 1.0 kcal/mole for the heat of formation of BaCO_3 at 298°K against -290.7 kcal/mole given in the tables.

PRODUCTION OF STABILIZED ZIRCONIA FOR USE AS A SOLID-STATE ELECTROLYTE

M.J. Bannister and W.G. Garrett

The production of stabilized zirconia for solid electrolyte use is reviewed. Topics covered include the phase systems of interest, the preparation of powders, calcination or prefiring, shaping, firing and the stability of the electrolyte in service. Special reference is made to the phase systems $\text{ZrO}_2\text{-CaO}$, $\text{ZrO}_2\text{-Y}_2\text{O}_3$ and $\text{ZrO}_2\text{-Sc}_2\text{O}_3$, to the effects of stabilizers and impurities on electrical properties, to the influence of the powder preparation method on powder properties, to reactions which occur during calcination and final firing, to sintering mechanisms and grain growth, and to the influence of impurities and agglomerates on fabrication. Alternative methods of fabricating electrolyte bodies are also considered.

JOINING OF LANTHANUM CHROMITE AND ZIRCONIA CERAMICS

Vu Tien, L.F. Cabannes and A.M. Anthony

An experimental procedure allowing the joining LaCrO_3 ceramic and stabilized ZrO_2 ceramic is described. Some micro-

structural characteristics of the joints are presented. In the thin joining area, no chromium is observed, the porosity is low and the lanthanum concentrations are high, corresponding to the compound $\text{La}_2\text{Zr}_2\text{O}_7$.

SOME USES OF ALKYL SILICATES IN REFRACTORY TECHNOLOGY

H.G. Emblem

The manufacture of alkyl silicates is outlined. Refractory binders which do not contain fluxing agents can be prepared from alkyl silicates by hydrolysis and gelation. The method of making refractory shapes by the alkaline hydrolysis and gelation of ethyl silicate is given. Intricate shapes having good refractoriness and thermal shock resistance can be made to close dimensional tolerance. «Composites» and thermal insulating refractories can also be produced. Special uses of alkyl silicates include the use of ethyl silicate in forming rigid shapes from ceramic fibres, producing dry-pressing mixes and the bonding of nitrides, borides and silicides. Some uses of aminoalkyl and chloroalkyl silicates are mentioned.

Vol. II, January/December, 1976

BUBBLES IN CERAMIC SYSTEMS

W.O. Williamson

The genesis and properties of bubbles are discussed, with ceramic examples selected from aqueous suspensions and pastes, dried bodies, molten and congealed glasses, glazes and vitreous bonds, natural and synthetic crystalline materials, and fluidized beds. Bubbles influence ceramic behaviour before, during and after firing, sometimes desirably, but often adversely. Most develop by heterogeneous nucleation or by the entrapment of gases. Their expansion and mobility, or the mobility of their surfaces, induce flow in ambient liquids which may, for instance, accelerate the corrosion of refractories or produce glaze defects. Corrosion is accelerated also by the enhanced chemical reactivity and material transport at bubble surfaces.

SUBSOLIDUS EQUILIBRIA IN THE PSEUDOTERNARY SYSTEM $\text{CaO-SrO-Fe}_2\text{O}_3$

E. Lucchini and G. Slocari

The phase relationships at 1100°C among the reaction products of CaO , SrO and Fe_2O_3 were determined by the air quenching technique. Extended regions of binary solid solutions based on $\text{SrO}\cdot 6\text{Fe}_2\text{O}_3$, $7\text{SrO}\cdot 5\text{Fe}_2\text{O}_3$, $2\text{CaO}\cdot \text{Fe}_2\text{O}_3$ and a pseudobinary one adjacent to $2\text{SrO}\cdot \text{Fe}_2\text{O}_3$ are formed. The variable oxygen content of $2\text{SrO}\cdot \text{Fe}_2\text{O}_3$ and $3\text{SrO}\cdot \text{Fe}_2\text{O}_3$ induces an extra degree of variance in the system. Based on experimental evidence obtained by X-ray diffraction, optical microscopy and titrimetric determination of Fe^{+4} , the phase diagram for the system $\text{CaO-SrO-Fe}_2\text{O}_3$ was derived.

HIGHLY REFRACTORY OXIDE SYSTEMS CONTAINING OXIDES OF RARE-EARTH ELEMENTS

L.M. Lopato

The paper describes the interactions of rare earth element (REE) oxides with magnesium, calcium, strontium, and barium oxides in a wide range of concentrations and temperatures from 1000 to 2450°C. The most typical binary phase diagrams found for these oxide systems are illustrated in the

paper. The existence of six types of compounds, i.e. $MeLn_2O_7$, $MeLn_2O_4$, $Me_3Ln_8O_{17}$, $Me_3Ln_4O_9$, $Me_2Ln_2O_5$, and $Me_3Ln_2O_6$, has been established. It has been shown that the compounds formed resemble other classes of compounds with REE oxide participation; this is demonstrated by spasmodic property changes in a given series of compounds of a single type (process of formation, X-ray and petrographic characteristics) and by changes of the composition of the compounds. These facts indicate an appreciable role of the 4f electrons of the REE atoms resulting in changes in the nearest environment of the REE atoms; in turn this leads to property and compositional changes of the compounds formed and, hence, to variations of the type of phase diagrams in the La-Lu series. Phase transformation in REE oxides (1800°C) have been investigated and the regularities observed in the effects of oxides of elements of the IIA subgroup on the transformations are discussed. The nature and kinetics of decomposition of magnesium oxide-based solid solutions have been studied in the Sc_2O_3 -MgO system. It is suggested that the regularities observed here may be valid for other oxide systems having a eutectic type of liquidus where the decomposition of the solid solution occurs into the starting components or into solid solutions on their base, without formation of intermediate compounds. Theoretical calculations of the phase-field boundaries of some types of phase diagrams of the systems studied have been carried out, assuming ideal or regular solution models.

MAGNETIC AND MICROSTRUCTURAL PROPERTIES OF SiO_2 -MODIFIED γ - Fe_2O_3 PREPARED IN A FLUID BED FURNACE

G. Fagherazzi

A method for minimizing the amount of micropores in γ - Fe_2O_3 acicular particles prepared from α -FeOOH is described. Reduction temperatures of α -FeOOH to Fe_3O_4 were employed in the range of 340°C - 600°C, in the presence of 0.5-2.0% silica, previously precipitated from a solution of Na_2SiO_3 added to the reagent suspension. The improvement reached in the microstructural characteristics of SiO_2 -modified γ - Fe_2O_3 particles was clearly shown by means of electron microscopy. Three main advantages were achieved: i) a more compact bulk structure of the particles combined with a drastic reduction of the number of micropores; ii) an improvement in the regularity and smoothness of particle shape; iii) a decrease of interparticle sintering. As a consequence, a H_c value of 375 Oe was achieved in a magnetic tape containing SiO_2 -modified γ - Fe_2O_3 . The trends of intrinsic coercivity H_c and of specific surface S_{BET} as functions of reduction temperature are reported both for SiO_2 -modified γ - Fe_2O_3 samples and for pure ones. The temperature at which oxidation of Fe_3O_4 to γ - Fe_2O_3 takes place does not affect the properties of the product in the range 260°C-380°C. All runs were carried out in a fluid bed furnace.

SEM AND ELECTRON MICROPROBE OBSERVATIONS OF SOME PHENOMENA OCCURRING IN MAGNESIA-CHROME REFRACTORIES

W. Piatkowski

Scanning electron microscopy (SEM) and electric microprobe (EMP) were used to study some phenomena occurring in the production of magnesia and magnesia-chrome clinkers, with special reference to the sintering process and to the formation of secondary spinel phases. Transformations occurring during firing of chrome-magnesite bricks, especially the development of the so-called «direct bonds» have also been reported.

ONCE PRESSED SINGLE FIRED GLAZED FLOOR TILES

T. Emiliani and G. Biffi

A technological process is described for producing glazed red stoneware floor tiles, whereby the clay constituting the body is rendered partially compact in the press, a layer of glaze in powder form is subsequently placed thereon and both layers are pressed. This process for the production of material of a good quality is, both from an aesthetic and a technological point of view, suitable for application in a fully mechanized and automated cycle. The cycle envisages spray drying of the glaze and clay, the use of hydraulic or friction screw presses with suitably modified feeders for pressing, rapid or natural drying and firing either single layer or in saggers. The 20% loss in efficiency of the presses (the number of strokes per minute) is largely compensated through the abolition of glazing lines, the consequential saving in the space taken up for the working area, the reduction in internal pollution and the fact that the entire production cycle is simplified.

REFRACTORIES BASED ON LIME: DEVELOPMENT AND PERSPECTIVES

F. Nadachowski

CaO as a refractory shows specific high-temperature reactions, differing in some important aspects from those of magnesia and even of dolomia. Lime-carbon composites offer much promise with regard to corrosion resistance to the attack of ferruginous slags. There has been a considerable development of refractory lime technology over the post-war period, including in recent years the so-called salt-lime materials of a wide range of properties. To secure future commercial manufacture, full advantage should be taken of the specific merits of CaO, as well as of the possibilities of low-cost production. The most promising fields of applications seem to be: full-lime linings for making pure and alloyed steel, cement rotary kilns, glass regenerators and roofs, lime kilns and some specialized installations.

MAGNESIUM ALUMINATE SPINEL PRECIPITATION IN MgO

C. Berthelet, W.D. Kington and J.B. Vandersande

Magnesium aluminate spinel precipitates forming in polycrystalline MgO containing 0.43 weight % Al and 0.031 weight % Al were examined by transmission electron microscopy after air quenching or rapid cooling. Precipitation in a variety of morphologies occurred at grain boundaries, low angle grain boundaries and dislocations. On reheating a virgin surface, precipitation occurs at temperatures above 730°C.

FABRICATION OF TRANSLUCENT CERAMICS BY ISOSTATIC HOT-PRESSING

M. Koizumi, K. Kodaira, Y. Ishitobi, M. Shimada and F. Kanamaru

Hot isostatic pressing of BeO and $Pb(Zr_{0.8}Ti_{0.2})O_3$ was performed using a glass as a pressure-transmitting medium in the range of 1000° to 1400°C for BeO and 700° to 900°C for $Pb(Zr_{0.8}Ti_{0.2})O_3$ at 2 kb. Translucent bodies of these materials with theoretical density were obtained. The present results indicate that the hot isostatic pressing technique of glassed-sealed BeO and PZT has the following characteristics. (1) Sealing in an evacuated state is feasible using a glass container instead of a metal one. (2) Translucent sintered bodies with theoretical density can be obtained under conditions of low temperature and short pressing time at 2

kb. (3) Grains are uniformly distributed and their sizes are quite small. (4) The closed system and high pressure involved in the present pressing technique permit sintering to proceed without interference from vaporization or environmental reactions.

CRYSTALLITE GROWTH AND CHANGES OF SOME RELATED CHARACTERISTICS OF MAGNESIA OBTAINED BY THERMAL DECOMPOSITION OF BASIC CARBONATE

N.A.L. Mansour

The effect of decomposition temperature and soaking time, of magnesia prepared from basic magnesium carbonate, on crystallite growth, surface area, agglomeration and lattice parameter was investigated. X-ray line broadening was used to measure the crystallite size of the powdered samples; lattice parameter was measured from (200) peak and surface area was measured by areameter. The results have shown that crystallite growth is governed by the equation $D^2 = kt$, the activation energy equals to 27.5 Kcal/mole for temperatures up to 770°C and 66 Kcal/mole for higher temperatures. A minimum value for lattice parameter was observed at crystallite size of about 200 Å. They have also shown that the specific surface area of the magnesia powder reached a limiting value at each decomposition temperature. This limiting value decreased rapidly with increasing the decomposition temperature up to 770°C. At higher temperatures the decrease was very slight.

EFFECTS OF RAW MATERIALS AND MIXING METHODS ON THE SOLID STATE REACTIONS INVOLVED IN FABRICATION OF ELECTRONIC CERAMICS

T. Yamaguchi, S.H. Cho, M. Hakomori and H. Kuno

Effects of raw materials and mixing methods have been studied in the solid state reactions in the systems $\text{BaCO}_3\text{-TiO}_2$ and $\text{PbO-ZrO}_2\text{-TiO}_2$. It is shown that the dispersion and aggregation state of reactants are responsible for the formation of intermediate phases and also for the densification characteristics of PZT. Behavior of additives has been interpreted in terms of dispersion of reactant particles.

HOT-PRESSING OF SOME PIEZOELECTRIC CERAMICS IN THE PZT SYSTEM

V.L. Balkevich and C.M. Flidler

The effect of different hot-pressing regimes on the physical, dielectric and piezoelectric properties of low-coercive and high-coercive piezoelectric ceramics was investigated. Ceramics with density approaching theoretical (98.3-99.5%) were obtained. Densification kinetics of piezoelectric ceramics were studied. It was concluded from the investigation results that the densification mechanism was of a complicated nature. Suitable choice of hot-pressing regime resulted in considerable improvement in the dielectric and piezoelectric properties was 15-20% on average. High values for the electrophysical properties were obtained at sintering temperatures 100-150° lower than those used in common annealing. It was observed that conditions giving maximum values for the electrophysical properties did not agree with conditions giving maximum values for relative density: in spite of the density increase there was a weakening of the piezoeffect at high pressure.

DENSIFICATION CHARACTERISTICS OF ULTRAFINE POWDERS

M. Hoch and K.M. Nair

Ultrafine (< 100 Å) and high purity (99.99%) powders of mullite ($3 \text{ Al}_2\text{O}_3 \cdot 2 \text{ SiO}_2$), Zyttrite® (Y_2O_3 stabilized ZrO_2), and

alumina-zirconia (58 wt. % Al_2O_3) were prepared from appropriate organo-metallic precursors. The materials were dried at 125°C and then calcined at 550°C for 1½ to 3 hours and cooled in desiccators in order to minimize the absorption of moisture. The calcined mullite and Zyttrite® and noncalcined alumina-zirconia powders were isostatically pressed up to 60,000 psi (4222.2 kg/cm²) and sintered at up to 1500°C using two different sintering pathways: (1) one-step sintering at up to 1500°C and (2) multi-step sintering (sintered at 1100°C, cooled, resintered at 1300°C, cooled, and finally sintered at 1500°C). Results show that these ultrafine powders sinter to 95% + theoretical density at 1500°C, irrespective of sintering pathways. Sintered materials showed a uniform grain size and change in the sintering pathways from one-step to multi-step has little or no effect on the grain size or microhardness. Surface reactivity of these powders is neither diminished nor increased by variation in the sintering pathways and thus the densification is dependent mainly on the final sintering temperature.

A NEW METHOD FOR ESTIMATING THE DRYING SENSITIVITY OF CLAYS

V.P. Varlamov, L.A. Kroichuk and A.A. Toporkova

Fourteen clays with different drying sensitivity were selected for developing a rapid method of estimation of their drying sensitivity. The clays were arranged in a series according to results of complex technological tests in a decreasing order of their drying sensitivity. It is proposed to determine only that portion of the losses that is released in the temperature range above the drying temperature, at 100-200°C in order to compare different clays as regards the interlayer moisture lost during drying. A relationship was found between the amount of moisture liberated at temperature up to 200°C, mineralogical composition and drying behaviour of clays. Having determined the amount of the interlayer moisture at 100-200°C, it is possible to quantitatively evaluate the content of component adversely affecting the drying sensitivity and predict the drying behaviour of a given clay.

EFFECT OF ENVIRONMENT ON FRACTURE OF CERAMICS

S.W. Freiman

This paper reviews the important work to date describing the effect of environment (particularly H_2O) on the fracture behavior of glasses, single crystals and polycrystalline ceramics. It is shown that since the environment predominantly affects rates of crack propagation, fracture mechanics techniques have proved useful in describing the phenomenon of «stress corrosion» in ceramics. Models describing the environment-crack interaction are presented and mechanisms of crack propagation are discussed. The temperature dependence of «stress corrosion» in ceramics is described and the effect of plastic deforction on a material's environmental sensitivity is briefly discussed. Finally, future research topics are suggested.

SUBSOLIDUS EQUILIBRIA AND KINETICS OF DECOMPOSITION OF SOLID SOLUTIONS IN THE HfO_2 ($\text{ZrO}_2\text{-MgO}$) SYSTEMS

A.K. Kuznetsov, P.A. Tikhonov, m.V. Kravchinskaya and E.K. Koehler

The subsolidus equilibrium diagram in the $\text{HfO}_2\text{-MgO}$ system has been constructed and contains a eutectoid point similar to the $\text{ZrO}_2\text{-MgO}$ system. A comparative study of the stabilities of solid solutions of MgO in HfO_2 and in ZrO_2 has been made. The difference in phase stability of the solid solutions in the temperature range 1300 to 1450°C is due to the difference of eutectoid temperatures in the two systems. The me-

chanism and kinetics of decomposition of the $\text{HfO}_2\text{-MgO}$ solid solutions have been studied. The decomposition process of solid solutions in this system and in the $\text{ZrO}_2\text{-MgO}$ system is a particular case of the wide-spread type of eutectoid decomposition which is governed by the laws of eutectoid equilibria. The decomposition of the cubic solid solutions in both systems proceeds in two steps.

THERMODYNAMIC ANALYSIS OF THE HIGH-TEMPERATURE STABILITY OF SILICON NITRIDE AND SILICON CARBIDE

S.C. Singhal

A thermodynamic analysis of the stability of Si_3N_4 and SiC is presented which can be employed to assess their suitability for use at high temperatures in various environments. Specifically, the decomposition and the volatilization of Si_3N_4 and SiC , and of SiO_2 , which is the major constituent in the oxide scales formed on their surfaces in oxidizing atmospheres, are discussed in terms of ambient environment and temperature. The calculated values of the lowest oxygen partial pressure up to which a protective SiO_2 layer should be maintained on the surface of Si_3N_4 and SiC are also presented.

THERMAL CRYSTALLIZATION OF CORDIERITE GLASS POWDER WITH PLATINUM AS A NUCLEATING AGENT

A. Negro, M. Murat and F. Sassi

Cordierite glass powder, synthesized with 100 ppm platinum as a nucleating agent, were preheated at different temperatures from 600 to 900°C for different times (up to 5 hours) and were studied by X-ray diffraction, differential thermal analysis, scanning electron microscopy, and IR absorption spectroscopy. The low content of platinum promotes, during preheating, phenomena which do not take place in the case of the pure glass, essentially nucleation of metastable μ -cordierite with low preheating temperatures, and crystallization of μ -cordierite followed by crystallization of α -cordierite when both the temperature and time of preheating become higher.

MECHANICAL AND THERMAL PROPERTIES OF BOEHMITE BONDED ALUMINA BODIES

K.S.E. Forssberg

The paper describes the fabrication and the properties of boehmite bonded alumina shapes. The term boehmite bonding refers to the utilization of steam cured reactive alumina as an intermediate binder in alumina shapes. Bodies were prepared by mixing tabular alumina. After drying the shapes were treated in an autoclave at around 200°C and saturated steam pressure. During steam treatment the reactive alumina is converted to boehmite, $\gamma\text{-Al}_2\text{O}_3\cdot\text{H}_2\text{O}$. Cold crushing strength figures up to 1200 kp/cm² have been obtained. Relations between mechanical properties and porosity have been examined. The paper gives details on reaction kinetics of the formation of boehmite as well as the dehydration of boehmite at around 500°C. Boehmite dehydrates to γ -alumina at 500-520°C. Due to the high reactivity of the so formed γ -alumina, ceramics bonds are formed at low temperatures. Therefore the conversion from boehmite to γ -alumina is followed by only a slight decrease of the strength. The dehydration process has been followed by means of surface area and pore size distribution measurements and X-ray diffraction and DTA-TGA investigations. The boehmite bodies have been subjected to normal refractory testing procedures i.e. hot modulus of rupture, Youngs modulus, creep, refractoriness under load, resistance to slag attack and spalling. The testing shows that the boehmite bonded ceramics have re-

fractory properties comparable with those of normal fired chemically bonded bricks. The boehmite bonding method have also been tested on aluminosilicate, i.e. cyanite, with good results. Possible applications of the method are discussed in the paper.

CERAMIC COMPOSITE MATERIALS BASED ON REFRACTORY OXIDES WITH NITRIDE AND OXYNITRIDE BONDS

J. Gusman

Some problems concerning the synthesis, structure and properties of products $\text{R}_n\text{O}_m\text{-Si}_3\text{N}_4$ (or Si_2ON_2) obtained by reaction sintering have been investigated. Al_2O_3 , MgO , ZrO_2 and others were used as R_nO_m . It was demonstrated that the nature of the bonding material, in particular when nitride (or oxynitride) bonds are used instead the oxide ones, radically influences many properties such as the thermal expansion, modulus of elasticity and thermal stability. In particular, the thermal expansion coefficients of the nitride and oxynitride bonded materials are generally controlled by that of the bond rather than that of the oxide.

SEMICONDUCTING BARIUM TITANATE FILMS BY A MODIFIED DOCTOR BLADE METHOD

Masayuki Nagai and Hiroaki Yanagida

Nonporous and dense semiconducting barium titanate films were obtained by a modified «doctor blade» method. The calcined semiconductive powders were dispersed into a polystyrene film. After decomposing and evaporating the organic vehicle, the powders left on the plate were pressed into the polystyrene film. Then, primary sintering was achieved and followed by sintering in various conditions. Thinner films consisted of single grains perpendicular to the direction of the film, thicker films had grain boundaries inside the film along the same direction. The films had a resistivity of $10^2 \sim 10^3 \Omega \cdot \text{cm}$ at room temperature. The positive temperature coefficient of resistivity was at least three orders of magnitude on properly sintered films.

THE TECHNOLOGY AND PROPERTIES OF FIBRE REINFORCED CERAMIC COMPOSITES

R.W. Davidge

Over the last decade a number of factors have contributed to the rapid development of a new class of material - fibre reinforced ceramics. Important factors include: a demand from materials users for ceramics with improved engineering properties; the availability of new fibrous materials for reinforcement; the development of fabrication techniques for composite production; and an improved understanding of the fundamental factors controlling the mechanical properties of the composites. Materials discussed range from those already in use such as asbestos or glass reinforced cement, to research materials for intermediate and high temperature use such as carbon fibre reinforced glasses and silicon carbide reinforced silicon nitride. Fabrication methods, and actual or potential applications are outlined. The properties of ceramic based composites differ from those of metal or plastic composites in that the matrix fails by fine scale cracking before the reinforcing fibres break. Nevertheless, useful increases in both strength and stiffness can be obtained in particular systems. More spectacular increases, of several orders of magnitude, in fracture energy are obtained by reinforcement. In this way the significance of the brittleness of ceramics is diminished which makes the greater engineering use of ceramic composites more likely.

PbTiO₃-PbZrO₃-In(Li_{3/5}W_{2/5})O₃ PIEZOELECTRIC CERAMICS FOR SURFACE WAVE FILTERS

N. Ichinose, T. Takahashi, Y. Yamashita and H. Iwasaki

Piezoelectric ceramics with a low-temperature coefficient of surface wave velocity have been obtained in the ternary system PbTiO₃-PbZrO₃-In(Li_{3/5}W_{2/5})O₃ with a small amount of MnO. The surface wave velocity temperature coefficient of the typical compound is 18 ppm/deg from -30° to 20°C and -3 ppm/deg between 20° and 80°C. Surface wave velocity is 2273 m/sec and propagation loss is 0.04 - 0.05 db/λ at about 22 MHz. Surface wave properties in this ternary system are suitable for surface wave devices, such as TV-PIF filters.

MECHANISMS OF DENSIFICATION DURING THE PRESSURE SINTERING OF ALPHA-SILICON NITRIDE

L.J. Bowen, R.J. Weston, T.G. Carruthers and R.J. Brook

Data obtained during a study of the hot-pressing of high purity α-silicon nitride, to which MgO was added as a sintering aid, are used to illustrate the use of available hot-pressing equations in attempting to identify the mechanism of densification. The shortcomings of using these in their integrated forms, as is customary, are pointed out. The processes of liquid phase (solution-reprecipitation) sintering and surface diffusion controlled (Coble creep) sintering are seen to differ only in the nature of the grain boundary phase; differences in the form of the equations for these processes lie in the geometries chosen for their derivation. The use of the differential form of the Coble intermediate stage sintering equation enables the linear relationship between MgO content and densification rate at constant density to be explained in terms of the thickness of the magnesium silicate boundary layer. Values of the diffusion coefficient of the rate controlling species in the boundary layers as a function of temperature are calculated.

MICROSCOPIC STUDY OF PORE STRUCTURE

J. Piekarzyk and R. Pampuch

The relative merits of optical microscopic methods in study of the pore structure of some ceramic materials (mainly graphite) are discussed on the basis of comparison of the results of this method with those from other current methods, such as apparent and true density measurements and mercury high-pressure porosimetry. A modified microscopic method has been developed in which direct replicas of polished sections are examined under an interference-polarisation microscope and indirect replicas under the electron microscope. In this method the main drawbacks of the microscopic method are suppressed to a great degree. In cases of materials containing pores of an irregular shape and of wide size distribution, such as the graphite studied, the optical microscopic method has many advantages in comparison with other methods when the random and systematic errors of this method are properly recognised and suppressed. The cumbersome evaluation of the microscopic images and/or photomicrographs may sometimes be avoided by using the image analysing computer but the latter proved to be of a lower accuracy in the case of the graphite studied.

INVESTIGATION ON FORMATION AND BEHAVIOUR OF THE PHOSPHATE BONDING IN ELECTROFUSED MgO

M. Gašić and F. Sigiński

Formation of the phosphate bonding in electrofused MgO by addition of ammonium and Mg phosphates was investigated and formation of amorphous compounds has been found. On heating these compounds undergo almost identical changes what leads to the conclusion that chemical properties of the

phosphate anion play essential role in this bonding reaction which does not depend to the same extent on the present cation. In the present work zero shrinkage sintering was observed. However, porosity substructure considerably changed during sintering. Electron microprobe analyses have shown that phosphate compounds concentrate at the grain boundaries. Phosphorus is present in MgO even after heating at 1660°C but it is no more continuously arranged at the boundaries of periclase grains.

ANALYSIS OF DYNAMIC FUSION PHENOMENA OF CERAMIC AND METALLIC POWDERS INJECTED INTO A ARGON PLASMA-JET

G. Perugini

Plasma-spray experiments have been carried out to study the velocity of Al, Al₂O₃, and W powders (mean size: 45 μm) at a distance of 5.65 cm from the nozzle. The experimental set-up is described. The profile of velocity and kinetic energy (of each powder in each of the several trajectories of the spray-projection) along the distance between the intercept point (in the flame axis) and the receiving surface has been calculated. The calculations have been developed on the basis of the experimental results and on the assumption of a uniformly decelerated flight of the particles under a Stokesian regime. Impact heat, together with the heat necessary to melt the injected powders are the other parameters examined. From the obtained data useful considerations are drawn for good operative procedures in order to obtain high-quality coating.

Vol. III, January/December, 1977

ADVANCES IN CERAMIC HOT FORMING AND PRESSING: THEORY AND PRACTICE

M.R. Notis

Advances in the understanding of the hot forming of ceramic materials and the mechanisms of sintering during the intermediate and final stages of densification during hot pressing are reviewed. The available diffusion and plastic flow models are critically examined and approaches to the development of quantitative multimechanism models for hot pressing are discussed. The effects of grain growth and grain boundary sliding in a porous body are described. Recent developments related to the interpretation of pressure-sintering kinetics through the use of «densification mechanism maps» are outlined. Technological advances that have recently been made in relation to fabrication by hot forming and by hot pressing are described. These include the production of large area-high transparency ceramics for optical applications, the development of controlled microstructure and improved properties in magnetic materials, and the preparation of hotpressed Si₃N₄ materials for ceramic turbine applications. Finally, significant areas for future study, where either fundamental understanding or technological development limit present capabilities, are considered.

SUBSOLIDUS PHASE RELATIONSHIPS IN THE SYSTEM BaO-CaO-Fe₂O₃

G. Slocchi and E. Lucchini

The phase relationships at 1100°C among the reaction products of BaO, CaO and Fe₂O₃ were determined by the air quenching technique. Two binary solid solutions are formed, one between barium hexaferrite and a hypothetical calcium tetraferrite and another pseudobinary one adjacent to 2BaO·Fe₂O₃. Based on experimental results obtained by x-ray diffraction, optical microscopy and titrimetric determination of Fe⁺, the 1100°C isothermal section for the system BaO-CaO-Fe₂O₃ was derived.

SOME REACTIONS OCCURRING IN LIME REFRactories CONTAINING CALCIUM CHLORIDE

F. Nadachowski, T. Rymon-Lipinski and M. Janiec

Refractory products made from $\text{CaO}-\text{CaCl}_2$ mixtures precalcined at low temperatures have shown a specific volume stability on further firing to 1500°C and higher, in contrast to phenomenon was studied using simplified systems, including their equivalents of pure CaO , MgO , or $\text{MgO}-\text{CaCl}_2$. This phenomenon was studied using simplified systems, including some additives specially chosen; an explanation is offered based on shrinkage data and the observed development of a unique microstructure, resulting from an early formation of a reactive liquid as well as gas evolution effects. The non-shrinking behaviour of the so-called calcite brick (made from ground limestone masses containing CaCl_2) is also dealt with.

EUROPIA CERAMICS FOR USE AS FAST REACTOR NEUTRON ABSORBERS

J.B. Ainscough, D.A. Moore and S.C. Osborn

The development of a fabrication route for europia, which is one of the few materials suitable for use as a neutron absorber in Fast Reactor control and shut-off rods, is described. The route is based on cold pressing and sintering with the most important stages being the control of powder surface area and of sintering atmosphere. An account is given of the various batches of dense sintered europia artefacts which have been prepared for experimental purposes and for irradiation testing with particular emphasis being given to the production of 12,000 pellets and a small number of relatively large square plates for a zero energy irradiation experiment. Difficulties encountered during the manufacture of the plates and the way in which they were overcome are also discussed.

THE INFLUENCE OF STARTING MATERIAL CHARACTERISTICS ON THE PROPERTIES OF HIGH-POROSITY FORSTERITE BRICKS

I. Stamenković and F. Sigulinski

In order to follow the interdependence between characteristics of raw materials and properties of low bulk density bricks several sample series on forsterite basis were made. The starting powders we employed in the brick production were dead-burned magnesite and dunite having different physico-chemical properties: impurity content, granulation, crystal structure and other relevant parameters. Using the cold and vibro pressing and sintering techniques bricks of total porosity 44% and 70% were produced. The bricks contained predominantly macropores having various shape: spherical, irregular and elongated. The relationship obtained between powder granulation, mineral and chemical composition and thermal conductivity, gas permeability, thermostability, mechanical and other properties were discussed.

THE ADAPTATION TO SPACE APPLICATIONS OF A 2000°C FURNACE IN AN OXIDIZING ATMOSPHERE

A.M. Anthony, K. Dembinski, J.L. Dunand, L. Dupont and R. Mottu

Materials Science in Space requires furnaces for high temperature designed to minimize the electrical power consumption. This experimental work demonstrates that it is possible to reduce the energy consumption within a furnace using a zirconia heating element working up to 2000°C in an oxidizing atmosphere. The time to reach this temperature is less than 1 h and the energy consumption at 2000°C for a hot zone of 20 mm diameter and 30 mm height is ± 350 W.

SYNTHETIC RAW MATERIALS FROM BENTONITE AND CONCENTRATED SALT SOLUTIONS

P. Reynen and M. Faizullah

Synthetic raw materials are successfully applied in the fields of electrical and special ceramics but are still unusual in silicate ceramics, because the quality improvement does not yet justify the higher costs. A review is given of possible ways to synthesize mullite and cordierite on a large production scale. One of these methods using bentonite and concentrated $\text{Al}_2(\text{SO}_4)_3$ and MgSO_4 as precursors was used to make larger quantities of powder (mullite and cordierite) by a spray drying process. These powders, heat treated at 1200°C have fully reacted to mullite and cordierite. The ceramic properties (pressing, slip casting, sintering) of these materials have been investigated.

MORPHOLOGY OF SILICON CARBIDE FORMED BY CHEMICAL VAPOUR DEPOSITION

R. Pampuch and L. Stobierski

Silicon carbide polycrystalline layers and particulate crystals were obtained in a modified van Arkel-de Boer apparatus on SiC -covered graphite and molybdenum susceptors. Gaseous $\text{SiCl}_4 + \text{CCl}_4 + \text{H}_2$ reactive mixtures with Si/C mole ratios varying between 0.9 and 1.4 and with $\text{Cl}/\text{Cl} + \text{H}$ ratios varying between 2.10^{-5} and 1.10^{-3} were used. The morphology and structure of SiC products obtained at temperatures between 1400 and 1900°C and input gas flow rates between 5.10^{-4} and 6.10^{-2} moles per hour have been systematically investigated by scanning electronmicrographs, x-rays (using the Laue, Weissenberg, and rotation photographs), IR-spectra, and under the polarising microscope. The ranges of temperature and input gas flow rates in which the given habits and forms of the SiC products are formed have been assessed. The habits of the particulate crystals as function of temperature have been interpreted in terms of the existing theories of heterogeneous nucleation assuming layer growth of the crystals by two-dimensional nucleation. The influence of the composition of the gaseous mixtures upon the formation of the 2H polytype as well as the probable reasons for the common occurrence of stacking fault twins in the 3C polytype have been discussed.

VACUUM SINTERING OF TRANSPARENT PIEZO-CERAMICS

K. Nagata, H. Schmitt, K. Stathakis and H.E. Müser

Transparent PLZT ceramics were fabricated by a new vacuum-atmosphere sintering method combining vacuum sintering and atmosphere sintering. Cold pressed powders were first sintered in vacuum for 15-30 minutes at 1150 - 1180°C and then heated in air for 60-90 hours with atmosphere powder. By this process, highly transparent PLZT ceramics were obtained. The production of nearly colourless small grain-size samples is possible.

REACTION SINTERED MgAl_2O_4 BODIES FROM DIFFERENT BATCH COMPOSITIONS

E. Kostić and I. Momčilović

Sintered MgAl_2O_4 bodies were obtained from batches of spinel (60%, 80% and 90%) and oxide powder mixtures. The density and microstructural characteristics of sintered samples, and the open porosity level at 1600°C to 1800°C were influenced by the starting batch composition. The densification of batches containing partially synthesized spinel powders with addition of CaO and SiO_2 mixtures was enhanced. With CaO and SiO_2 present, the densities after 1600°C were equal to those after 1800°C , without additions. Differences of densification path were also observed for batches containing

ning additive as the spinel phase content varied. These differences were especially evident at lower temperatures. It was found that liquid phase intensified grain growth at lower temperatures.

STUDY OF THE BEHAVIOUR OF ZINC OXIDE IN DIRECT-ON ENAMELS

A.M. Vogels, R. Derie and M. Ghodsi

The properties of direct-on enamels obtained by replacing TiO_2 , totally or partially, by ZnO have been studied. The first experiments were made with a frit containing 20 wt% ZnO in place of TiO_2 , the other constituents being the usual ones. The optimal fusion temperature of the frit was 1150°C: this shows that ZnO acts as a flux (the normal fusion temperature is about 1200°C). Decarburised steel sheets were enameled using this ZnO -frit, for various firing time at 800°C. The binding strength, estimated with an adherence-meter, was satisfactory, but the coats were translucent. The incorporation of several colouring agents has been tested. Opaque enamels of good adherence have been obtained by replacing only a fraction (up to 70%) of TiO_2 by ZnO . The interface reactions have been studied, in each case, by means of the electron microprobe, the scanning electron microscope and X-ray diffraction. The irregular, corroded-like appearance of the interface may be attributed to the formation of an FeO layer on the support, during the heating period, and to the subsequent dissolution of this layer in the fused coat. A compound is formed at the interface, which contains essentially iron, silicon and zinc oxides. It has been identified by X-ray diffraction as a willemite-type solid solution. The fact that willemite only appears at the interface led us to study the influence of FeO on the formation and crystallization of this compound. One may reasonably think that this willemite formation promotes adherence.

PORCELAIN FOR FAST FIRING

H. Moertel

Fast-fired porcelain may be produced by use of raw materials with very small particle sizes. Firing times of two hours were obtained. Especially the quartz must be very fine so as to change to cristobalite during fast firing. The casting slips show thixotropic behaviour, but with suitable deflocculants these difficulties may be overcome. There are also no serious problems with dry and wet pressing. The firing cycle was as follows: heating up to 1300°C (1 hour) constant temperature at 1300°C (40 min) rapid cooling to 750°C (5 min) followed by cooling to 500°C (10 min). The microstructure of this porcelain is unusual; it consists of a glassy matrix containing spherical mullite. It has outstanding properties: high strength combined with high thermal shock resistance. Its transparency and whiteness equal those of high quality standard porcelain. This porcelain should also be of interest for technical applications.

METAL-BARIUM HEXAFERRITE COMPOSITES AS PERMANENT MAGNETS

G. Asti, P. Cavallotti and R. Roberti

Barium ferrite powders have been coated with a thin layer of a cobalt phosphorus or nickel phosphorus alloy by chemical reduction from aqueous solutions with hypophosphite, after the usual sensitization-activation pretreatments. The operation parameters of the deposition baths have been varied to modify the phosphorus content, the morphology and crystallographic structure of the coating, pointing out their influence on the magnetic and mechanical characteristics of the composites. The utilization of slurry electrodes has shown the possibility of producing composites of barium ferrite with various metals, such as cobalt, nickel, iron, copper and zinc by

electrochemical treatments. The different powders produced with these new methods have been compacted and sintered at several temperatures; the influence of the thermal treatment on the characteristics of the produced magnets is pointed out. Encouraging results have been obtained, showing the possibility of producing magnets with improved magnetic and/or mechanical characteristics.

CRYSTALLITE GROWTH OF A SODIUM BETA-ALUMINA POWDER DETERMINED BY X-RAY LINE BROADENING

A. Bellosi and P. Vincenzini

Short communication.

THE SUBSYSTEM $BaO \cdot 6Fe_2O_3 - CaO \cdot 4Fe_2O_3$ $SrO \cdot 6Fe_2O_3$

G. Slocardi, E. Lucchini and G. Asti

Short communication.

THE SYNTHESIS, COMPOSITION AND PROPERTIES OF PELLITE: $Ba_2Ca(Mg, Fe^{2+}, Zn, Co)_2 Si_6O_{17}$

F.P. Glasser and J. Marr

Pellite, $Ba_2Ca(Mg, Fe^{2+}, Co)_2 Si_6O_{17}$, is a framework silicate containing three essential divalent ions. It is readily synthesized either by sintering or by devitrification of appropriate glass compositions. It occurs in nature as the mineral pellite, which has $Fe^{2+} > Mg^{2+}$. Natural and synthetic phases are, however, isostructural; the synthesis of Mg^{2+} , Zn^{2+} and Co^{2+} phases has been achieved. The synthetic Mg , Zn and Co phases melt congruently at 1177°, 1114° and 1121°C respectively. Indexed powder X-ray data are given. Ba may be partially replaced by Sr or Pb ; Be may be substituted in tetrahedral sites.

DENSIFICATION OF TiO_2 BY HOT PRESSING

S. Pejovnik, D. Sušnik and D. Kolar

TiO_2 was hot pressed to nearly zero porosity at 1200°C and 300 kp/cm². The influence of various +2, +3 and +5 valent dopants was analyzed and it was concluded that oxygen vacancies are the predominant type of defect in slightly understoichiometric rutile. An analysis of possible deformation mechanisms indicated diffusion mechanisms to prevail in hot pressing of rutile.

THERMODYNAMIC AND GEOMETRIC CONSIDERATIONS OF SOLID STATE SINTERING

Carl E. Hoge and Joseph A. Pask

Thermodynamic analysis of model sintering systems indicates that the minimum free energy configuration is represented geometrically by interpenetrating spheres of increasing size with no neck formation. The dihedral angle formed at the grain boundary increases as densification proceeds; the limit is the equilibrium angle determined by the ratio of the solid/solid and solid/vapor interfacial energies for the system. An intermediate free energy configuration favored by kinetic factors is the formation of a neck at grain/grain contacts with an equilibrium dihedral angle; the resulting reverse curvature in the surfaces of the particles provides the driving force for densification in this case. Conditions and mechanisms under which both configurations develop are discussed and are illustrated by experiments on MgO powder compacts that densify considerably more rapidly in flowing water than in static air.

MICROWAVE DIELECTRIC MATERIALS IN THE SYSTEM (Sr_{1-x} Ca_x)_{1-y} (Li_{1/4} Nb_{3/4})_{1-y} Ti_y O₃

N. Ichinose, T. Mizutani, H. Hiraki and H. Ookuma

Dielectric properties of ceramics in the system (Sr_{1-x} Ca_x)_{1-y} (Li_{1/4} Nb_{3/4})_{1-y} Ti_y O₃ were investigated. In the composition range 0 ≤ x and y ≤ 0.12, dielectric permittivities and their temperature coefficients can be varied from 38.2 to 45.8 and +30 to -70 ppm/°C, respectively. In many compositions, zero temperature coefficient of permittivity has been found. A typical compound has the following properties at X-band frequency (9 GHz): K = 42.3, 1/K · dK/dT = 0 ppm/°C and Q₀ = 3500.

DEFORMATION PROCESSES DURING HIGH TEMPERATURE CREEP OF LIME, MAGNESIA AND DOLOMA

J.A. Coath and B. Wilshire

For single-phase lime and magnesia and also for two-phase doloma (consisting essentially of a dispersion of MgO crystals in a lime crystal matrix), the creep rate, $\dot{\epsilon}$, varies with stress, σ , and temperature, T, as

$$\dot{\epsilon} = A \sigma^n \exp(-Q_c/RT)$$

where A and n are constants and Q_c is the activation energy for creep. The creep properties of doloma appear to be determined by the deformation behaviour of the ductile lime matrix. Stress change experiments during creep indicate that, over the stress ranges examined for these materials, the rate-determining process during creep is the recovery-controlled generation and movement of dislocations. The transition from a stress exponent, n, in the range 3 to 5 at high stress levels to a value near unity at low stresses is then associated with a rapid increase in the contribution of grain boundary sliding to the overall creep strain.

SERICITE CLAY AS A RAW MATERIAL FOR THE FABRICATION OF WHITEWARE BODIES

J. Espinosa De Los Monteros, M.A. Del Rio, R. Martinez Caceres, D. Alvarez-Estrada and V. Aleixandre

The possibility was investigated of obtaining porcelain bodies using a sericitic clay, whose fundamental characteristics are to form a very reactive glassy phase, to have an exceptional firing range and a very fine grain size, and a tendency to produce bodies with a very high mullite content at low temperature. The second aim was to obtain porcelain bodies at low firing temperatures with a high flexural strength and large mullite content using only the above-mentioned clay, alumina and a small and constant amount of feldspar. To cover different porcelain types, both silicious and alumina, eight compositions were formulated and fired between 1200°C and 1320°C and the technological properties, microstructures, phases, etc., were studied. For comparison with the results obtained with the new compositions, two industrial porcelain bodies were formulated and studied at the same time under the same conditions. The paper shows the possibility of obtaining porcelain bodies with much better properties than present industrial ones, and at the same time with a significant saving in the cost of raw materials.

INTRODUCTION OF VARIOUS GRADES OF RAW MATERIALS IN FERRITE MAGNET PRODUCTION

C.A.M. Van Den Broek

This paper gives some information concerning the present state of the technology of slurry preparation for making anisotropic hexaferrite magnets. The main conclusion is that

cheaper and less defined raw materials can be used, provided a flexible technology and the existing knowledge on raw materials and phenomena during prefireing are applied.

THE GRAIN BOUNDARY COMPOSITION OF MnZn FERRITES WITH CaO, SiO₂ and TiO₂ ADDITIONS

P.E.C. Franken, H. Van Doveren and J.A.T. Verhoeven

Short communication.

GRAIN GROWTH IN PRESSURE-SINTERED Al₂O₃ CERAMICS

Y. Ishitobi, M. Shimada, M. Koizumi and R. Hayami

Short communication.

CALCULATION OF DIFFUSION COEFFICIENTS OF MANGANESE IN DEBASED ALUMINA

J. Ranachowski and W. Włosinski

Short communication.

EFFECT OF CATION SUBSTITUTION ON THE EUTECTOID DECOMPOSITION OF CuFe₅O₈

T. Yamaguchi and H. Sutoh

Effects of cation substitution on the eutectoid decomposition of CuFe₅O₈ into CuFeO₂ and Fe₂O₃ have been studied by means of X-ray diffraction analysis and optical microscopy. It is shown that the eutectoid temperature decreased with increasing amount of cation with a more pronounced effect for Ni and Zn, and that the site preference of the cations in the host spinel phase plays no significant role on the stabilization of the spinel phase. All the cations studied retarded the rate of decomposition without changing the maximum-rate temperature in the time - temperature - transition diagram. Microscopic observations of the sintered bodies revealed that the cations are grouped into two with respect to their effect on the eutectoid structure. The obtained results have been interpreted in terms of the dilution effect of the cation substituted.

PHASE RELATIONSHIPS IN THE HAFNIA-GADOLINIA SYSTEM

P. Durán

Phase relationships in the system HfO₂-Gd₂O₃ have been studied by X-ray diffraction. The formation of the pyrochlore structure compound Gd₂Hf₂O₇ (a = 10.498 Å) was found. This compound undergoes an order-disorder transformation at very high temperature to yield a fluorite-type structure. The range of existence of the solid solutions based on HfO₂, Gd₂Hf₂O₇ and Gd₂O₃ was determined using the lattice parameter method. In the gadolinia-rich region, two hexagonal compounds have been formed. The first is formed between 57 and 60 mol% Gd₂O₃, and the second is formed between 75 and 90 mol% Gd₂O₃. Both of them decompose above 1700°C into cubic phases of the fluorite and C-type rare earth structures respectively.

ZrO₂ POWDERS PRODUCED BY VAPOR PHASE REACTION

Y. Suyama, T. Mizobe and A. Kato

The formation of ZrO₂ powders by vapor phase reaction of the system ZrCl₄-O₂ was studied with emphasis on the effects of reaction conditions on the particle size and crystal

structure of the products. The particle size of ZrO_2 powders decreased with decreasing $ZrCl_4$ concentration. The formation and stability of tetragonal ZrO_2 are closely related to its particle size, and it was found that there is a critical particle size below which the tetragonal ZrO_2 is stable thermodynamically. The vapor phase reaction gives metastable tetragonal ZrO_2 -particles besides the thermodynamically stable ones. The presence of the critical size is in favor of the surface energy mechanism for the stabilization of the tetragonal phase. The formation process of tetragonal and monoclinic ZrO_2 particles was discussed.

DENSIFICATION KINETICS OF VACUUM HOT-PRESSED SODIUM BETA-ALUMINAS

G.N. Babini, A. Bellosi and P. Vincenzini

Hot pressing of two sodium beta-alumina powders of nominal composition $Na_2O \cdot 6.9Al_2O_3$ and $Na_2O \cdot 8.5Al_2O_3$ at 1100-1600°C and 150-350 kg/cm² in inductively heated graphite dies under vacuum, proved an easy method for obtaining fully dense materials in very short pressing times. Densification rates and microstructures developed are strongly dependent on the characteristics of the starting powders. The microstructure of the materials obtained from the first powder consisted of approx. equiaxed grains of the β and β'' phases; the intermediate and final stages of densification ($\rho > 85\%$) obeyed first-order kinetics and showed stress exponents in the steady state creep equation ($\dot{\epsilon} \sim \sigma^n$) from 0.74 to 1.76. The apparent volume diffusion coefficients at 90% relative density for which n values close to unity were found, calculated on the assumption of the Nabarro-Herring diffusional creep model were of the order of $10^{-9} \text{ cm}^2/\text{sec}$. The apparent activation energy for densification was 55 kcal/mole. A duplex microstructure was observed in the materials hot-pressed from the second powder consisting of nearly equiaxed grains and strongly anisotropic elongated crystals grown perpendicularly to the hot-pressing direction. First-order densification kinetics were observed also for this powder but with much lower densification rates. The apparent activation energy for densification was 130 kcal/mole. A strong texture was observed in the materials hot-pressed from both powders with most of the c axes oriented parallel to the hot-pressing direction.

OBSERVATIONS ON SOME PLASMA-SPRAYED METAL CARBIDES

S. Basinska - Pampuch and T. Gibas

Results of a study into plasma-sprayed coatings of W and Cr-carbides are presented. The investigations comprised the assessment of phase composition, microstructure, carbon losses, hardness and scratch resistance of coatings obtained at the same spraying conditions. Of practical importance are the changes occurring in the carbides in the plasma stream, namely evaporation, melting, phase-changes, oxidation, and decomposition which bring about different microstructures and variations of the properties of the coatings. These changes have been evaluated on the basis of a detailed characterization of the starting powders and of the microstructure of the coatings.

DEVELOPMENT OF SLIP MOULDING METHODS

A.G. Dobrovolskiy

A review of the factors affecting the basic properties of ceramic slips, i.e. viscosity, settling rate, tixotropy and dilatancy, is given. The main technological features of slip casting in porous forms, electrophoretic moulding and thermoplastic slip casting are described. It is shown that the slip casting process may be used not only for manufacturing complex shaped products also for the production of special ceramics,

such as fibre reinforced materials, porous materials with oriented channel, cellular materials, multi layer ceramics, thin films, and others.

INTERFACIAL PHASES IN A METAL-TO-ALUMINUM OXIDE CERAMIC SEAL

J. Ranachowski, M. Stepniewski and W. Włosinski

The interface of metal-to-alumina ceramic seals was examined by an electron probe and by X-ray methods. The thickness of the interface was found to be 11 to 15 μm . About 75% of the interface was amorphous glassy phase and the remaining 25% was $Mn_{0.9}Fe_{0.1}Al_2O_4$ spinel. Because of the replacement of Mn^{+2} by Fe^{+2} , the lattice of the spinel was decreased from that of $MnO \cdot Al_2O_3$ ($a_0 = 8.184 \pm 0.004\text{\AA}$).

PROPERTIES OF $Al_2O_3 \cdot SiO_2$ HEAT INSULATING REFRactories

I. Stamenković, V. Simić, F. Sigulinski, P. Martinović and R. Stefanović

A short description of high-porosity brick production is given. The technology included the preparation of starting materials, forming by extrusion, firing and finishing. The investigation included physical, thermal, structural and microstructural measurements. Apparent brick density ranged from 0.6 to 1.3 g cm^{-3} , the minimum Al_2O_3 content was 34-36%. Micro and macropores distributions were determined and discussed in relation to mechanical and/or heat conductivity properties.

Vol. IV, January/December, 1978

CERAMIC SELF-SEALING COATINGS FOR HIGH-TEMPERATURE SURFACES

G. Perugini

The ceramic self-sealing coatings are described by their composition, structural and functional properties; their applications are discussed taking into account some peculiar surface characteristics. Considering the positive results obtained in some applications, it seems possible that ceramized surfaces can give several contributions (anticorrosive, anti-pollution, technological, energetic) towards solving the problems of high-temperature technology.

PHASE DIAGRAMS OF THE SYSTEMS $HfO_2 \cdot Pr_2O_3$ AND $Dy_2O_3 \cdot Pr_2O_3$

M.V. Kravchinskaya, A.K. Kuznetsov, P.A. Tikhonov and E.K. Koehler

The phase diagrams for the systems $HfO_2 \cdot Pr_2O_3$ and $Dy_2O_3 \cdot Pr_2O_3$ have been constructed in the temperature range 1000°-3000°C under vacuum. Phase relations in these systems were studied by X-ray and high-temperature thermal analyses and by electrical conductivity measurements to 2000°C. In the $HfO_2 \cdot Pr_2O_3$ system, the compound $Hf_2Pr_7O_{12}$ exists which has a pyrochlore-type structure and the lattice parameter $a = 10.662 \pm 0.004 \text{ \AA}$. The region of existence of the pyrochlore phase lies within the limits of 20 to 50 mole % Pr_2O_3 . The heterogeneous regions of existence of the fluorite cubic phase C and the pyrochlore-type phase P as well as of the cubic face-centered phase C' and the pyrochlore-type phase P extend from 20 to 30 mole % and from 38 to 50 mole % Pr_2O_3 , respectively. In the $Dy_2O_3 \cdot Pr_2O_3$ system, there are solid solutions of the A, B and C - structures of the

rare-earth oxides. The phase diagram for this system belongs to the diagram type having a temperature minimum in the liquidus and solidus curves and an eutectoid at 78 mole % Pr_2O_3 at 1780°C.

GRAIN GROWTH AND CREEP IN POLYCRYSTALLINE MAGNESIUM OXIDE FABRICATED WITH AND WITHOUT A LiF ADDITIVE

J.D. Hodge and R.S. Gordon

Grain growth and diffusional creep phenomena were studied in high purity, polycrystalline MgO which was fabricated with and without the use of a LiF additive. Small amounts of residual fluorine were believed to be responsible for enhanced rates of grain growth and diffusional creep by increasing both the magnesium lattice and magnesium grain boundary diffusivities. Diffusional creep was clearly identified in polycrystalline MgO at low stresses and small grain sizes.

THE PHASE DIAGRAM OF THE SYSTEM $\text{ZrO}_2\text{-CaO-MgO}$ BETWEEN 1200°C AND 1700°C

V. Longo and L. Poddia

Solid state phase relations in the system $\text{ZrO}_2\text{-CaO-MgO}$ were investigated at 1700°, 1600°, 1500°, 1400°, 1300° and 1200°C. The most significant equilibrium isotherms are reported and the phase diagram of the system in the 1700° to 1200°C temperature range is proposed.

VARIATION OF SOME PHYSICAL PROPERTIES WITH CALCINATION AND ANNEALING TEMPERATURE OF MAGNESIA OBTAINED BY THERMAL DECOMPOSITION OF BASIC MAGNESIUM CARBONATE

N.A.L. Mansour

The influence of calcination temperature and annealing conditions on crystallite growth, firing density and lattice constant was investigated. X-ray broadening was used to measure the crystalline size of the powdered samples. Lattice parameter was measured from the (200) peak and the bulk density was measured by mercury balance. Crystallites of magnesia obtained by calcining basic carbonate at 800°C and then by annealing at lower temperatures, break down to smaller sizes probably due to the sudden expansion of the entrapped gases in the micropores. Crystallite growth obeys the equation $D^2 - D_0^2 = 2 Kt$ with an activation energy of 66 Kcal/mole at temperatures higher than 770°C. The activation energy at lower temperatures was found to be 43.5 and 32 Kcal/mole for magnesia prepared at 500 and 800°C. Compacts of magnesia prepared at 500°C sintered to a higher density than magnesia prepared at 800°C when the annealing temperature is lower than 770°C and to a lower density above this temperature with a maximum density at 800°C annealing temperature and 2 hours annealing period. For longer periods temperatures lower than 770 and 800°C were obtained. Independent on the calcination temperature, an equilibrium lattice constant at every annealing temperature was obtained which decreases with temperature up to 770°C, then remains constant.

MICROSTRUCTURAL CHANGES DURING THE FIRING OF WALL TILE AND SANITARYWARE

V. Lach

The influence of firing temperature and soaking time on phase composition, porosity and some other microstructural parameters of porous wall tile and sintered sanitaryware was investigated by means of X-ray diffraction, mercury porosimetry, SEM, dilatometry, DTA, TG and ultrasonic thermal analyses. The results were interpreted on the basis of the so cal-

led «New Silicate Concept» developed by the Author. The influence of various parameters of the microstructure on the physical properties was investigated.

ON THE EFFECT OF CRACK GROWTH ON THE SCATTER OF STRENGTH OF BRITTLE MATERIALS

D.P.H. Hasselman and G. Ziegler

Short communication.

COMPATIBILITY RELATIONS IN THE SYSTEM $\text{Al}_2\text{O}_3\text{-P}_2\text{O}_5\text{-WO}_3$

Jelena Brun Langensiepen and F.A. Hummel

Short communication.

ON THE DEFECT STRUCTURE IN NONSTOICHIOMETRIC METAL OXIDES

S. Mrowec

A number of important physical and chemical properties of nonstoichiometric transition metal oxides are influenced by kind and concentration of defects in the crystalline lattice of these materials. Until quite recently it was thought that the relation between the nature of defects in the lattice of these oxides and their physical and chemical properties could be explained satisfactorily based on point defect theory. Today it is known that such an approach is correct only in the case of very small defect concentrations. At higher concentrations the mutual interaction between point defects results in formation of complexes and defect clusters called extended defects. These extended defects can become further ordered, which leads to superstructure ordering and to formation of intermediate phases. In some cases point defects can become eliminated in the process of crystallographic shear which is connected with formation of a whole series of intermediate phases.

MICROSTRUCTURAL AND PHYSICAL PROPERTIES OF $\text{Al}_2\text{O}_3\text{-Fe}$ CERMETS

J.T. Klomp and R.H. Lindenhovius

$\text{Al}_2\text{O}_3\text{-Fe}$ sintered compacts were prepared in order to find experimental evidence for the hypothesis that during sintering Fe evaporates and condenses on the Al_2O_3 grains increasing the probability that metal-metal contacts occurs. The electrical and thermal properties of these cermets were measured. The electrical resistivity of cermets containing up to 17.5 vol% Fe is equal to that of pure alumina. The thermal expansion characteristics show that the interfacial adherence is maintained during heating and cooling. This is attributed to the occurrence of pores or cracks in the particle interior. The thermal conductivity of cermets with an Al_2O_3 matrix is up to 6% higher than that of pure Al_2O_3 -ceramic. The experimental results give no evidence for the validity of the hypothesis.

THE INFLUENCE OF VARIATIONS IN COMPOSITION ON THE CREEP BEHAVIOUR OF DOLOMA

J.A. Coath and B. Wilshire

A study has been made of the high temperature creep behaviour of natural doloma and a wide range of synthetic CaO-MgO samples. Over the stress and temperature ranges examined, the rate-determining process during creep of these two-phase ceramics is diffusion-controlled generation and movement of dislocations, independent of variations in the magnesia content (from 25 to 75% MgO), crystal sizes (from

VC
1
19

1.5 to 11 μm) and impurity levels (i.e. SiO_2 , Al_2O_3 and Fe_2O_3 contents up to a total of 5.6 wt%). Under these conditions, whilst variations in crystal size have comparatively little effect, the creep strength can be significantly improved by decreasing the CaO/MgO ratio and by minimizing the impurity levels (particularly Fe_2O_3).

PREPARATION AND PROPERTIES OF SINTERED HYDROXYLAPATITE

J.G.J. Peelen, B.V. Rejda and K. De Groot

The preparation of a bioceramic material is described, which resembles natural bone in its chemical composition and in its porous structure. Hydroxylapatite powder with the composition $\text{Ca}_5(\text{PO}_4)_3\text{OH}$ is used as starting material. The porosity of the ceramic product is determined by the forming process (macroporosity) and by the sintering schedule (microporosity). The relationship between preparation conditions and crystallographic structure, microstructure and strength is discussed. This strong but still porous ceramic has already successfully been used in animal implantation experiments.

IR AND RAMAN STUDIES OF THE STABILIZATION OF $\beta\text{-Ca}_2\text{SiO}_4$

M. Handke and W. Ptak

Laser Raman and Fourier transform infrared spectroscopic investigations have been performed on powdered samples of $\beta\text{-Ca}_2\text{SiO}_4$ and on monocrystalline samples obtained by the Verneuil method. The polarized Raman spectra are consistent with monocrystalline behaviour in the translational modes region but a polycrystalline one in the internal and rotational modes region of SiO_4 tetrahedra. This phenomenon can be explained by an existence of domains with different orientation of SiO_4 tetrahedra between domains; the orientation of adjacent SiO_4 tetrahedra is incongruent. The domains should be small enough to prevent the formation of nuclei of the γ -phase within them and in consequence also the initiation of polymorphic transition. To make the nucleation of the γ -phase possible, the boundaries between domains must be free to move.

CERAMIC AND MAGNETIC PROPERTIES OF STRONTIUM HEXAFERRITE POWDERS PREPARED BY A FLUIDIZED BED TECHNIQUE

L. Giarda, G. Bottone, D. Candolfo, A. Cecchetti and F. Masoli

The properties of strontium hexaferrite powders prepared by a laboratory fluidized bed technique are examined in order to obtain powders suitable for plastically bonded or ceramic permanent magnets. Ceramic and magnetic parameters are analysed as a function of the reaction temperatures. A comparison is made between two sets of hexaferrite powders obtained from the oxides $\alpha\text{-FeOOH}$ and $\alpha\text{-Fe}_2\text{O}_3$.

THE EFFECT OF GROG TYPE ON THE QUALITY OF SURFACE OF SANITARY WARE MADE OF FAIENCE GROG

N.S. Belostotskaya and L. Ja Shapiro

This paper discusses the influence of grain size and grain shape of the grog composition on the quality of surface of sanitary ware casts made of faience grog. The use of fine grogs possessing spherical particles provides a better surface on both cast and finished ware while also allowing for elimination of base glazing, thereby reducing the required production time.

TEXTURE-CONDUCTIVITY RELATIONSHIPS IN POLYCRYSTALLINE LITHIA-STABILIZED β'' -ALUMINA

G.E. Youngblood and R.S. Gordon

Hot-pressed polycrystalline β'' -alumina (lithia-stabilized) possesses an (OOL) texture which is perpendicular to the pressing direction. The sodium ion resistivity, measured at 300°C in a direction parallel to the hot-pressing direction, was a factor of 1.4 to 1.8 larger than the resistivity measured in the perpendicular direction for small ($\sim 2 \mu\text{m}$) to large ($\sim 100 \mu\text{m}$) grained microstructures, respectively. The lowest resistivities (1.8 ohm-cm) and activation energies (3.1 kcal/mole) were observed perpendicular to the pressing direction for the large-grained material. The highest resistivities (6.8 ohm-cm) and activation energies (5.1 kcal/mole) were observed parallel to the pressing direction for small grain size material. An X-ray texture parameter was developed for polycrystalline β'' -alumina and related to the measured anisotropy in sodium ion conduction for hot-pressed material. Finally this relation was extended to qualitatively explain why the radial resistivity for an isostatically pressed and sintered β'' -alumina tube is typically 25% higher than the axial resistivity.

PREMETALLIZING OF HIGH ALUMINA CERAMICS

G. Visomblin and D. Tchoubar

Premetallizing with a Mo-Mn-SiO₂ mixture was studied on corundum single crystal and sintered alumina surfaces. The oxide phase formed after heat treating is described with the aid of scanning electron microscopy, X-ray diffraction and microprobe analysis. The $\text{Al}_2\text{O}_3/\text{SiO}_2$ and CaO/SiO_2 ratios in this phase were correlated with the behaviour of the manganese and the purity of the support (presence of silica and lime). Specially, if the CaO/SiO_2 ratio is higher than 0.1, undesirable crystallization of anorthite occurs at the alumina-molybdenum interface.

HYDROTHERMAL REACTIONS IN THE SYSTEMS $\text{CaCO}_3\text{-SiO}_2$ and $\text{MgCO}_3\text{-SiO}_2$

R.G. Anthony and E.R. McCartney

Hydrothermal reactions in the systems calcite-quartz and magnesite-quartz have been studied over the temperature range 200°C to 600°C and the steam pressure range 1.5 to 70 MPa. In the calcite-quartz system, a hydrothermal reaction was found to occur at temperatures in excess of 450°C to form wollastonite. In the magnesite-quartz system, at temperatures above 300°C, formation of talc was observed in all compositions studied, with some formation of serpentine evident at higher magnesite compositions. Above 450°C and at magnesite contents above 80%, talc and forsterite formed. In all cases, the reaction mechanism appears to be the displacement of CO_2 by a mobile silica species. To assess the potential utilization of these reactions in ceramic manufacture, a series of samples was made from carefully graded mixtures and their compressive strengths were measured. Mixtures of calcite and quartz developed a maximum strength of 18 ± 2 MPa at 300°C. In the magnesite-quartz system, the strength was found to increase from 11 ± 2 MPa at 200°C to 31 ± 2 MPa at 300°C and 30 ± 2 MPa at 500°C. The strength rose with time of treatment in each case, reaching a maximum at about forty hours, after which no further increase in strength with time was evident.

LEAD TITANATE ZIRCONATE-BASED PYROELECTRIC CERAMICS

B. Hardiman, K.V. Kiehl, C.P. Reeves and R.R. Zeyfang

Ceramics with a base composition $\text{PbTi}_x\text{Zr}_{1-x}\text{O}_3$ ($x = 0.07$) and modified materials by additions of Nb_2O_5 , Fe_2O_3 and

U_3O_8 in ≤ 1 wt. % concentration were pressure sintered to near theoretical densities. The effect of these additives on the microstructure and on the dielectric properties are reported and discussed in terms of the A- and O-position vacancy model in the ABO_3 perovskite lattice. The pyroelectric properties are also affected by the characteristics of the $\text{F}(\text{R}_{\text{LT}})-\text{F}(\text{R}_{\text{HT}})$ phase transition.

THE SIGNIFICANCE OF NON-ELASTIC DEFORMATION IN THE FRACTURE OF HETEROGENEOUS CERAMIC MATERIALS

G.A. Gogotsi, Ya. L. Groushevsky and K.K. Strelov

The classification of refractory ceramic materials is considered according to the magnitude of their brittleness i.e. the ratio of the specific elastic energy stored in the specimen at the moment of fracture, to the total amount of deformation energy of the specimen prior to its fracture. The materials are classified as brittle ($\chi = 1$) and relatively brittle ($\chi < 1$). Deformation peculiarities of these materials are analysed and distinctive features of their mechanical behaviour are pointed out. It is shown that macronelastisity of relatively brittle materials is caused by microfractures. It is proved that these features must be taken into consideration when developing design criteria for these materials. The known thermal shock resistance criteria are considered and a new criterion is proposed in which brittleness is introduced as a parameter. The validity of the approach is confirmed by results of tests of single-phase and composite ceramic materials based on aluminium oxide, yttrium oxide, zirconium dioxide, and titanium carbide.

THE USE OF CUBIC SHAPED SAWDUST IN HEAVY CLAY PRODUCTS

M.J. Murray and R.M. Liversidge

The effect of the addition of sawdust on the properties of extruded heavy clay bodies before and after firing is described. It was found that sawdust particles of cubic shape, produced by swage-set band saws, could be added in greater quantities and had less adverse effect on the physical properties than the elongated particles produced by spring-set circular saws.

VOLTAMMETRIC TECHNIQUES IN CERAMIC ANALYSIS. THE STATUS OF THE ART

P.L. Buldini

A comprehensive bibliography covering the period from 1922 to 1977 deals with the determination of Al, As, Au, B, Ba, Bi, Ca, Cd, Co, Cr, Cu, Fe(II), Fe(III), In, K, Li, Mg, Mn, Mo, Na, Nb, Ni, Pb, S, Sb, Se, Si, Sn, Ti, Tl, U, V, Zn, Zr in ceramics and related materials. Several voltammetric techniques are compared. Different methods for sample dissolution are suitable for voltammetric analysis. Advantages and limitations of ceramics analysis by means of voltammetric techniques are discussed.

FIGURES-OF-MERIT FOR THE THERMAL STRESS RESISTANCE OF HIGH-TEMPERATURE BRITTLE MATERIALS: A REVIEW

D.P.H. Hasselman

A review is presented of the selection rules for brittle structural ceramics subjected to severe thermal stress. A total of twenty-two figures-of-merit are presented for a total of twenty-nine different heat transfer environments and/or criteria of thermal stress resistance, involving steady-state or transient heat transfer, internal heat generation, thermal

buckling as well as thermal fatigue and unstable crack propagation.

SINTERING CHARACTERISTICS OF PORCELAIN

E.M.H. Sallam and A.C.D. Chaklader

Sintering experiments in the temperature range 1050° to 1300°C using a eutectic glass (as present in a triaxial porcelain) and several constituents in porcelain compositions indicate that shrinkage behaviour of porcelain is primarily controlled by the reaction between glass (or felspar) and clay components. An equation to predict the relationship between the relative density change and shrinkage has been developed, which is based on the liquid phase formation on particles and migration of liquid from the neck regions to the void space. The predicted relationship $\Delta L/L_0 = 4\pi/9\beta (1/\rho_0 - 1/\rho)$ (where β is a geometric constant and calculable) fitted the data well. The mechanism of densification appears to change with temperature - initially controlled by reaction then followed by precipitation. The calculated apparent activation energy during the second stage (~ 60 Kcal/mole) is about half of that obtained by previous workers.

HIGH TEMPERATURE OXIDATION OF DISILICIDES IN THE SYSTEM MoSi_2 - TiSi_2

J. Schlichting

The oxidation behaviour of silicon ceramics e.g. MoSi_2 at temperatures up to 1600°C is due to the formation and stability of glassy SiO_2 -surface layers. The oxidation behaviour of two-component silicides is a function of crystallization and segregation phenomena in the oxidic surface layer. Small amounts of titanium in the SiO_2 -layer lead to devitrification of the glass resulting in low O_2 -transport. But with high Ti content in the MoSi_2 different oxides (TiO_2 and SiO_2) are formed isolated and therefore the oxidation rate increases rapidly.

EFFECT OF CdO ADDITIVE ON SINTERING OF LiNbO_3

S. Shimada, K. Kodaira, T. Matsushita, K. Ichijo and R. Maeda

The effect of CdO additives on the sintering of LiNbO_3 at 805-1100°C was studied and is discussed on the basis of Kingery's model of initial sintering and cubic grain growth kinetics. The sintering appears to be controlled by the volume diffusion of oxygen ion in both cases. Exaggerated grain growth in pure LiNbO_3 occurs at 1050-1100°C and hinders the attainment of sintered densities higher than 83-87%. Addition of CdO increases the diffusion coefficient of oxygen by about 500 times during initial sintering and causes rapid densification. DTA curves indicated a reaction between CdO and LiNbO_3 at 750-895°C; the second phase thus formed probably hinders exaggerated grain growth.

HIGH QUALITY CHROME-BEARING BASIC REFRactories FROM BRINE MAGNESIA

E.A. El-Rafei

Pure magnesia (>96% MgO) was recovered from marine brine of high MgCl_2 content using calcined dolomitic magnesite as alkali precipitating agent. High quality chrome-bearing refractories were obtained from clinkers produced by joint fine grinding and firing at 1550°C of the dried $\text{Mg}(\text{OH})_2$ paste with different amounts (10, 20, 35 wt. %) of common chrome ore and chemically enriched ore. The technical characteristics of the basic refractories were improved as the chrome content is increased up to 20% com-

VO
1
19

mon ore and 35% chemically enriched ore. On substituting the common ore by the chemically enriched one the properties of the refractories were remarkably improved due to lower silicate level (about 2%) and higher chrome spinellide content. The properties of the basic refractories were correlated with their different constituent phases.

LATTICE PARAMETERS OF CUBIC SOLID SOLUTIONS IN THE SYSTEMS uR_2O_3 -(1-u)MO

V.B. Glushkova, F. Hanic and L.V. Sazonova

Short communication.

Vol. V, January/December, 1979

MAGNETIC PROPERTIES OF AI, Ga, Sc, In SUBSTITUTED BARIUM FERRITES: A COMPARATIVE ANALYSIS

G. Albanese and A. Deriu

A comparative analysis of the magnetic properties of $BaFe_{12-x}Me_xO_{19}$ ($Me = Al, Ga, Sc, In$) ferrites is given. The influence of the substitution of iron ions on the magnetic ordering and on the magnetic properties is pointed out. The reported data indicate that the occupation by non magnetic ions of lattice sites inside the R-block leads to peculiar helical spin structures. Further confirmation of the relevant contribution of iron ions in the 12 K sublattice to the single ion uniaxial anisotropy has been obtained.

THE SOLID SOLUBILITY OF Sc_2O_3 , Al_2O_3 , Cr_2O_3 , SiO_2 and ZrO_2 in MgO

A.F. Henriksen and W.D. Kingery

Scanning electron microscopy and X-ray diffraction lattice parameter measurements have been used to determine the extent of solid solubility of oxides in MgO . The solubility of Sc_2O_3 ranges between 0.005 and 0.044 mole fraction in the temperature interval from 1270°C to 1600°C, with an experimental heat of solution equalling 36.8 kcal/mole. Cr_2O_3 has a similar solubility range, between 0.007 and 0.038 mole fraction in the temperature interval from 1200°C to 1600°C, and the heat of solution was determined to be 43.6 kcal/mole. Much smaller solubility was found for Al_2O_3 , between 0.0004 and 0.007 mole fraction in the temperature interval from 1200°C to 1600°C, and the heat of solution was 97.2 kcal/mole. The solubility of SiO_2 is less than 0.00034 mole fraction at 1850°C and the solubility of ZrO_2 is less than 0.000075 mole fraction at 1885°C.

SURFACE TENSION AND DENSITY OF MOLTEN GLASSES IN THE SYSTEM La_2O_3 - $Na_2Si_2O_5$

A. Passerone, R. Sangiorgi and G. Valbusa

Surface tension, density, and volatility of sodium disilicate, modified by additions of 1%, 5%, 10%, mole La_2O_3 , have been evaluated at temperatures varying from 900 to 1500°C, under highly reducing conditions. These results and related data (such as activation energy of evaporation reaction; thermal expansivity; temperature coefficient of surface tension; nonideal behaviour; surface adsorption) have made possible interpretation of the role played by lanthanum in modifying the properties of the base glass.

ELECTRICAL CONDUCTIVITY OF POLYCRYSTALLINE $3Y_2O_3$ • WO_3 AT HIGH TEMPERATURES

K. Kuribayashi and T. Sata

The electrical conductivity of polycrystalline Y_6WO_{12} ($3Y_2O_3$ • WO_3) and of polycrystalline Y_6WO_{12} doped with alkaline earth oxides or ZrO_2 were measured over the temperature range from 800 to 1400°C under oxygen partial pressures of 10^{-5} to 10^0 atmospheres. Y_6WO_{12} showed a p-type conductivity at higher oxygen pressures and an n-type conductivity at lower oxygen pressures. Additions of alkaline earth oxides increased the conductivity of Y_6WO_{12} in the higher oxygen pressure region. The conductivity of alkaline earth oxides-doped Y_6WO_{12} decreased monotonically with decreasing oxygen partial pressures and approached constant values at lower oxygen partial pressures. The ZrO_2 addition caused a decrease in the conductivity of Y_6WO_{12} in the higher oxygen pressure region. The variations of the conductivity with oxygen pressure are discussed assuming various defects models.

THE CORROSION RESISTANCE OF STRONTIUM ZIRCONATE CERAMICS TO COAL ASH CONSTITUENTS AND POTASSIUM SEED OF MHD-GENERATORS

M. Zborowska, M. Grylicki and J. Zborowski

The resistance of dense strontium zirconate ceramics to corrosion by Al_2O_3 , CaO , MgO , SiO_2 and K_2CO_3 as well as coal ash was investigated by the «crucible method» for 2 hrs at 1700°C. The corrosion process was investigated by optical polarizing microscopy, X-ray microanalysis and scanning electron microscopy. The results showed that strontium zirconate ceramics have excellent corrosion resistance against K_2CO_3 . No corrosion effect by Al_2O_3 , CaO and MgO was observed as well. Considerable corrosion occurred when silica was used which formed a baddeleite dispersed phase in a glassy matrix of a variable composition. A similar effect was observed in crucibles corroded by coal ash containing silica.

KINETICS AND MECHANISM OF THE SOLID-STATE HIGH-TEMPERATURE TRANSFORMATION OF ANDALUSITE (Al_2SiO_5) INTO 3/2-MULLITE ($3Al_2O_3$ • $2SiO_2$) AND SILICA (SiO_2)

H. Schneider and A. Majdić

The kinetics of the high-temperature transformation of andalusite ($<40\mu m$) were investigated by means of X-ray techniques. The transformation interval was determined to lie between about 1250 and 1500°C. The best fitting of the kinetic data was achieved with an exponential law of the type: $1-\alpha = \exp(-kt + ct/(t+1))$. The kinetic curves are associated with a topotactic transformation mode with preservation of the aluminium-oxygen octahedral chains and diffusion of aluminium, silicon and oxygen atoms. Below 1380°C, mullite ($+SiO_2$) formation is essentially restricted to an initial rapid period of the transformation, because nucleation and product growth occur only at energetically favored lattice sites (e.g. grain boundaries). Above 1380°C, mullite and SiO_2 nucleation and growth may take place throughout the volume of the low-temperature phase (andalusite) over the whole range investigated.

KINETICS AND MECHANISM OF THE REACTION BETWEEN SODIUM CARBONATE AND SILICA

W. Richard Ott

The kinetics and mechanism of the reaction between sodium carbonate and silica were studied using thermogravimetric analysis to monitor the percent reaction versus time. A

modified form of the rate constant in the Ginstling and Brounstein model has been shown to describe the sodium carbonate - silica reaction of dried samples. This equation is:

$$(a) K = 1 - 2x/3 - (1-x)^{2/3}$$

$$2DC_a \left(1 - R_n k_1 \left[\frac{M+Q}{2M} + \frac{1}{2} \right]^{1/3} - 1 \right)$$

were $K = \frac{2DC_a}{k_2 R_n^{2/3} \text{SiO}_2}$

t is the time, D is the diffusion coefficient of the rate controlling species, C_a is the concentration gradient, k_1 and k_2 are constants, R_n is the sodium carbonate particle size, $R_n^{2/3}$ is the silica particle size, and M and Q are the total volumes of the sodium carbonate and silica, respectively. Surface diffusion was shown to cover all silica particles rapidly and supply Na^+ and O^- ions to the reaction interface. The activation energy of the process was found to be 30 k - cal/mole. The presence of water vapor caused the diffusion rate to increase rapidly and the rate controlling step became chemical processes which occurred at the phase boundary. This process was determined to have an activation energy of 35 k - cal/mole.

SYNTHESIS OF MULLITE BY A FREEZE-DRY PROCESS

T.A. Wheat, E.M.H. Sallam and A.C.D. Chaklader

A freeze-drying technique has been developed to synthesize fine-grained stoichiometric mullite ($3\text{Al}_2\text{O}_3 \cdot 2\text{SiO}_2$) by doping a silica sol with an appropriate quantity of a one molar $\text{Al}_2(\text{SO}_4)_3$ solution followed by spray freezing in liquid N_2 and freeze drying the mixture. The freeze-dried powder when calcined at 1400°C produced a single-phase stoichiometric mullite as determined by X-ray diffraction. The final product was very friable and could be easily broken down to a mean particle size of $\sim 7 \mu\text{m}$ (equivalent spherical diameter).

EFFECT OF CALCINATION TEMPERATURE ON LATTICE DEFECTS IN IMPURE MAGNESIUM OXIDE

S.A. Abdel-Hady, N.A. Ahmed, A.R. El-Dib and M.S. Farag

The crystallite size and the strain of powdered MgO prepared by decomposing magnesium carbonate in the range 600 - 1300°C were measured in [100] and [111] crystallographic directions by analyzing the X-ray line broadening. The Warren and Averbach multiple order method was used. The results showed that the crystallite size and the strain are anisotropic. The lattice parameter was calculated from the centre of gravity of the $k_{\alpha 1}$ line profile of all planes using Wagner's extrapolation method. The changes in the density of the powdered samples and the changes in the unit cell constant showed that the Schottky defects are probably present at low firing temperatures and there are adsorbed contaminant agents on the primary surfaces of the crystallites. The impurities affected the properties of the polycrystalline material. Their effects were very evident in the magnetic susceptibility values, in the sudden increase of the crystallite size above 1000°C and in the high value of the strain at that temperature.

OBSERVATIONS ON THE GRAIN-BOUNDARY OF Al_2O_3 BICRYSTALS

O. Maruyama and W. Komatsu

The grain-boundary thickness of alumina bicrystals, fabricated without the aid of sintering additives and pressure, was measured with an optical microscope. The thickness was 500 to 550 \AA and independent of the tilt angle. Impurities segregated at the grain-boundary and the surface of the same sample was studied with an ion microanalyser. The segregation of Ca and Si at both interfaces was

noticeable but that of Mg was not. The thickness of the segregation region for both interfaces was 600 to 800 \AA . The spheroidization of tubular voids into pores at the grain-boundary was controlled by surface diffusion. Discussion of the fabrication process of the bicrystal in terms of initial sintering kinetics concluded that the process was controlled by the surface diffusion.

EFFECTS OF STRAIN ENERGY ON PRECIPITATE MORPHOLOGY IN MgO

A.F. Henriksen and W.D. Kingery

Differences between the morphology of MgFe_2O_4 precipitates, which form octahedra with {111} habit planes and grow into dendritic forms propagating along $<100>$; MgCr_2O_4 and MgAl_2O_4 , which assume plate-like morphology with a {100} habit plane; and Sc_2O_3 , which precipitates as randomly oriented platelets, are discussed in terms of the differences in strain energy associated with exsolution of the phases in MgO . The strain energy effects, which occur both during nucleation and subsequent growth, provide a rational explanation of the observed behavior.

FABRICATION OF STABILIZED ZrO_2 BY HOT PETROLEUM DRYING METHOD

Su-Il Pyun

A series of MgO - and CaO - partially and fully-stabilized ZrO_2 bodies were produced from sulfate and acetate powders using a wet chemical drying method («hot petroleum drying method»). The optimum sintering conditions for powders produced from sulfates and acetates were found: calcining at 1200°C for 2-5 h, followed by sintering for 5 h at 1600°C . This drying process proved to be a very effective method for preparing stabilized ZrO_2 without conventional ceramic process of mixing, milling, and granulating.

HOT PRESSING OF LITHIA-STABILIZED β'' -ALUMINA

A.V. Virkar, T.D. Ketcham and R.S. Gordon

Fine-grained ($<5 \mu\text{m}$), dense (3.26 - 3.27 g/cm^3), and strong ($>200 \text{ MN/m}^2$) polycrystalline β'' -alumina (lithia-stabilized) ceramics can be fabricated by vacuum hot-pressing at temperatures $\geq 1330^\circ\text{C}$ and pressures between 28 and 41 MN/m^2 . By suitable low temperature annealing ($<1400^\circ\text{C}$), a fine-grained, high strength β'' -alumina body can be fabricated with a low resistance ($<5 \text{ ohm-cm}$ at 300°C) to sodium ion conduction. The relatively high sodium ion resistivities (6-11 ohm-cm) obtained directly after hot-pressing are caused by an incomplete phase conversion to β'' -alumina during densification and not to a small grain size. Low temperature annealing can promote phase conversion and yet prevent any significant grain growth. The high strength ceramics produced by hot-pressing can serve as the standard to be achieved in conventional sintering.

TRANSPARENT HOT-PRESSED ALUMINA I: HOT PRESSING OF ALUMINA

J.G.J. Peelen

The densification of alumina to nearly full density by continuous hot pressing is described. The influence of the atmosphere on hot pressing is discussed as well as the influence of the process parameters temperature, pressure and transit rate. The microstructure of hot-pressed alumina is examined and compared with that of normally sintered alumina. X-ray diffraction is applied to investigate a possible

crystallographic texture of the grains in hot-pressed alumina. The optical properties of the material are treated in a second paper.

MECHANISMS OF HOT PRESSING OF MAGNESIUM OXIDE POWDERS

R. Pampuch

Estimation of the rate controlling mechanisms of mass transport during the initial, intermediate and a portion of the final stage of hot pressing of powder compacts by an adequate application of the theory of creep of non-porous polycrystals at elevated temperature is first discussed and their significance for understanding of the relations between powder characteristics and their densification during hot pressing stressed. Review of recent developments of the creep theory indicates that if intraparticle (intracrystallite) i.e. dislocation mechanisms are acting to a negligible extent only, the steady-state strain rate $\dot{\epsilon}_s$ should be controlled entirely either by boundary reactions (emission/absorption of point defects at sources and sinks, e.g. at boundary line-defects) or by diffusion between sources and sinks (Nabarro-Herring and/or Coble creep). An analysis has been made in these terms of $\dot{\epsilon}$ observed with well characterised MgO powders, having a rather uniform crystallite size, during hot pressing at 775-975K under loads of $P_A = 60-295$ MPa. Two types of powders, obtained by thermal decomposition of $Mg(OH)_2$ at different temperatures, have been studied, namely i. powders constituted by well-annealed fine crystallites ($d = 28-56$ nm) showing no lattice microstrains, and ii. powders constituted by fine crystallites (25-45 nm) showing appreciable microstrains of the lattice and, consequently, a high density of the line defects. Experimental determination of the stress sensitivity, n , particle sensitivity, m , and true activation energy for creep, Q_{c_1} , has shown that the data correspond very closely to $\dot{\epsilon}_s \propto P_A^{2/d}$ in the first, and to $\dot{\epsilon}_s \propto P_A^{1/d}$ in the second case, respectively. The first situation is expected for strain rates controlled by boundary reactions while the second for the ones controlled by Coble creep, respectively. The different rate-controlling mechanisms enable to explain rationally the different densifications obtained under comparable conditions of hot pressing with the two types of MgO powders.

SUBMICRON TiO_2 - ZrO_2 POWDERS PRODUCED BY VAPOUR PHASE REACTION OF $TiCl_4$ - $ZrCl_4$ - O_2 SYSTEM

Y. Suyama, M. Tanaka and A. Kato

Submicron TiO_2 - ZrO_2 powders were prepared by the vapor phase reaction of the $TiCl_4$ - $ZrCl_4$ - O_2 system. The phases appeared were TiO_2 ss, ZrO_2 ss and $ZrTiO_4$ ss. The major crystal forms of TiO_2 and ZrO_2 were rutile and tetragonal system, respectively. Pure TiO_2 was predominantly anatase and consisted of single crystalline particles with square and plate-like shape. As $ZrCl_4$ concentration increased, the particle size decreased, the content and lattice constants of rutile increased and particles became polycrystalline. The compound $ZrTiO_4$ was formed most abundantly as the ratio $ZrCl_4/TiCl_4$ approached 1 and the effective reaction temperature was raised. It was found that $TiCl_4$ accelerates the oxidation of $ZrCl_4$ and $ZrCl_4$ retards that of $TiCl_4$ in the vapor phase reaction of the $TiCl_4$ - $ZrCl_4$ - O_2 system. It was concluded that the formation process of TiO_2 - ZrO_2 particles consists of the preferential nucleation of TiO_2 and the growth by codeposition of TiO_2 and ZrO_2 .

GRAIN GROWTH DURING SINTERING OF ALUMINA SUBSTRATES

A. Bellosi and P. Vincenzini

Short communication.

DEVELOPMENT OF POROUS SINTERED-CERAMIC SEPARATORS FOR APPLICATION IN A Li-Al/LiCl-KCl/FeS BATTERY

G. Bandyopadhyay, J.T. Dusek and T.M. Galvin

The procedure for fabrication of porous sintered-ceramic separators and the technical feasibility of using such separators in Li-Al/molten LiCl-KCl/FeS battery cells have been investigated. Processing techniques have been developed to fabricate ~1.5-2.5 mm thick, ~35-60% porous, flat, sintered Y_2O_3 and MgO separator plates with sufficient strength to allow handling prior to and during cell assembly. These separators performed successfully in laboratory-scale cells for up to ~2000 h and 283 cycles, indicating that the concept of a sintered separator, is viable for Li-Al/FeS batteries. The particularly attractive features of these separators are potentially low cost, prefabricated form that allows easy cell assembly, and small pore size (average diameter 0.5-1.0 μm) which provides good particle retention. The test results from the sintered-separator cells indicate that Y_2O_3 is probably unsuitable for long-term performance in Li-Al/FeS cells because of its reaction with the positive active material. This is in agreement with the recently reported data on cells with Y_2O_3 felt and powder separators. Sintered MgO separators, however, showed good chemical and mechanical stability in the cell environment.

PHASE EQUILIBRIA IN THE Si, Al, Be/C, N SYSTEM

G. Schneider, L.J. Gauckler and G. Petzow

Phase equilibria studies in parts of the system Si, Al, Be/C, N were carried out at 1760 and 1860°C. In the carbide system Al_4C_3 - SiC - Be_2C seven new compounds were found and characterized by their chemical composition and crystal symmetry. In the nitride system AlN - Si_3N_4 - Be_3N_2 a solid solution between AlN and $BeSiN_2$ was found to exist besides the already known compounds. The carbonitride system showed solid solution between α - Al_2SiC_4 and α - Al_5C_3N . Furthermore the compound AlN - SiC - Al_2C_3 was found to exist.

CONTRIBUTION TO THE SYSTEM EUROPiUM-BORON-CARBON

K.A. Schwetz, M. Hoerle and J. Bauer

By means of chemical preparation techniques and x-ray analysis the ternary system Eu-B-C was studied, with special emphasis on the technologically important sections EuB_6 -C and EuB_6 -B₂C. It was possible to prove the existence of a hexaboride-carbon solid solution $EuB_{6-x}C_x$ ($0 \leq x \leq 0.25$), a ternary phase EuB_2C_2 , the europium carbides EuC_x (Eu_2C), EuC_2 , as well as another carbide of the approximate composition Eu_2C_3 .

POST-SINTERING OF REACTION-BONDED SILICON NITRIDE

A. Giachello and P. Popper

Reaction-bonded silicon nitride, RBSN, may be used as the starting material for a post-densification process carried out at about 1800°C in nitrogen at atmospheric pressure. The sintering aids used are similar to those employed in hot pressing and pressureless sintering (e.g. MgO , Y_2O_3). They may be added to the silicon powder before nitridation or, in the case of MgO , by diffusing the vapour into preformed RBSN. High densities (98.5% theoretical) have been achieved accompanied by a shrinkage of only 6.2%. The strength at R.T. was about 1000 MN/m²; the strength at H.T. depends on devitrification. The process thus offers complex components to be formed by injection moulding, with strength values after sintering similar to those of hot-pressed silicon nitride.

TRANSPARENT HOT-PRESSED ALUMINA II: TRANSPARENT VERSUS TRANSLUCENT ALUMINA

J.G.J. Peelen

The optical properties of very dense hot-pressed alumina are compared with those of normally sintered alumina with equal pore volume. The influence of the pore size on the in-line and diffuse transmission of light through these materials is considered. The concept of transparency and translucency is critically discussed and it is demonstrated that alumina powder can be hot pressed to form a really transparent material. Relations between the degree of translucency and the microstructure and the preparation conditions of dense alumina are given.

EFFECT OF TITANATE ADDITIONS ON SINTERING TEMPERATURE OF Al_2O_3

G. Wroblewska

The effect of small additions of magnesium titanate, calcium titanate, strontium titanate, and barium titanate on the sintering temperature of aluminum oxide was investigated. The dependence of linear shrinkage and density on sintering temperature and dopant concentration and type was studied. X-ray analysis, microscopic examination, and electron microprobe analysis indicate that sintering occurred through a liquid phase and that Ti^{4+} diffused into the Al_2O_3 grains. When CaTiO_3 , SrTiO_3 , and BaTiO_3 were added, the compounds $3\text{CaO}\cdot\text{Al}_2\text{O}_3$, $\text{SrO}\cdot 6\text{Al}_2\text{O}_3$, and $\text{BaO}\cdot 6\text{Al}_2\text{O}_3$ were formed. The sintering temperature was reduced to 1500°C by adding less than 2 mol% of magnesium, calcium, strontium, or barium titanate.

ON THE FRACTURE STRENGTH OF TAPE-CASTED ALUMINA SUBSTRATES

C. Fiori, G. Fusaroli, A. Krajewski and P. Vincenzini

Short communication.

EFFECT OF DATA SCATTER ON APPARENT THERMAL STRESS FAILURE MODE OF BRITTLE CERAMICS

G. Ziegler and D.P.H. Hasselman

Short communication.

GRAIN BOUNDARY SEGREGATION OF IRON IN POLYCRYSTALLINE MAGNESIUM OXIDE OBSERVED BY STEM

T. Mitamura, E.L. Hall, W.D. Kingery and J.B. Vandersande

Utilizing X-ray microanalysis in samples studied with scanning transmission electron microscopy, substantial grain boundary segregation of Fe is found in grain boundaries in polycrystalline MgO . Samples studied contained between 540 and 5400 cation ppm Fe. Grain boundary segregation in the region within 200 \AA of the boundary was found in all cases, with the amount of segregation increasing with increasing Fe content. Samples slow-cooled from 1500°C showed an increased amount of segregation attributed to continued diffusion during cooling. Samples quenched from 1100°C showed greater segregation than those quenched from 1500°C , consistent with space charge theory. In some samples precipitates were observed which are correlated with a low-temperature phase diagram for the solidus in the iron oxide-magnesium oxide system. In addition to Fe, grain boundary segregation of Ca and Si impurities in the samples was also observed.

CHARACTERIZATION OF METASTABLE TETRAGONAL HAFNIA

O. Hunter, Jr., R.W. Scheidecker and Setsuo Tojo

Conditions for retaining metastable tetragonal HfO_2 at room temperature were determined. Mechanical properties were measured as a function both of the fraction of retained metastable HfO_2 and of the porosity. The metastable phase was retained by 1) thermal decomposition of pure $\text{Hf}(\text{OH})_4$ or HfOCl_2 and 2) hot pressing of $\text{HfO}_2 + 1\%$ Er_2O_3 . The critical size for retaining pure tetragonal HfO_2 at room temperature in a stress free condition in 100 \AA , whereas the critical size for the 1% Er_2O_3 hot pressed composition is significantly larger. The elastic moduli were found to vary linearly with porosity and showed a small effect due to the metastable phase presence.

PREPARATION AND PROPERTIES OF NEW OXYGEN ION CONDUCTORS FOR USE AT LOW TEMPERATURES

K. Keizer, M.J. Verkerk and A.J. Burggraaf

Two new systems, $\text{Bi}_2\text{O}_3\text{-Er}_2\text{O}_3$ and $\text{ZrO}_2\text{-Y}_2\text{O}_3$ ($\text{CaO}\text{-Bi}_2\text{O}_3$), were investigated. The first system has a homogeneous cubic, fluorite phase between 17.5 and 45.5 mol% Er_2O_3 and can be sintered to densities near 95% at 1200 K . At temperatures between 700 K and 1000 K the highest value of the a.c. oxygen ion conduction in this system is twice as much as the highest value found in the literature. In the second system concentrations of 1-3 mol% Bi_2O_3 act as an excellent sintering aid for $\text{ZrO}_2\text{-Y}_2\text{O}_3$ and $\text{ZrO}_2\text{-CaO}$ samples which can be sintered to densities higher than 95% at temperatures of 1350 K . During this procedure a liquid $\text{ZrO}_2\text{-Bi}_2\text{O}_3$ phase exists from which Bi_2O_3 partly evaporates with increasing sintering time. The oxygen ion conduction is little affected by the Bi_2O_3 -rich second phase. The influence of annealing procedures up to 1570 K on the conduction in the $\text{ZrO}_2\text{-Y}_2\text{O}_3\text{-Bi}_2\text{O}_3$ system is small despite weight losses up to 4%.

CHARACTERISTICS AND SINTERING BEHAVIOUR OF ZIRCONIA ULTRAFINE POWDERS

K. Haberko

Coprecipitation from water solution of chlorides was used to obtain yttria-stabilized zirconia powders. It was shown that precalcination processing of the coprecipitated gel greatly affects the microstructure of the resultant powder as well as its cold compaction behaviour and hence its sinterability. Relative densities of +98% theoretical have been achieved at sintering temperature as low as 1300°C .

SELF-DIFFUSION IN ALPHA AND BETA SILICON CARBIDE

J.D. Hong, M.H. Hon and R.F. Davis

The self-diffusion coefficients of ^{14}C and ^{30}Si have been measured for lattice transport in high purity and N-doped $\alpha\text{-SiC}$ single crystals and in high purity polycrystalline CVD $\beta\text{-SiC}$ in the temperature range of $2123\text{-}2573\text{ K}$. Grain boundary diffusion of ^{14}C has also been determined in the $\beta\text{-SiC}$ material. The results of these studies reveal a vacancy mechanism wherein ^{14}C diffuses considerably faster than ^{30}Si in both materials. Furthermore, D_c in the N-doped single crystals is smaller than for the undoped materials, while the opposite is true for the ^{30}Si transport in these crystals. Changes in the concentration of the charged C and Si vacancies are reasoned to be the underlying cause of this last phenomena. A discussion of the effect of Si evaporation and its effect upon the value of the diffusion coefficient is also presented.

VO
1
19

THE CORROSION OF TIN OXIDE SEMICONDUCTING GLAZES

G. Bagnasco, P. Pernice and P. Giordano Orsini

An $\text{SnO}_2\text{-Sb}_2\text{O}_5$ glaze, which seems the most promising among semiconducting porcelain glazes for high voltage applications, has been operated as electrode in Na_2SO_4 solution, to study under controlled conditions its corrosion behaviour. The morphology of the corrosion has been observed by microscopy. Metallic tin produced by electrochemical reduction has been identified by X-ray diffraction.

YOUNG'S MODULUS-POROSITY RELATIONSHIP FOR ALUMINA SUBSTRATES

G. De Portu and P. Vincenzini

Short communication.

SOME OBSERVATIONS ON OPACIFICATION IN K_2O -CONTAINING BOROSILICATE GLASSES

H. Takashima

Short communication.

Vol. VI, January/December, 1980

HIGH TEMPERATURE STRUCTURAL CERAMIC MATERIALS MANUFACTURED BY THE CNTD PROCESS

J.J. Stiglich, Jr., D.G. Bhat and R.A. Holz

Controlled Nucleation Thermochemical Deposition (CNTD) has emerged from classical chemical deposition (CVD) technology. This paper describes the techniques of thermochemical grain refinement. The effects of such refinement on mechanical properties of materials at room temperature and at elevated temperatures are outlined. Emphasis is given to high temperature structural ceramic materials such as SiC , Si_3N_4 , AlN , and TiB_2 and ZrB_2 . An example of grain refinement accompanied by improvements in mechanical properties is SiC . Grain sizes of 500 to 1000 Å have been observed in CNTD SiC with room temperature MOR of 1380 to 2070 MPa (4 pt bending) and MOR of 3450 to 4140 MPa (4 pt bending) at 1350°C . Various applications of these materials to the solution of high temperature structural problems are described.

DEFORMATION MECHANISM MAPS FOR APPLICATIONS AT HIGH TEMPERATURES

Terence G. Langdon

Deformation mechanism maps provide a very simple and convenient method of displaying mechanical properties data at high temperatures. Several different types of maps are available, and these are discussed with reference to polycrystalline Al_2O_3 and MgO . Ambipolar diffusion is important in ceramic materials, and this leads to four different types of diffusion creep which may be illustrated directly on the deformation mechanism maps. In practice, the accuracy of the maps depends on the purity level, and this is demonstrated by comparing maps for nominally pure Al_2O_3 and Al_2O_3 doped with MgO above the solubility limit.

FRACTURE MECHANICS STUDY OF A TRANSFORMATION TOUGHENED ZIRCONIA ALLOY IN THE CaO-ZrO_2 SYSTEM

R.C. Garvie, R.H.J. Hannink and C. Urbani

The flexural strength, elastic modulus, fracture toughness (K_{Ic}) and grain size were determined for a partially stabilized calcia-zirconia alloy (Ca-PSZ) which was progressively aged at 1300°C . Data for the same properties were obtained also for a fully stabilized cubic magnesia-zirconia alloy (Mg-CSZ) which was used as a reference material. The growth of the zirconia precipitate phase in the Ca-PSZ material was monitored. The flexural strength and fracture toughness increased smoothly to peak values of 645 MPa and 9.6 MPa $\text{m}^{1/2}$, respectively, at a critical value of the ageing time and thereafter declined rapidly. The precipitate phase coarsened during ageing. Its structure was tetragonal up until the critical ageing time and thereafter the majority of the particles transformed to monoclinic. The peak strength increased three times relative to the cubic stabilized material. The grain size and elastic modulus showed only a slight dependence on ageing time. The study confirmed the hypothesis that the enhanced strength of transformation toughened zirconia alloys arises from an increase in the fracture energy. This increase is brought about by the presence of tetragonal particles, metastable at room temperature, which can be transformed by stress.

EFFECT OF POROSITY ON THE THERMAL SHOCK BEHAVIOUR OF REACTION-SINTERED SILICON NITRIDE

G. Ziegler and J. Heinrich

Reaction-sintered silicon nitride was investigated to determine the effect of its pore size on thermal stress resistance to fracture initiation. Samples of controlled pore structure were prepared by using an organic component to incorporate pores in the green silicon compact as well as by using silicon starting powders with different particle size. Critical temperature differences ΔT_c after water quenching is discussed in relation to changes in most important variables affecting thermal shock, such as fracture strength, Young's modulus of elasticity and thermal conductivity. The results show that when total porosity as well as other microstructural parameters are held constant, an increase in pore size leads to a decrease in ΔT_c . Moreover, the results indicate that thermal conductivity plays a significant role in the interpretation of the thermal shock behaviour of reaction-sintered Si_3N_4 .

THERMAL STRESS BEHAVIOUR OF YTTRIA, SCANDIA AND ALN CERAMICS

G.A. Gogotsi

Results of an investigation of ceramics based on yttria (Y_2O_3), scandia (Sc_2O_3) and aluminum nitride (AlN) are given. Test procedures used for evaluating their mechanical behaviour as well as their thermal shock resistance on quenching and monotonic heating are described. Special emphasis was placed on yttria from which one- and two-phase materials were fabricated. It was found that, of the materials studied, ceramics of AlN possessed the highest strength and thermal shock resistance. The analysis involved also the use of data from fractographic studies.

STUDIES ON THE APPLICATION OF HOT-PRESSED SILICON NITRIDE CERAMICS AS CUTTING-TOOLS

Miao Ho-Cho, Chow Chia-Bao, Liu Yuan-Ho, Chiang Tso-Chao, Liu Kuo-Liang and Tang Chen-Huei

Studies on the application of hot-pressed Si_3N_4 as cutting

tool were carried out and satisfactory results achieved. In cutting hardened tool steels, chilled cast iron, pure molybdenum and pyrolytic graphite, the tool life of Si_3N_4 cutting tools is several times as long as that of sintered carbide tools. In threading, the Si_3N_4 cutting tool also performs satisfactorily. In order to test its cutting property under shock load, a milling test was made. The results show that the Si_3N_4 cutting tool can resist the shock load in milling. In cutting cast iron with high cutting speed, the Si_3N_4 cutting tool was also successful. These results indicate that hot-pressed Si_3N_4 is a cutting tool material which should be developed extensively.

SOME PHENOMENA OCCURRING IN BASALT GLASS FIBRES AT HIGH TEMPERATURES

J. Rzechula and M. Grylicki

It is well known that at high temperatures basalt glass wool loses its elasticity; crystalline phases appear and the fibres eventually disintegrate. Experiments reported here show that one of the factors responsible for this processes is oxidation of Fe^{2+} to Fe^{3+} . Other possible physicochemical processes, which can effect the behaviour of basalt glass fibres at high temperatures were also analysed.

INTERACTION BETWEEN CREEP, OXIDATION AND MICROPOROSITY IN REACTION-BONDED SILICON NITRIDE

G. Grathwohl and F. Thümmel

Kinetic studies have been performed on primary and secondary (minimal) creep of reaction-bonded silicon nitride in 4-pt-bending tests up to 1500°C. The creep deformation depends strongly on the extent of internal oxidation. In spite of the very marked dependence of the creep rate on material and pretreatment parameters, the stress exponents ($n = 1.7-1.8$) and activation energies (360-390 kJ/mole) are hardly influenced, suggesting similar creep mechanism. Creep deformation is provided by relative motion and separation of grain boundaries. Oxidation and deformation lead to remarkable changes of the pore size distribution; the creep processes are accompanied by deformation of the pores. The creep rupture strain is very limited in highly creep resistant materials and vice versa. Methods for the determination of oxidation products and oxide profiles along sample cross section have been developed and the chemical changes which the material can undergo during creep are outlined.

ON THE α TO β PHASE TRANSFORMATION AND GRAIN GROWTH DURING HOT-PRESSING OF Si_3N_4 CONTAINING MgO

H. Knoch and G.E. Gazza

The α/β phase transformation and correlated grain growth during hot-pressing of silicon nitride containing MgO has been studied. The reconstructive transformation appears to be reaction controlled with the rate dependent on the amount of pre-existing β phase and $\alpha/\text{liquid}/\beta$ interface formed during hot-pressing. The microstructure of the dense, hot-pressed product, i.e. grain size, shape, and distribution, is influenced by the starting α/β ratio and nucleation rate of the β phase. Different growth rates perpendicular and parallel to the crystallographic c-axis of β result in an elongated microstructure. Increasing the hot-pressing pressure increases the transformation rate as a consequence of the enhanced nucleation rate of β . This produces a fine, uniform microstructure with good mechanical strength. If hot-pressing time is extended beyond that required for α/β conversion, coarsening of the β grains will degrade mechanical properties.

EXPANSION DURING THE REACTION SINTERING OF PTZ

Yoshikazu Nakamura, Sudhir S. Chadratreya, and Richard M. Fulrath

Expansion during the reaction sintering of PTZ from PT and PZ constituents was studied at different temperatures: compositional and particle size effects were observed. The expansion is related to the size of the PT particles present and exhibits a maximum at 50 mole % PT for equal sizes of PT and PZ.

KINETICS OF THE THERMAL DECOMPOSITION OF KYANITE

H. Schneider and A. Majdić

The kinetics of the solid state high-temperature transformation of kyanite ($\text{Al}_2\text{SiO}_5 = \text{Al}_2\text{O}_3 \cdot \text{SiO}_2$) powders ($\leq 40 \mu\text{m}$) to 3:2-mullite ($3\text{Al}_2\text{O}_3 \cdot 2\text{SiO}_2$) and silica (SiO_2) were investigated by means of quantitative X-ray diffraction techniques. The transformation interval was found to lie between about 1150 and 1350°C. The reaction law best fitting the kinetic data is: $1-\alpha = kt^n$. The transformation is believed to be reconstructive, with decomposition of the kyanite structure, solid-state atom diffusion, and (epitactic) rearrangement of mullite and cristobalite. Cristobalite represents part of the «free» silica, the rest being present as a glassy phase. Addition of Fe_2O_3 and TiO_2 to the starting material exerts a marked decrease of the transformation temperature, with TiO_2 having a somewhat stronger influence than Fe_2O_3 . The reason may be an oxide-catalyzed reaction; the decomposition begins at nuclei formed at the surfaces of the kyanite particles, which are coated with thin layers of hematite and rutile respectively.

ELECTRON MICROSCOPY OF SOME WOLLASTONITE BASED PORCELAINS

C. Coma Díaz, J.M. González Peña and D. Alvarez-Estrada

Electron microscopy studies were made on five calcium porcelains whose starting batches consisted of kaolinite clay, wollastonite and a lead borate frit. Transmission and scanning electron microscopy, as well as X-ray energy dispersive microanalysis were used. The mineral composition of the resulting porcelains was found to be primarily anorthite, wollastonite and quartz. Anorthite, the most abundant crystal phase, was found to be present in a wide range of sizes and shapes, suggesting that it is formed in these porcelains by more than one mechanism. This may be related to the presence of a vitreous phase of special characteristics. It seems possible to direct the growth of the anorthite crystals, not only towards different sizes but also towards specific shapes for the purpose of inducing convenient microstructures.

THERMAL INSULATIONS FROM RICE HUSK ASH, AN AGRICULTURAL WASTE

P.C. Kapur

Rice husk ash, an agricultural waste material, is available in large quantities in the rice paddy growing countries of the world at little or no cost. This ash is highly porous, mostly silica and possesses refractory and thermal insulation properties. It is therefore an attractive starting raw material for the manufacture of low to moderate cost thermal insulations for dryers, ovens, kilns and furnaces, including those employed in the ceramic industry. This paper deals with manufacture, properties and usage of a spectrum of low to high temperature thermal insulations and insulating refractories that can be made from rice husk ash, namely: (i) Calcium ferrite bonded porous silica refractory; (ii) Sodium

VOL
11
1985

silicate bonded porous silica refractory; (iii) Fired and chemically bonded forsterite insulating refractory; (iv) Hydraulic setting calcium silicate / silica thermal insulation.

PREPARATION OF CORUNDUM AND STEATITE CERAMICS BY THE FREEZE-DRYING METHOD

A. Kwiatkowski, K. Reszka and A. Szymanski

The flexural strength and surface and fracture structures of ceramics samples dried by the traditional thermal method were compared with those of equivalent samples dried by the freeze-drying method. The freezing temperatures of the corundum, mullite and steatite slips, were determined. Drying by the freeze-drying technique resulted in smoother sample surfaces and increased flexural strength of the corundum and mullite ceramics.

FORMATION AND PROPERTIES OF GLASS-MICA COMPOSITE MATERIALS

Normal L.P. Low

Glass-mica composite material of different physical structures has been developed from mixtures of recycled soda-lime waste glass powder and a locally produced phlogopite-type mica powder by a simple sintering process at temperatures above 780°C for 30 minutes or longer. The composite material can be fabricated into products having either a cellular-structure consisting of both closed and open cells or a highly densified ceramic structure having very little porosity. The fabricated glass-mica composite product with the densified ceramic structure is found to have a compressive strength higher than 53 MN/m² and thermal conductivity values in the range of 0.198-0.250 W/m, °C when measured over the temperature range, 25-180°C. These mechanical and thermal properties are found to be superior than those of the conventional building materials, such as concrete, masonry products and cement mortar. This suggests that the glass-mica composite is a potential material for building construction applications because it could contribute to energy conservation.

HOT PRESSING OF SILICON NITRIDE WITH CERIA ADDITIONS

G.N. Babini, A. Bellosi and P. Vincenzini

Hot pressing kinetics, α/β conversion reaction and β -phase texture were studied for (1 - 20) wt% CeO_2 - Si_3N_4 compositions hot pressed at $T = 1823 \div 1973$ K and $P_a = 14.7 \div 39.2$ MNm⁻², in a nitrogen atmosphere. Sintering is likely to occur in the presence of an intergranular cerium orthosilicate $\text{Ce}_{4.67}(\text{SiO}_4)_3\text{O}$ liquid phase by a multicomponent mechanism including rheologic rearrangement, solution / reprecipitation and grain boundary sliding. The same solution / diffusion / reprecipitation mechanism seems to apply for densification and for the α/β conversion reaction in the early stages of hot pressing. An appreciable dependence of the β -phase texture on hot pressing parameters and amount of liquid phase is also featured.

THE PREPARATION AND PROPERTIES OF STRONTIUM ZIRCONATE CERAMICS FOR CHANNELS OF OPEN-CYCLE MHD GENERATORS

M. Zborowska, M. Grylicki and J. Zborowski

A two-stage procedure of preparation of dense strontium zirconate ceramics capable of being used as electrically insulating material in MHD generators is described. A small addition of TiO_2 was introduced at the first stage to favour development of the properties, especially low apparent

porosity, required for MHD purposes. The effect of TiO_2 on sintering temperature, phase composition and microstructure of the bodies is described. Properties of the resulting ceramics i.e. porosity, cold crushing strength, microhardness as well as electrical conductivity over the temperature range of 20-2000°C were measured. The results of successful testing of these ceramics in the channel of an experimental MHD generator are presented.

FORMATION AND TRANSFORMATION OF ALKOXY-DERIVED BaB_2O_4

O. Yamaguchi, K. Tominaga and K. Shimizu

Barium metaborate was formed by the simultaneous hydrolysis of barium and boron alkoxides. The dehydrated compound of the as-prepared BaB_2O_4 is termed $\gamma\text{-BaB}_2\text{O}_4$. The IR pattern of $\gamma\text{-BaB}_2\text{O}_4$ was able to be ascribed to a chain anion made up of $(-\text{BO}_2^-)_n$ units. The transformation of γ into $\beta\text{-BaB}_2\text{O}_4$ and of β into $\alpha\text{-BaB}_2\text{O}_4$ was observed at 590-650°C and 870-940°C, respectively. From the results of the high-temperature X-ray analysis as well as the DTA data, both transformations were found to be irreversible. Transformation isotherms of γ into $\beta\text{-BaB}_2\text{O}_4$ were described by the first-order equation and activation energies were determined as 69 kcal/mol and 48 kcal/mol for nucleation process and propagation process, respectively. The kinetics of transformation of β into $\alpha\text{-BaB}_2\text{O}_4$ was best interpreted by the contracting cube equation. Activation energies were 126 kcal/mol and 76 kcal/mol for initial and final stages, respectively.

PHASE EQUILIBRIA IN THE $\text{SiO}_2\text{-TiO}_2$ BINARY AND THE EFFECT OF TiO_2 ON THE $\alpha\text{-}\beta$ TRANSFORMATION IN CRYSTOBALITE

S. Kaneko, H.N. Tran, Y. Kubo and F. Imoto

The solid solubility of TiO_2 in cristobalite at 1450°C is ~4.7 wt%. The variation of the lattice constant and of the $\alpha\text{-}\beta$ transformation temperature of cristobalite with increasing TiO_2 content was also studied.

NEW APPROACHES TO PORCELAIN DOSIMETERS FOR MEASURING FAST NEUTRON FLUXES

M.A. Fadel, I.A.F. Wafa and D.S. Al-Alousi

The induced damage effects of 14.3 Mev neutron fluxes on quartz-based porcelain and alumina-based porcelain were studied using X-ray diffraction analysis and electric resistivity measurements. The results showed that both the degree of crystallinity and the electric resistivity of the samples decreased upon irradiation. Resistivity values plotted as a function of neutron flux proved to fit semi-empirical formulae that could be used for measuring neutron fluxes ($10^{10} \div 2 \times 10^{11}$ n/cm²) in the presence of gamma radiation (up to 5 megarads). Moreover, plots of the area under the X-ray peaks as a function of neutron flux were found to fit empirical formulae which could be used for the sample purpose. The effect of storage at temperatures up to 50°C and for periods of up to 2 weeks on the radiation induced changes in the porcelain were studied.

EFFECT OF MgO AND NiO ON THE SINTERING OF SLIP CAST ALUMINA

N.A. Haroun

Similar to pressed compacts, slip cast alumina can be sintered to near theoretical density if minor additions of MgO or NiO are made. Sintering kinetics of alumina were analyzed

ed in terms of the Wong and Pask model which was shown to give the more realistic representation of powder compacts. The rate controlling step with and without additions is the migration from the neck along the pore surface rather than diffusion along the grain boundaries to the neck. Both MgO and NiO retard mass transport probably due to changes in surface energy. However, they allow sintering to near complete densification. Although grain growth limitation via second phase inclusions or solute segregation is expected, the final density improvement was shown to result from modifying pore kinetics such that the pores remain attached to the grain boundaries during grain growth until complete densification.

PHENOMENA AT THE POWDER-WALL BOUNDARY DURING DIE COMPACTION OF A FINE OXIDE POWDER

S. Strijbos

Fine powders (particle size smaller than $0.1 \mu m$) are often used for the fabrication of modern fine-grained ceramics. During die compaction of such fine powders, special phenomena at the powder-wall boundary can be expected because the size of the particles is of the same order as the size of the wall asperities. In the present paper, the principles of powder mechanics are applied to experimental results obtained with a fine ferric oxide powder. The appearance of a dense boundary layer on the surface of compacts could be related to the occurrence of powder failure during compaction at the die wall.

CHARACTERIZATION OF METALLIZED CERAMIC INTERFACES

D.E. Clark and S.M. Clark

Using a variety of surface analytical tools, the interfaces of several metal-ceramic composites have been characterized. Three processes that lead to the bonding of a metallizing to a ceramic substrate are illustrated. When a pure refractory metallizing is deposited onto a 94% Al_2O_3 , bonding is achieved by glass migrating from the ceramic into the metallizing during firing. During cooling, the glass forms a mechanical-chemical bond between the ceramic and metallizing. In order to achieve bonding to a 99% Al_2O_3 or 99% BeO , the metallizing itself must contain a sufficient quantity of glass for wetting the ceramic, or be capable of forming a direct chemical bond to the ceramic.

YOUNG'S MODULUS OF SILICON NITRIDE HOT PRESSED WITH CERIA ADDITIONS

G. De Portu and P. Vincenzini

Possible relationships between Young's modulus at room temperature of (1-20) wt% CeO_2 -fluxed HPSN and some microstructural features such as amount of the intergranular phase, porosity, α/β ratio and crystallographic β texture have been investigated. The dependence of Young's modulus on amount of intergranular phase expressed in terms of the Cohen-Ishai model resulted in the relation: $E = 98.0 [1 + V_N/(1.45 - V_N^{1/3})] GN/m^2$. A quadratic relationship, $E = 290.0 (1 - AP + BP^2)$, proved the most adequate to account for the effect of porosity on Young's modulus over the 0-36% porosity range. α/β ratio and β texture did not seem to have an appreciable effect.

HOT FORMING OF DOLOMITE BRIQUETTES

W. Piatkowski and B. Rózanowski

Results of experiments to study the production of dolomite

clinker having a density close to the theoretical density of pure sintered dolomite are discussed. Density values are reported for samples obtained by the following process: decarbonization of dolomite, hot briquetting at 300-700°C, firing the semi-product at 1500°C. A similar procedure was also developed using salt-doped dolomite. The technology used leads to especially good results when dealing with 'hard to sinter' dolomites. It also avoids the necessity to use extremely high temperatures for the sintering process, thus making the process more economical from the point of view of energy consumption.

AN ALTERNATIVE TECHNOLOGY FOR MAKING CARBON CONTAINING BASIC REFRactories

T. Rymon - Lipinski

A new technological procedure is outlined involving a hot pressing operation at 400-500°C; this operation, carried out using existing commercial equipment, can replace the traditional high temperature sintering of basic raw materials. Test results indicating the optimum conditions for hot pressing are given along with some characteristics of the resulting materials.

REFRACTORY AND ELECTRIC INSULATING MATERIALS BASED ON NON-METALLIC NITRIDES

P.S. Kisly, M.A. Kuzenkova, L.I. Prikhod'ko and V.K. Kazakov

Non-metallic nitrides and alloys based on them are used as refractory and electric insulating materials in modern high temperature technology. The properties of these materials depend on powder production techniques and on technological industrial processes. With efficient control of production conditions and chemical composition, materials of given property levels can be obtained.

HIGH-PRESSURE SINTERING OF SILICON NITRIDE

M. Shibata, N. Kinomura and M. Koizumi

Short communication.

THE REACTIONS OF SILICON NITRIDE WITH VANADIUM OXIDES

M.B. Trigg and E.R. McCartney

Short communication.

FORMATION AND GROWTH PROCESSES OF RARE EARTH NIOBATES AND PHOSPHATES

I.A. Bondar', M.G. Degen, L.P. Mezentseva and L.N. Koroleva

Short communication.

PRECIPITATION OF CeO_2 CRYSTALS IN A GLASSY OXIDE PHASE FORMED DURING OXIDATION OF CeO_2 -DOPED HOT PRESSED SILICON NITRIDE

G.N. Babini, A. Bellosi and P. Vincenzini

Short communication.

VO
1
19

Vol. VII, January/December, 1981

PHASE RELATIONSHIPS, ELECTRICAL CONDUCTIVITIES AND VAPORIZATION RATES IN THE SYSTEM $\text{La}(\text{Fe}_{0.5}\text{Cr}_{0.5})\text{O}_3\text{-Sr}(\text{Fe}_{0.5}\text{Cr}_{0.5})\text{O}_3\text{-SrZrO}_3$ IN AIR

T. Sasamoto, W.R. Cannon and H.K. Bowen

The properties of the mixed perovskite $(\text{La},\text{Sr})\text{FeO}_3\text{-SrZrO}_3$ with LaCrO_3 additions were investigated. In general, an increased melting point is achieved with these additions without significant change of the electrical conductivity. However, phase separation into end-member compounds was observed up to 1700°C . The vaporization rates were measured for several compositions by the weight loss at 1700°C in still air, and it has been found that the additions of SrZrO_3 up to 20 mol% reduced the vaporization rate greatly.

EFFICIENCY OF CERAMIC ABSORBER COATINGS FOR SOLAR-THERMAL CONVERSION

Seung-Am Cho, Raymond Fookes and Charles A. Garris

Local solar constants both at 1750 m altitude and at sea level were measured by a simple and cheap, but practical water calorimetric technique, and its reliability has been proved. From the incident solar energy flux, solar absorptances of a semipolished metallic copper surface, fourteen common oxides, one sulfide and two local minerals, laterite and hematite, all sprayed on copper substrates, have been measured. All the absorptance data are presented in order of merit.

PREPARATION AND PROPERTIES OF NEW SILICON OXYNITRIDE BASED CERAMICS

M. Billy, P. Boch, C. Dumazeau, J.C. Glandus and P. Goursat

Silicon oxynitride based ceramics containing magnesia or yttria additives were prepared by hot-pressing. Their properties are very similar to those of related silicon containing nitrogen ceramics, with special reference to mechanical properties, thermal shock resistance in particular. The oxidation resistance of these materials exceeds that of Si_3N_4 and by using Y_2O_3 as a densification additive, the limiting temperature for utilization in air is about 1600°C .

ALKALINES VAPOUR ATTACK ON A HIGH ALUMINA REFRACTORY

E. Criado, J.S. Moya and S. De Aza

The sequence of attack by vapours of Na_2CO_3 and K_2CO_3 under oxidizing conditions on plates of a high alumina refractory (98%) bounded with calcium hexaluminate was studied. The damage caused by alkaline attack was evaluated and the results obtained compared with data reported in the literature on experiments done under reducing conditions.

EFFECT OF THE MAIN WHITEMEARE COMPONENTS ON THE DISSOCIATION OF BARITE

Tahany El Adly, Doreya M. Ibrahim and Mohamed T. Hussein

The effect of certain whiteware constituents clay, quartz, feldspar or alumina on the dissociation of barite was studied by thermogravimetric analysis of two series of powder mixes. In addition discs of the powders were semi-dry-pressed and their weight loss determined. The dissociation process of barite is influenced by two reactions which occur with increasing temperature. A solid state reaction occurs at 600°C

in the presence of all additions and results in a slight loss in weight. The products of this superfacial reaction hinder reaction between the barite grains and quartz until 1000°C is reached. In the case of clay, this reaction proceeds slowly up to 1200°C . A second reaction starts at 1250°C where a liquid phase is present, accelerating the dissociation process. Alumina appears inert even at 1250°C . Only 50.4% of the original amount of barite in mixes reacted with the clay and even less reacted with feldspar and quartz. The main crystalline phases detected were barite together with sanbornite or mullite and celsian.

BARITE AS A MAIN CONSTITUENT IN WHITEMEARE COMPOSITION

Tahany El Adly, Doreya M. Ibrahim and Mohamed T. Hussein

Two series of mixes lying in the field of celsian $\text{BaO}\cdot\text{Al}_2\text{O}_3\cdot2\text{SiO}_2$ in the ternary system $\text{BaO}\text{-Al}_2\text{O}_3\text{-SiO}_2$ were investigated. These compositions were obtained using 35 to 60% barite together with either clay and feldspar or clay, feldspar and quartz. The amount of unreacted BaSO_4 , was determined by chemical means. The effect of barite addition on physical properties, reversible linear thermal expansion and modulus of rupture of the produced bodies was verified. Results showed that 35 to 40% barite was consumed in the reaction with other constituents forming celsian $\text{BaO}\cdot\text{Al}_2\text{O}_3\cdot2\text{SiO}_2$ and sanbornite $\text{BaO}\cdot2\text{SiO}_2$. Higher additions of barite left unreacted BaSO_4 as a constituent of the fired product. Unreacted barite increased the bulk density, 2.2-2.9 g/cm³, raised the linear thermal expansion coefficient, 4.2-8.5 $10^{-6}/^\circ\text{C}$, between 20-1000°C and lowered the modulus of rupture, 450-180 kg/cm².

OPTICAL PROPERTIES OF LOW-TERMPEARTURE B_2O_3 -AND ZrO_2 -OPACIFIED GLAZES

O.S. Grum-Grzhimailo

A method for the quantitative determination of the Light Scattering Capacity (LSC) of glazes is described. Using equations previously employed for milky white glasses, a method was developed for defining the LSC of low melting borozirconium glazes. It is shown that this method may be taken as a basis for use with regard to any other glaze. The evidence indicates that an exponential dependence exists between the amount of the opacifying crystalline phase and the LSC of the investigated glazes.

EQUILIBRIUM MOISTURE DIAGRAMS FOR THE DRYING OF CLAYS

P. Bálint, B. Szóke, Z. Juhász and T. Skvorecz

The values of equilibrium moisture content shown by desorption isotherms of the clays are of utmost importance for ceramic drying processes. The desorption isotherms — the course of which depends on the mineral composition of the clays, as well as on the parameters of drying — facilitate the optimization of the drying processes. With the aid of the diagrams, the drying parameters required for obtaining the prescribed equilibrium-, resp. final moisture content of the dry product can be selected and the equilibrium moisture content obtainable at the given drying parameters can be easily determined. Examples are given for five different clay sorts.

BLOATING OF SLIP CAST MgO

N.A. Haroun and M.A.A. El-Masry

Short communication.

COMPOUNDS IN THE $\text{Na}_2\text{O}-\text{Y}_2\text{O}_3-\text{SiO}_2$ SYSTEM

F. Cervantes Lee, J. Marr and F.P. Glasser

Data on the synthesis and characterization of six ternary phases in this system are presented. $\text{NaY}_9\text{Si}_6\text{O}_{26}$ is confirmed as having the apatite structure: 39 indexed powder reflections are given. The synthesis of $\text{Na}_3\text{YSi}_2\text{O}_7$ is reported, together with unindexed powder data. Much interest centres about the sodium-ion conductor, $\text{Na}_5\text{YSi}_4\text{O}_{12}$, for which indexed powder data are presented. This phase is shown to be one of a family of compounds which have the general formula $\text{Na}_{24-3x}\text{Y}_x\text{Si}_{12}\text{O}_{36}$. In this notation, $x = 3$ for $\text{Na}_5\text{YSi}_4\text{O}_{12}$. At least three other phases are stable up to liquidus temperatures and characterization data are presented for $\text{Na}_9\text{YSi}_6\text{O}_{18}$ ($x = 2$), $\text{Na}_3\text{YSi}_3\text{O}_9$ ($x = 4$) and NaYSi_2O_6 ($x = 6$).

γ -ALUMINA OBTAINED BY ARC PLASMA SPRAYING: A STUDY OF THE OPTIMIZATION OF SPRAYING CONDITIONS

M. Vardelle and J.L. Besson

γ -alumina massive samples have been made by arc-plasma spraying. Measurements of the temperature and the velocity of the plasma stream as well as surface temperatures and velocities of the alumina particles have been performed which have identified relations between the microstructure and crystallography of the deposits and the working conditions of the arc-plasma spraying device. After optimization of the process, samples 98% dense and containing less than 2% of α phase have been obtained.

CERAMIC ELECTRODES FOR PHOTOELECTROLYTIC DECOMPOSITION OF WATER

J.M. Kowalski and H.L. Tuller

In the last decade a number of semiconducting oxides have been identified which serve as essential components in the photoassisted electrolytic decomposition of water to produce hydrogen fuel. To date, this attractive process still suffers from relatively low solar energy conversion efficiencies. In this paper we outline the operating principles characterizing photoelectrolytic cells, and discuss those materials properties which appear most relevant to their efficient operation. Recent data obtained for BaTiO_3 and other photoelectrodes are presented which illustrate the importance of materials preparation.

PROPERTIES OF SOME HIGH ALUMINA REFRactories OBTAINED FROM DIFFERENT ALUMINA SOURCES

Ibrahim Nasr, F.M. Abdel-Kader and H.K. Embabi

Within the same alumina level, refractories made using different sources of alumina vary widely in their densification and refractory properties. Refractories based on the more volume stable synthetic mullite and sillimanite grains are dense and more creep resisting than the continuously bloating easily deformed bauxite ones. The mineralogical composition of the grog grain used and the matrix developed in a fired brick appears to be the most important factor determining its resistance at high temperatures.

SINTERING CHARACTERISTICS OF CHINESE BAUXITES

Zhong Xiangchong and Li Guangping

The sintering behaviour of Chinese bauxites of the diasporo-kaolinite type proceeds in three stages, viz: decomposition

stage (400-1200°C), secondary mullitization stage (1200-1400 or 1500°C) and recrystallization sintering stage (above 1400 or 1500°C). The sinterability of different grades of bauxites is dependent on the Al_2O_3 content. The closer is the composition of calcined bauxite to that of mullite, the more difficult is it to sinter. It is postulated that secondary mullitization and liquid phase action are the two principal factors influencing the sintering of these bauxites. Grade II bauxites characterised by maximum secondary mullite formation and relatively low glass content are found to be most difficult to sinter.

NEPHELINE SYENITE-TALC LOW TEMPERATURE VITRIFIED BODIES

D.M. Ibrahim, E.H. Sallam, A.A. Khalil and S.M.H. Naga

Compositions in the system, talc-nepheline syenite-quartz-china clay (Kaolinite) were studied. The content of nepheline syenite was kept constant, 25%, while talc was added in the range of 5-15% at the expense of quartz. This study extended the range of fusible talc/nepheline mixes from 15 to 28%. The content of talc dissolved in the glassy phase is limited to 3-4%. Addition of talc to the compositions caused the dissolution of mullite and increased the glassy phase. The addition of nepheline syenite counteracts the effect of talc on the thermal expansion coefficient of the bodies.

KINETICS OF THE FORMATION OF ALKOXY-DERIVED $\text{MgO}\cdot 2\text{TiO}_2$ AND $\text{MgO}\cdot \text{TiO}_2$

Osamu Yamaguchi, Shigeharu Yamamoto and Kiyoshi Shimizu

The compounds of $\text{MgO}\cdot 2\text{TiO}_2$ and $\text{MgO}\cdot \text{TiO}_2$ were formed directly from mixed powders prepared by the simultaneous hydrolysis of magnesium and titanium alkoxides. Both crystallization isotherms were described by the first-order equation $-\ln(1-f) = k(t-t_0)$. Activation energies corresponding to nucleation and propagation are 57 kcal/mol and 21 kcal/mol with $\text{MgO}\cdot 2\text{TiO}_2$ and 61 kcal/mol and 29 kcal/mol with $\text{MgO}\cdot \text{TiO}_2$, respectively.

PETROGRAPHIC AND X-RAY IDENTIFICATION OF PHASES FORMED BY OXIDATION OF SILICON CARBIDE

V.A. Lavrenko, S. Jonas and R. Pampuch

Short communication.

OXIDATION OF SILICON NITRIDE HOT PRESSED WITH CeO_2 AND SiO_2 ADDITIONS

G.N. Babini, A. Bellosi and P. Vincenzini

($\text{CeO}_2 + \text{SiO}_2$)-doped hot pressed silicon nitride shows parabolic oxidation kinetics in dry flowing air at $T = 773$ to 1673 K. Possible oxidation mechanisms have been proposed. The apparent activation energy for oxidation ($\sim 350 \text{ kJ mol}^{-1}$) suggests migration of impurity cations through the grain boundary phase to the silicon nitride/oxide reaction interface as the probable rate-limiting step. The very low solubility of cerium in silicate melts appears to be an important factor for oxidation. Cristobalite and ceria were the main crystalline oxidation products, the genesis and morphology of CeO_2 crystals being strictly related to oxidation temperature and cooling rate. A previously unknown hexagonal high-temperature form of ceria crystallized in samples subjected to very fast quenching.

INFLUENCE OF MIXING MEDIUM ON SINTERING AND COUPLING COEFFICIENT OF PZT CERAMICS

Michihiro Nishioka, S.S. Chiang, Richard M. Fulrath and Joseph A. Pask

Mixtures of PZT, PbO and a water solution of PVA were prepared with distilled water and isopropyl alcohol. Better cold pressing behavior and more uniform microstructures free of large pores were obtained with use of the alcohol. Nature of grain boundaries was essentially unaffected as indicated by K_p measurements.

THE SUBSOLIDUS PHASE EQUILIBRIA AND MELTING TEMPERATURES OF MgO - Al_2O_3 - SiO_2 COMPOSITIONS

R.M. Smart and F.P. Glasser

Phase equilibrium relations in the MgO - Al_2O_3 - SiO_2 system at 1 bar pressure are strongly temperature-dependent. Information obtained from a study of 53 compositions has been combined to show a series of isothermal sections at 1350, 1450, 1470, 1490, 1525 and 1575°C. The compositions of synthetic sapphires may be represented by the general formula $Mg_7Al_{22-x}SiO_{0.75x}O_{40}$: depending upon temperature, x may vary from ~1.5 to ~5.6. Assemblages which at lower temperatures contain cordierite and corundum, give way to assemblages containing spinel and mullite at higher temperatures.

ELECTRO-MECHANICAL DEGRADATION OF POLYCRYSTALLINE BETA-ALUMINA

Kuo Chu-Kun and Li Shan-Tin

Deposition of metallic sodium under conditions of current flow of sodium ions through beta-alumina ceramics is an important cause of their breakdown when the solid electrolyte is used as a separator in various electrochemical devices. Cells of different combinations: Na/Beta-Alumina/Na amalgam, Na/Beta-Alumina/Cu (probe), and Na/Beta-Alumina/Na, etc. have been investigated for sodium deposition at room temperature and at 350°C. A method is presented by which the progress of sodium deposition may be followed. A mechanism of formation of sodium deposition centers at impurity rich spots and other defect sites has been proposed.

CRYSTALLOGRAPHIC CHARACTERISTICS OF THE SOLID SOLUTION $SrCeO_3$ - $BaCeO_3$

V. Longo, D. Minichelli and F. Ricciardiello

Short communication.

THE INVESTIGATION OF HIGH-TEMPERATURE STRENGTH OF SiC BASED REFRACTORIES

M. Komac

The Brew-Instron apparatus was used in order to investigate the temperature dependence of bend strength of SiC based refractories in the range from room temperature up to 1400°C. The results obtained show that the strength of the samples strongly depends on the type and amount of bonding phase used (silicate, nitride) as well as on the grain size and the grain size distribution of the SiC phase. Nitride bonded materials are superior to silicate bonded and by decreasing the SiC grain size the high-temperature strength can be markedly increased. The extent of deformation is governed mainly by the SiC grain size, whereas the amount of binder phase does not influence it significantly. The results are discussed with reference to other methods which are used to characterize the performance of the refractories.

FERROELECTRIC FERROMAGNETICS

R. Röttenbacher, H.J. Oel and G. Tomandl

Composite materials $MgMn$ -ferrite/ $BaTiO_3$ prepared by conventional powder technology behave as ferroelectric ferromagnetics at room temperature in a range of compositions from 30:70 to 50:50 w/o.

PROGRESS OF CERAMIC RESEARCH IN THE SHANGHAI INSTITUTE OF CERAMICS, ACADEMIA SINICA

Tung-Sheng Yen

Research activities in the Shanghai Institute of Ceramics of the Chinese Academy of Sciences started in the early fifties after the founding of the People's Republic of China. The Institute is now an establishment devoted essentially to studies of inorganic materials with a broad spectrum of research projects relating to single crystal studies, glass (amorphous material) research, oxide and non-oxide ceramics research, ferroics studies, fast-ion conductor research, inorganic coating materials studies and research on ancient Chinese porcelain and glazes. Problems concerned with processing, characterization, microstructure and properties are involved. Other major branches of ceramic science and engineering are being studied in other institutions run by the Building Materials, Light Industries and Metallurgy Departments of the Government and some Universities and Institutions of Technology. This review gives an account of the works that are being carried out in the Shanghai Institute. It is, however, not intended to be a complete coverage.

MICROCHEMICAL COMPOSITION AND CELL DIMENSIONS OF MULLITES FROM REFRactory-GRADE SOUTH AMERICAN BAUXITES

H. Schneider and K. Wohlleben

Two different types of mullite could be determined in differently coloured fragments of South American bauxites: — Mullites, occurring in light bauxite fragments with low impurity contents (Σ wt% $(Fe_2O_3 + TiO_2) \leq 2.5$), and cell dimensions close to that of 3/2 mullite, the b parameter being slightly shorter. — Mullites, occurring in grey to dark grey, and in brown bauxite fragments, with high impurity contents (Σ wt% $(Fe_2O_3 + TiO_2) \leq 4.0$) and a and c cell dimensions close to those of 2/1 mullite. The b constant of these mullites is slightly expanded with respect to impurity free mullites. Increasing impurity contents in mullite are linearly correlated with a b expansion. The expansion was structurally explained with a substitution of Al^{3+} by Fe^{3+} and Ti^{4+} at octahedral lattice sites, which causes stretching of the AlO_6 octahedra along to the elastic Al_1-D_D bond in mullites which is 30° to either side of b . The substitution-produced expansion is superimposed by an expansion due to the change of the structural state of mullite from the 3/2 to the 2/1 type. The greatest variation in any cell parameter with the change of the structural state is the a constant.

REDUCTION OF $LaMnO_3$, STRUCTURAL FEATURES OF PHASES $La_8Mn_8O_{23}$ AND $La_4Mn_4O_{11}$

F. Abbattista and M. Lucco Borlara

Two new phases with ordered anion vacancies, $La_8Mn_8O_{23}$ and $La_4Mn_4O_{11}$, both having the general formula $A_nB_nO_{3n-1}$, form during the reduction of perovskites of the type $LaMnO_{3+\nu}$. The solid $LaMnO_{3.07}$, obtained in air at 1100°C and subsequently reduced in flowing carbon monoxide at 350°C, gives the stoichiometric perovskite $LaMnO_{3.00}$, whose reduction starts at 420°C and is completed at 450°C with formation of the phase $La_8Mn_8O_{23}$. The second reduction stage

starts at approximately 500°C and is completed at 520°C with formation of $\text{La}_4\text{Mn}_4\text{O}_{11}$. The solids in the range of composition $\text{LaMnO}_{3.00}$ - $\text{La}_8\text{Mn}_8\text{O}_{23}$ and $\text{La}_8\text{Mn}_8\text{O}_{23}\text{-La}_4\text{Mn}_4\text{O}_{11}$ would seem by X-ray examination to be biphasic but the behaviour during reduction is typical of a monophasic substance, the oxygen pressure of which at constant temperature progressively decreases as the composition tends to the limiting values $\text{La}_8\text{Mn}_8\text{O}_{23}$ and $\text{La}_4\text{Mn}_4\text{O}_{11}$. The crystal lattice of $\text{La}_8\text{Mn}_8\text{O}_{23}$ can be considered as resulting from a sequence of seven octahedral sheets, MnO_6 , alternated with tetrahedral sheets, MnO_4 , and the crystal lattice of $\text{La}_4\text{Mn}_4\text{O}_{11}$ from a sequence of three MnO_6 sheets alternating with MnO_4 sheets.

BULK AND GRAIN BOUNDARY DIFFUSION OF ^{14}C IN TUNGSTEN HEMICARBIDE

D. Treheux, J. Dubois and G. Fantozzi

Dense tungsten hemicarbide specimens were used to study the bulk and grain boundary diffusion of ^{14}C into W_2C at temperatures of 1200 to 2000°C. The bulk diffusion coefficient is given by:

$$D_v = 18.3 \exp\left(-\frac{91,500}{RT}\right) (\text{cm}^2 \text{s}^{-1})$$

The grain boundary diffusion coefficient is represented by the expression:

$$P_{GB} = 1.8 \cdot 10^{-4} \exp\left(-\frac{68,880}{RT}\right) (\text{cm}^3 \text{s}^{-1})$$

A comparison is given with preceding results on other carbides.

Vol. VIII, January/December, 1982

THE STRUCTURE OF SiO_2 - CURRENT VIEWS

E. Görlich

Silicon dioxide or silica, one of the most important raw materials in ceramics, undergoes rather complex phase transformations under varying conditions of temperature, pressure and chemical purity. The flexibility of the silica framework, consisting of $[\text{SiO}_4]$ tetrahedra bonded together into a giant polymeric "open molecule" by sharing oxygen atoms, is primarily due to the easy adjustment of the Si-O-Si angles between tetrahedra in response to changing conditions. The structure reinvestigations of silica polymorphs done in recent years allow a comprehensive review of the structure problems, including the high-pressure and amorphous states of SiO_2 and the mechanism of some of the phase transformations. The most difficult and still controversial problem of the structure of vitreous silica is rather extensively discussed in view of the technical importance of silica glass.

CHARACTERIZATION AND SINTERING OF Mg-Al SPINEL PREPARED BY SPRAY-PYROLYSIS TECHNIQUE

Y. Suyama and A. Kato

Magnesium, aluminate spinel was prepared by the spray-pyrolysis technique at 740°-1030°C from a corresponding nitrate solution. The spinel powders were characterized by poor crystallinity, large specific surface area, and hollow spheres 1-20 μm in size. The crystallinity, strength of the hollow shells, and stoichiometry affected the density of sintered bodies. Densification was inhibited when skeletons

of the hollow spheres remained in the green compacts. The pre-exclusion of the possibility of pore-formation originating from the hollow spheres was effective for densification. It was found that the highest density was obtained by the combination of low crystallinity and weak shells prepared by using ethyl alcoholwater as the solvent; the bulk density reached 93% TD with sintering at 1590°C for 2 h under atmospheric pressure.

STATISTICAL STUDIES OF THE STRENGTH OF INELASTIC CERAMICS

G.A. Gogotsi, J.A.L. Groushevsky

Test results for inelastically deformable ceramics - silicon nitride, cordierite, and also glass, - are given. The scatter of strength of these materials is shown to be adequately described by a two-parameter Weibull equation regardless of deformation features. This equation is also shown to be applicable for the description of ultimate strain values. The distribution of stresses at which acoustic emission in specimens begins has been found to correlate with the strength distribution in the same specimens.

CRYSTALLIZATION OF GLASS OF THE SYSTEM

$\text{K}_2\text{O}(\text{Na}_2\text{O})\text{-Al}_2\text{O}_3\text{-SiO}_2$

S.P. Chaudhuri

In a whiteware composition, the glassy phase derives from the molten feldspar in which a portion of quartz, clay and other crystalline constituents are dissolved. This glass is the major and continuous phase in the whiteware body and is the potential source of the crystalline phase, viz. mullite. Synthetic glass has been prepared by melting mixtures of feldspar and quartz comparable to whiteware-glass in composition. Glasses were also synthesized by melting mixtures of feldspar, quartz and mineralizers. All of these glasses were heat-treated and their mullite contents were estimated by X-ray analysis supported by TEM & SEM study. Among thirtyone (31) different mineralizers tried, only thirteen (13) are found to be effective mullite builders. The cation of the mineralizer helps replacement of the Al^{3+} ion from the glass which subsequently diffuses through the residual SiO_2 and mullite is formed. The replacement reaction and hence the degree of mullitization is dependent on factors, e.g. charge, radius, field strength of the cation as well as on the cation-oxygen bond strength. This last appears as the most predominant factor for mullitization.

SINTERING, OXIDATION AND MECHANICAL PROPERTIES OF HOT PRESSED ALUMINIUM NITRIDE

P. Boch, J.C. Glandus, J. Jarrige, J.P. Lecompte and J. Mexmain

Aluminium nitride samples were prepared by hot pressing of fine powder without additives. The sintering process is described. Different porosities were obtained and the ratio total porosity/open porosity was measured. Tests of corrosion in air were performed. The main mechanical properties (hardness, strength, toughness, thermal shock resistance...) were measured and the effects of porosity and temperature studied. The results obtained are compared with the mechanical properties of other structural ceramics.

POWDER SYNTHESIS FROM METAL-ORGANIC PRECURSORS

K.S. Mazdiyasni

Thermal conversion of organic polymers such as polymethylsilane $[(\text{CH}_3)_2\text{Si}]_n$, polymethylphenylsilane, and polysilazane or inorganic polymer such as silicicimide

VO
1
19

[Si(NH)₂]_n, and thermal and hydrolytic decomposition of metal alkoxides, M(OR)_n, have been employed to obtain sub-micron size 30-500 Å powders, continuous fibers and thin films of refractory carbides, nitrides and oxides. The high surface activity associated with these powders make possible relatively low temperature processing of the powders compact to near theoretical density and uniform fine grain size bodies. Transmission electron microscopy is used to show nucleation, growth crystallite morphology of the powders synthesized, and microstructural features observed.

SINTERING OF α -Al₂O₃ - AMORPHOUS SILICA COMPACTS

Y. Nurishi and J.A. Pask

Sintering of α -Al₂O₃ — fused SiO₂ compacts at temperatures of 1350-1500°C is affected by metastable and stable phase reactions. Shrinkage maxima in the range 10 to 30 mole % Al₂O₃ are the result of cristobalite in the fused SiO₂ and its reaction with α -Al₂O₃ to form the eutectic of the metastable phase equilibrium diagram for SiO₂ (cristobalite) — α -Al₂O₃ without mullite. The retardation of densification of α -Al₂O₃ compacts with additions of SiO₂ up to about 50 mole % at temperatures about 1400°C and above is associated with the appearance of mullite.

EFFECTS OF Cr₂O₃ ADDITIONS ON THE SINTERING AND MECHANICAL PROPERTIES OF Al₂O₃

H. Tomaszewski

The effect of Cr₂O₃ additions on the penetration of the intergranular phase between alumina grains of 96 wt % alumina ceramics has been investigated by applying the principles of quantitative metallography. From microsections, values of the true dihedral angle have been measured. Cr₂O₃ additions increased the dihedral angle and decreased the density of alumina ceramics. As a result, distinct deterioration of the mechanical properties of alumina ceramics was observed.

A MATHEMATICAL MODEL FOR CALCULATION OF n, p-TYPE CONDUCTIVITY SURFACES OF SOLID OXIDE ELECTROLYTES: AN APPLICATION TO 15 m/o CSZ

D. Gozzi and R. Gigli

A mathematical model to calculate the n, p-type conductivity surfaces of solid oxide electrolytes based on a limited number of experimental data is presented. Reliable results have been obtained by its application to 15 m/o CSZ by using an input data a well established set of conductivity vs temperature equations reported in literature. Also in terms of Schmalzried's parameters ($\log P_{-}, +$, $\log P_{-}$ and $\log P_{+}$), the values obtained support the potentialities of this mathematical procedure and in addition it shows that the P_{O₂} dependence of activation energies Q₋ and Q₊ is also a mathematical consequence.

EUTECTOID DECOMPOSITION PROCESSES OF SOLID SOLUTIONS IN THE HfO₂-PrO_{1.5} AND HfO₂-MgO SYSTEMS AND THEIR INFLUENCE ON THE PHYSICO-CHEMICAL PROPERTIES OF REFRACTORY MATERIALS

M.V. Kravchinskaya, P.A. Tikhonov and E.K. Koehler

Microscopy and electron microprobe analysis were used to study the process of eutectoid decomposition of cubic solid

solutions in the HfO₂-PrO_{1.5} and HfO₂-MgO systems. In the first system this occurs by forming of a Pr-rich pyrochlore-type phase and monoclinic HfO₂ solid solution. In the HfO₂-MgO system, magnesium concentrates mainly at crystal boundaries yielding a MgO solid solution; the second, MgO-poor phase is a HfO₂-based monoclinic solid solution. As a result of decomposition the electrical conductivity of the cubic solid solutions is reduced by two orders of magnitude in the HfO₂-PrO_{1.5} system and more than orders of magnitude in the HfO₂-MgO system.

BEHAVIOUR OF Cr³⁺ AND Fe³⁺ IONS IN THE GAHNITE CRYSTALLIZED FROM ZINC OPAQUE GLAZES

H. Takashima

The amount of gahnite spinel crystallized in a glaze containing a large amount of ZnO and Al₂O₃ as well as the behaviour of Cr³⁺ ions in the glaze were studied. Crystallization of gahnite containing a small amount of Cr₂O₃ gave a pink opaque glaze. Almost all the Cr³⁺ ions migrated into the gahnite phase. The measurement of the lattice constant by X-ray diffraction analysis, as well as chemical analysis of the crystallized gahnite separated from the glaze, used to determine the amount of Cr³⁺ ions in the gahnite phase. A similar phenomenon occurred when Fe₂O₃ was added to the base glaze composition.

REACTION SINTERING OF MgO-TiO₂ MIXTURES

F. Cambier, C. Leblud and M.R. Anseau

Short communication.

EFFECT OF EXPLOSIVE SHOCK WAVES ON MULLITE POWDERS

H. Schneider, A. Majdić and H.D. Werner

Short communication.

RARE-EARTH SILICATES

I.A. Bondar

Binary systems of the type Ln₂O₃-SiO₂ were studied. Three types of compounds were established for them: Ln₂O-SiO₄ (1:1) diorthosilicate, Ln₂Si₂O₇ (1:2), and the apatite-like silicate, Ln_{4.67}O [SiO₄]₃ (7:9), the latter being stable for the large cations. Systematization of the physical-chemical properties of rare earth silicates was made. Based on the model of ideal solutions the liquidus curves were calculated for several Ln₂O₃-Ln₂O₃SiO₂ systems. The solid solution limits were determined for complex systems formed by rare-earth and alkaline-earth silicates. A series of rare-earth single crystals of simple and complex composition were grown by crystallization from molten solutions. Classification of the same type compounds into structural groups (morphotropic series) was made and participation of the 4f-orbitals in bonding was considered. The spectralluminiscence characteristics of the rare-earth silicates are given.

THE INFLUENCE OF IMPURITIES ON THE MIGRATION ENERGY OF CATION VACANCIES IN MgO

E.A. Colbourn and W.C. Mackrodt

Calculated activation energies for cation vacancy migration in the presence of Ca_{Mg}²⁺, Al_{Mg}³⁺, Sc_{Mg}³⁺ impurity substitution ions are reported. The results are related to the recent experimental observations of vacancy mobility by Sempolinski and Kingery.

DENSIFICATION OF α -AND β -Si₃N₄ UNDER PRESSURE

Tetsuo Yamada, Atsuhiko Tanaka, Masahiko Shimada and Mitsue Koizumi

Effect of phase transformation, microstructural changes and bonding between grains of Si₃N₄, without additives was studied by high pressure hot-pressing using α - and β -Si₃N₄ as starting materials. Densification of Si₃N₄ did not depend on the difference of the phase in starting materials. During the hot pressing of α -Si₃N₄, a drastic change in grain morphology took place with the progress of phase transformation, and the final microstructure showed the existence of self bonding and the development of polyhedral grains. In the hot-pressing of β -Si₃N₄, no appreciable change in grain morphology was observed and densification was proceeded only due to a plastic deformation mechanism. Phase transformation seems to play a significant role in the bonding between grains.

FORMATION MECHANISM AND CERAMIC PROCESS OF THE FERROELECTRIC PEROVSKITES: Pb(Mg_{1/3}Nb_{2/3})O₃ AND Pb(Fe_{1/2}Nb_{1/2})O₃

M. Lejeune, J.P. Boilot

The formation of the Pb(Mg_{1/3}Nb_{2/3})O₃ and Pb(Fe_{1/2}Nb_{1/2})O₃ phases with a perovskite type structure is directly dependent on the reactivity of magnesium and ferric oxides to other phases belonging to the binary system PbO-Nb₂O₅. Moreover, it is shown that the ceramic process influences the proportion of perovskite phases in comparison with parasite phases and also the densification of the samples. The optimization of the ceramic process allows to obtain a pure Pb(Fe_{1/2}Nb_{1/2})O₃ phase, but as far as Pb(Mg_{1/3}Nb_{2/3})O₃ is concerned, a parasite phase is never entirely eliminated.

RECENT DEVELOPMENTS OF CEMENT CHEMISTRY IN CHINA

Xue Junan

In recent years, much work has been done by the cement chemists in China centering on energy saving in cement and concrete making and improving the properties of both.

EFFECT OF REACTANT DISPERSION ON FORMATION OF PZT SOLID SOLUTIONS

A.I. Kingon, P.J. Terblanché and J.B. Clark

The reactions in the formation of PZT solid solutions were studied with particular reference to changing the dispersion of the reactants by altering the mixing conditions. The final homogenisation step was studied in detail. The effect on the electromechanical properties of the PZT ceramics were measured. The results of these studies are discussed.

SEM, TEM AND EPMA STUDY OF INTERGRANULAR PHASES IN ALUMINA CERAMICS

H. Tomaszewski, L. Kulig, J. Toruń, H. Kozłowska and M. Wójcik

Short communication.

ELECTRICAL AND MECHANICAL LOSSES IN FERROELECTRIC CERAMICS

H.H. Härdtl

The magnitude of the electrical and mechanical losses of devices made from ferroelectric ceramics, which are current-

ly widely used in electronic circuits, often determines the applications of these materials. In this article the current understanding of the mechanisms and their dependence on the composition of the ceramic and on the experimental parameters is reviewed. The electrical and mechanical losses are proportional to each other. The proportionality factor is determined by material parameters, such as dielectric constant, spontaneous polarization etc., and is independent of the specific loss mechanism. The losses below the Curie temperature are mainly caused by domain wall movements. Above the Curie temperature the losses drop rapidly to a residual level, caused by lattice- and microstructural effects. At higher temperatures the losses are governed by the electrical conductivity of materials. Of major importance for applications are the domain wall losses. Their dependence on doping, aging, field strength, frequency and temperature is described and discussed. Models are presented that attribute the losses to the damping of a moving domain wall.

PRELIMINARY OBSERVATIONS ON THE MICROSTRUCTURE OF NUCLEAR WASTE GLASSES

J.F. DeNatale, D.K. McElfresh, and D.G. Howitt

The microstructures of simulated nuclear waste glasses prepared by the mixing of glass frit and calcined waste oxides at 1000°C are shown to contain well defined boundaries that are depleted of heavy elements. The development of small crystallites and phase separation have also been observed but no evidence of microcracking or interfacial separation at these discontinuities was found. The same glasses prepared at 1350°C were quite uniform at the microstructural level.

HISTORY OF BIOCERAMICS

S.F. Hulbert, L.L. Hench, D. Forbers, L.S. Bowman

The history of bioceramics is reviewed and the current status of the use of nearly inert, surface reactive, and resorbable bioceramics discussed.

PREPARATION OF GLASS-CERAMICS Pb₅Ge_{3-x}Si_xO₁₁ (0 ≤ x ≤ 1.75)

Hiroshi Hasegawa, Masahiko Shimada and Mitsue Koizumi

Glass-ceramics with a high transparency were prepared by the crystallization of 5PbO·(3-X) GeO₂·XSiO₂ glass. From the results of temperature dependence of the permittivity, the Curie temperatures of the products were estimated to be 175°C, 115°C and 65°C for the glass-ceramics 5PbO·3GeO₂, 5PbO·2.5·GeO₂·0.5SiO₂ and 5PbO·2GeO₂·SiO₂, respectively.

ACOUSTIC ACTIVITY IN A QUARTZ CONTAINING PORCELAIN SUBJECTED TO LOW RATE THERMAL CHANGES

J.D. Fridez, C. Carry and A. Mocellin

A typical quartz containing porcelain was subjected to various controlled temperature-time treatments in the 20-950°C range and for up to several days. Special precautions were taken and acoustic emission internally generated by the material during these treatments were recorded. Both experimental observations and analysis for stress in the vicinity of quartz particles show that the following process accounts for a significant part of the overall material response: development of circumferential microcracks, even at room temperature, following some (possibly absent if the initial size of the crack initiating defect is sufficient) subcritical defect growth. Parameters affecting the detailed distribution

of acoustic activity include size and shape of the quartz grains and their variations, distribution of initial defect size and material dependent defect growth kinetic parameters.

SINTERING OF α -Al₂O₃ / QUARTZ, AND α -Al₂O₃ / CRYSTOBALITE RELATED TO MULLITE FORMATION

Amar P.S. Rana, Osamu Aiko and Joseph A. Pask

Cristobalite and quartz react differently in mixtures with α -Al₂O₃ at 1415°C. With cristobalite, an eutectic liquid forms in accordance with the metastable phase equilibrium diagram for α -Al₂O₃-SiO₂ (cristobalite) in the absence of mullite. With quartz, a liquid first forms on the surface of quartz because of the occurrence of an intermediate liquid phase on transformation of quartz to cristobalite. These liquids act as precursors to the formation of mullite by reacting with α -Al₂O₃. Mullite was detected earlier in the cristobalite-containing mixtures under similar firing conditions because the growth of mullite becomes significant with the formation of the eutectic liquid at the α -Al₂O₃ - cristobalite interface since it is already saturated with Al₂O₃. The kinetics of sintering are affected by the rates of the step reactions.

ELECTRON MICROSCOPY STUDY OF THE MICROSTRUCTURE OF A HOT-PRESSED SILICON NITRIDE

T. Epicier and G. Orange

A microstructural investigation of a commercial hot-pressed silicon nitride variety is reported here; electron microscopy observations have been performed in attempt to precisely characterize the microstructure of the material. In particular, grain boundary structures have been studied by transmission electron microscopy using bright and dark-field techniques; a typical amorphous phase has been revealed in triple junctions and along grain boundaries.

sewing rings, percutaneous access devices, and tendon and ligament replacements.

Other forms of carbons, e.g. fibers and fiber composites, are currently being used clinically in orthopedic surgery. The impact of carbon on current replacement surgery and some possibilities for future applications will be described.

INFLUENCE OF YTTRIA CONTENT ON PHASE COMPOSITION AND MECHANICAL PROPERTIES OF Y-PSZ

K. Haberko and R. Pampuch

Coprecipitation technique was used to obtain powders in the system Y₂O₃-ZrO₂ of yttria concentration from 0.5 to 6.5 M/o. Fields of the existence of the monoclinic and the tetragonal ZrO₂ s.s. were calculated in the coordinate system: grain size vs. Y₂O₃ concentration. Experimental data are in good agreement with the calculations. It has been found that bodies of low yttria concentration (below 2 M/o) are monoclinic and their mechanical strength is low. Sintered bodies of Y₂O₃ concentration ranging between 3 and 5 M/o are entirely tetragonal, and those of Y₂O₃ content of 2 M/o have a thin monoclinic surface layer while the bulk is tetragonal. The ability to undergo the tetragonal to monoclinic transformation in front of a crack tip has been found to be dependent on the distance of the solid solution composition from the tetragonal/cubic phase boundary. Bodies demonstrating a higher degree of the crack induced transformation show higher K_c values.

The modulus of rupture increases with the K_c value and attains the highest level with bodies having a thin monoclinic surface layer at 2 M/o Y₂O₃.

FUSED SALT SYNTHESIS OF Bi₄Ti₃O₁₂

T. Kimura and T. Yamaguchi

Bismuth titanate powders were prepared in the presence of chloride or sulfate fused salts. In both fluxes, aggregate particles formed during the formation process and differently-shaped primary particles were obtained depending on the flux species. The aggregates changed to discrete plate-like particles on further heating. The crystal structure of the specimens obtained at low temperatures was defective with disturbed long-range order along c-axis and a/b close to unity. The effects of flux species on the nature of the products have been explained in terms of the interaction between Bi ions and flux anions.

FORMATION OF ALKOXY-DERIVED 3Al₂O₃•2GeO₂

Osamu Yamaguchi, Tatsuro Kanazawa, Masami Yokoigawa and Kiyoshi Shimizu

Germanium-mullite (3Al₂O₃•2GeO₂) is formed directly as a single phase at lower temperatures from amorphous material with 50-66.7 mole% Al₂O₃ prepared by the alkoxy-method. The kinetic data of the 3Al₂O₃•GeO₂ crystallization with 50 and 60 mole% Al₂O₃ are represented by different solid-state equations. The difference of the crystallization mechanism is possibly explained in terms of the morphology of the 3Al₂O₃•GeO₂ particles.

ON THE NATURE OF THE CRYSTALLOGRAPHIC DISORDER IN SUBMICROMETER PARTICLES OF Ca(OH)₂ PRODUCED BY VAPOUR PHASE HYDRATION

D. Beruto, G. Spinolo, L. Barco, U. Anselmi Tamburini and G. Belleri

Poorly crystalline form of Ca(OH)₂ can be produced by reaction of water vapours at room temperature with CaO powders and are highly reactive towards liquids and gases. Nitrogen

The variability of the crystalline structure of carbon allows a correspondingly wide range of possible properties. By controlling the structure of carbon through processing as for example in the deposition of carbon in a fluidized bed it is possible to produce deposits with unique combinations of properties. Certain of these carbons have been found to be extremely useful in prosthetic devices. The isotropic carbons deposited at relatively low temperatures (below about 1500°C), often called LTI carbons, are biocompatible in the broadest sense. They do not induce thrombosis or hemolysis or otherwise affect either the formed or molecular element of blood. They have exceptional wear and fatigue properties which are not degraded by the body environment. Accordingly, these carbons are widely used in the construction of prosthetic heart valves.

The modulus of elasticity of LTI carbon is unusually low for a material of such strength and falls within the limits reported for the elasticity of bone. This property, together with its ability to interface with both soft and hard tissue without eliciting a foreign body response, makes it possible to produce orthopedic joint replacements that can attach directly to bone without using polymethylmethacrylate bone cement. Using special vacuum deposition techniques, it is possible to deposit thin, impermeable isotropic carbons that mimic the structure and properties of the LTI carbon. Materials such as polymers and fabrics can be coated with such carbons and these coatings are finding use on vascular grafts, heart valve

adsorption isotherms, X-ray broadening analysis and S.E.M. observations were made on different samples either before or after a thermal treatment (essentially an irreversible process) that transforms these hydroxides into more crystalline materials. It is shown that the vapour phase hydration yields not only small size particles and high porosities but also crystallographic defects, and that the irreversible transformation is mainly connected to a recovery of defects.

THE PROPERTIES OF MAGNESIA POWDERS FOR THE HOT WELDING PROCESS

J. Zborowski

A number of powders derived from MgO calcined at various temperatures within the range 770-1770 K was submitted to the treatment usually used in preparation of the batches to welding process (hot-pressing in the presence of liquid salt phase).

Changes in powders characteristics during this treatment have been discussed based on results of sedimentation analysis and specific surface area measurement (BET method).

The samples made of these powders with and without salt addition ($CaCl_2$ - $LiCl$ eutectic mixture) were examined using mercury porosimetry and SEM. It has been shown that powder characteristics and the presence of liquid salt phase essentially influence the results of densification process. Sharp differences have been discovered in apparent densities and total amounts of open pores between the samples hot-pressed with and without salt additions. The former reached densities of about 85% theoretical and the latter were usually lower than 50%.

GRAIN BOUNDARY SEGREGATION OF IRON, CHROMIUM AND SCANDIUM IN POLYCRYSTALLINE MAGNESIUM OXIDE

N. Mizutani, A.J. Garratt-Reed and W.D. Kingery

Utilizing x-ray microanalysis in samples studied with scanning transmission electron microscopy, segregation of Fe, Cr and Sc has been found at grain boundaries of polycrystalline MgO . Samples studied contain between 500 and 1200 cation ppm of each solute, or of all three. The level of grain boundary segregation of Fe and Sc was approximately proportional to the bulk concentration while the boundary concentration of Cr was less than the other solutes, more so at higher concentrations. This result is attributed to the higher association energy of $Cr_{Mg} - V_{Mg}$ and $Cr_{Mg} - V_{Mg} - Cr_{Mg}$ complexes which have a negative or neutral charge in the MgO matrix, thus not contributing to the space charge layer.

REMARKS ON THE La_2O_3 - Li_2O BINARY SYSTEM BETWEEN 750° AND 1000°C

F. Abbattista and M. Vallino

The La_2O_3 - Li_2O binary system has been re-examined between 750° and 1000°C where $LaLiO_2$ occurs as the only binary compound. It is characterized by a monoclinic cell ($a_0 = 5.88 \text{ \AA}$; $b_0 = 6.22 \text{ \AA}$; $c_0 = 5.84 \text{ \AA}$; $\beta = 102.53^\circ$) and is isomorphous with α - $EuLiO_2$. Any orthorhombic polymorph of this compound is excluded between 750° to 1000°C. Moreover, the cubic phase ($a_0 = 12.22 \text{ \AA}$) reported by previous researchers and said to have composition close to $LaLiO_2$ formula, actually belongs to the La - Pt - Li - O system. It has a variable composition: $LaPt_xLi_{1-x}O_2 + 1.5x$ ($x = 0.14 \pm 0.25$) and its lattice parameter varies from 12.215 \AA ($x = 0.14$) to 2.284 \AA ($x = 0.25$). An isomorphous ternary cubic phase, in which titanium replaces platinum, has also been prepared and the lattice parameter of the $LaTi_{0.16}Li_{0.84}O_{2.24}$ compositions is 12.21 \AA .

PREPARATION AND STRENGTH OF FORSTERITE-ZIRCONIA CERAMIC COMPOSITES

Shen Yangyun and R.J. Brook

Forsterite ceramics, toughened with zirconia inclusions, have been prepared by heat treating mixtures of zircon and magnesia. The ceramics have been sintered both with and without applied pressure. The extent of reaction, the fraction of tetragonal zirconia and the density of the product materials have been determined. The strength has been measured in 3 point bend tests. Owing to the fact that the rate of reaction is faster than the rate of pore removal during pressureless sintering, suitable microstructures have not been prepared by this technique. However, hot pressing yields dense, fully reacted, materials with 35% of the zirconia present in the tetragonal form; these materials have strengths ($>350 \text{ MPa}$) substantially greater than those of conventional forsterite ceramics.

SYNTHESIS OF ALUMINA AND ZIRCONIA FIBERS

P.A. Vityaz, I.L. Fyodorova, I.N. Yermolenko, T.M. Ulyanova

The results of the investigations of conversions occurring during synthesis of aluminum oxide and zirconium dioxide porous fibres with alloying additions in the temperature range from 20 to 1300°C are presented. The analysis of the experimental results enabled to reveal features typical for pyrolytic conversion and sintering of aluminum oxide — and zirconium dioxide — base ceramic fibres.

DENSIFICATION OF SILICON NITRIDE POWDER WITH VARIOUS ADDITIVES

S.K. Bhattacharya and A.C.D. Chaklader

Cold compaction behavior of a sub-micron size silicon nitride powder with additives has been studied at various loading rates up to about 450 MPa. Liquid lubricants are found to be more effective than the solid lubricants. A marked increase in relative density has been obtained with the aid of 10 weight percent polyethyleneglycol after surface treatment of the powder with a dispersant solution. The loading rate between 0.8 and 800 MPa per minute has no effect on the densification process. Results are analysed with various theoretical equations available in the literature. The Cooper and Eaton's equation and also its modified form are used to determine the mechanism of densification during cold compaction.

INTERACTION OF LiBr WITH CALCITE AND CALCIUM OXIDE POWDERS

D. Beruto, G. Belleri, L. Barco, V. Longo

The interaction of LiBr with calcite and calcium oxide powders have been studied with and without the calcite decomposition reaction, using DTA and TG analysis plus SEM and RX observations. Interactions in LiBr - $CaCO_3$ system show two possible phase transformations at the temperature of 748 K and 786 K. The second one is due to the formation of an eutectic liquid phase in the LiBr-rich region. The rate of decomposition of calcite powders was measured in dry nitrogen and in a high partial pressure of CO_2 with and without LiBr. The addition of LiBr causes the decomposition reaction to occur at a lower temperature. The LiBr changes the mechanism of the reaction. The decomposition process occurs through a liquid-phase path given by the eutectic of LiBr- $CaCO_3$. The total rate of reaction as well as the temperature dependence are related to the liquid phase. The $CaCO_3$ powders obtained have a very dense structure with a high degree of crystallization. Probably the LiBr- CaO eutectic provides a solution path for CaO

recrystallization. The effectiveness of salt addition in lowering the decomposition temperature of carbonates seems promising in saving energy, as well as in promoting changes in morphology of important commercial oxide powders.

INFLUENCE OF PRECIPITATION PROCEDURE ON SINTERABILITY OF Y_2O_3 PREPARED FROM HYDROXIDE PRECURSOR

M.D. Rasmussen, G.W. Jordan, M. Akinc, O. Hunter, Jr. and M.F. Berard

The sinterability of Y_2O_3 prepared from reverse strike hydroxide precursors was found to be highly dependent on final pH and precursor dewatering procedure, high pH precursors yielding poorly-sinterable oxides if oven dried, but quite sinterable oxides if dewatered either by acetone-toluene-acetone or controlled-humidity treatments. Direct strike hydroxide precursors yielded highly-sinterable Y_2O_3 regardless of final pH or dewatering procedure.

INHIBITION MECHANISM OF THE ANATASE-RUTILE PHASE TRANSFORMATION BY RARE EARTH OXIDES

S. Hishita, I. Mutoh, K. Koumoto and H. Yanagida

The effect of rare earth oxide additions on the anatase-rutile transformation in doped TiO_2 was investigated. Y_2O_3 , La_2O_3 , CeO_2 , Nd_2O_3 , Sm_2O_3 , Gd_2O_3 , Tb_2O_3 , Ho_2O_3 , Dy_2O_3 , Er_2O_3 , Tm_2O_3 and Yb_2O_3 , were found to suppress the transformation. The transformation process occurs in three stages. In the first stage, rare earth metal ions dissolve into interstitial sites in anatase. The resulting decrease in oxygen vacancies caused by the solid solution suppresses the nucleation of the transformation. In the second stage, the activation energy of the transformation was found to be 124 ± 3 Kcal/mol and 138 ± 4 Kcal/mol for pure anatase and anatase with 1 mol% Dy_2O_3 , respectively. The transformation mechanism of this stage is not necessarily affected by additives. The final stage is affected by the amount of rare earth oxide-titania compound phase.

THE USE OF MOLTEN MAGNESIUM CHLORIDE IN THE PREPARATION OF CRYSTALLINE CERAMIC POWDERS

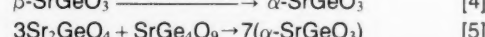
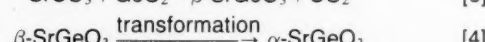
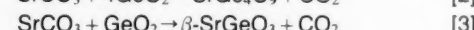
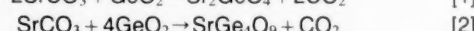
Emanuel I. Cooper and David H. Kohn

The interaction of molten $MgCl_2$ with various oxides and oxide minerals is described. Within several hours, at temperatures of 700-1100°C, components such as oxides of Fe, K, Ca and — under proper conditions — Ti are largely converted into the corresponding chlorides, the more volatile of which evaporate, the others being extracted into the liquid phase. By proper choice of stoichiometry, crystalline cordierite, forsterite, enstatite and spinel could be prepared; they contained a total < 0.2% of oxides of Na, K, Ca and Fe, and their average-diameter range was usually 1-10 μm (or larger for forsterite). The preparation of other microcrystalline powders in molten $MgCl_2$ is briefly discussed.

FORMATION AND TRANSFORMATION OF $SrGeO_3$

Osamu Yamaguchi, Hiroto Sasaki, Koji Sugiura and Kiyoshi Shimizu

The reaction of an equimolar mixture of $SrCO_3$ and GeO_2 proceeds in five stages, [1]-[5]. The overall reaction of [1], [2], and [3]



is best described by the Jander equation, the apparent activation energy being 47.6 kcal mol⁻¹ irrespective of the ball-milling time. β -Strontium metagermanate is formed directly at lower temperatures from amorphous material prepared by the simultaneous hydrolysis of strontium and germanium alkoxides. Kinetic studies of $\beta-SrGeO_3$ formation and $\beta \rightarrow \alpha$ - $SrGeO_3$ transformation are carried out by means of X-ray diffraction.

OXIDATION OF SINTERED ALUMINIUM NITRIDE

V.A. Lavrenko, A.F. Alexeev

The oxidation of sintered aluminium nitride samples having porosity of 12-16% has been studied at temperatures of 900-1100°C and 98.66 kPa oxygen pressure. It has been established that the reaction of AlN with oxygen obeys the parabolic law. The main products of AlN oxidation are α - Al_2O_3 and nitrogen with nitrogen oxides traces. The corresponding rate constants and apparent activation energy (61 kcal/mole) were calculated from the experimental data. It has been demonstrated that sintered aluminium nitride is resistant enough to high-temperature oxidation and can be used as a refractory material up to 1100°C.

RAPID SOLIDIFICATION IN THE Al_2O_3 - ZrO_2 SYSTEM

N. Claussen, G. Lindemann and G. Petzow

Eutectic compositions of Al_2O_3 and ZrO_2 have been melted and rapidly solidified by shock-wave quenching, flame-pressure atomization and high-pressure water atomization. Quenching rates $> 10^4$ K/s resulted in amorphous particles which, on annealing, crystallized at 1310°C. Microcrystalline particles with tetragonal ZrO_2 distributed in an ϵ - Al_2O_3 matrix formed at lower quenching rates. ϵ - Al_2O_3 transformed into α - Al_2O_3 on annealing at 953°C.

PRODUCTION OF HIGHLY-SINTERABLE RARE-EARTH OXIDE POWDERS BY CONTROLLED HUMIDITY DEWATERING OF PRECURSORS

G.W. Jordan and M.F. Berard

The sintering behavior of rare-earth oxide powders produced from reverse strike hydroxide, oxalate and carbonate precursors was studied. The influences of controlled humidity dewatering of precursors on powder morphology and sintering behavior were extensively studied, and were compared with those produced by oven drying or dewatering by using organic washes (ATA method). Significant differences in behavior were observed for hydroxide- and carbonate-derived powders dewatered in different ways; oxalate-derived powders showed little behavioral dependence on dewatering method. In general, controlled humidity dewatering proved effective in leading to highly-sinterable powders from any of the three precursors investigated. ATA treatment was effective for hydroxide and oxalate precursors, and oven drying generally led to good sinterability only for oxalate-derived powders. Compaction behavior and surface area of the powders were also determined and attempts were made to correlate these characteristics with sintering behavior.

FORMATION OF A NEW SOLID β TRICALCIUM ORTHOPHOSPHATE STRUCTURE, FROM REACTION BETWEEN HYDROXYAPATITE AND AMMONIUM SULFATE

M. Marraha, J.-C. Heughebaert, G. Bonef

The reaction which occurs during heating, from room temperature to 1100°C, of a mixture of hydroxyapatite, $Ca_{10}(PO_4)_6(OH)_2$ [HAP] and ammonium sulfate $(NH_4)_2SO_4$

[AS] are studied. The formation of $\text{Ca}_2(\text{NH}_4)_2(\text{SO}_4)_3$, $\text{Ca}_2\text{P}_2\text{O}_7$ and $\text{Ca}(\text{PO}_4)_2$ is observed between 200°C and 300°C; at 400°C CaSO_4 appears. From 500 to 700°C, $\text{Ca}(\text{PO}_4)_2$ reacts with CaSO_4 and with HAP and gives $\beta\text{-Ca}_2\text{P}_2\text{O}_7$. Lastly, from 700°C to 1000°C, $\beta\text{-Ca}_2\text{P}_2\text{O}_7$ reacts with HAP and with CaSO_4 and gives $\beta\text{-Ca}_3(\text{PO}_4)_2$ [$\beta\text{-TCP}$]; from 1000 to 1100°C, $\beta\text{-TCP}$ and CaSO_4 react and form a sulfate ion containing calcium phosphosulfate, the structure of which is $\beta\text{-TCP}$.

COMPLETE RHEOLOGICAL CURVES FOR CLAY DISPERSIONS AND PASTES AND THEIR ASSOCIATED ENERGETICS

N.N. Krugliski and V. Ya. Kruglitskaya

The mechanism of structural formation within ceramic systems is determined by the chemical, physical, crystal chemical mineralogical, surface and adsorption properties of the raw materials. Clay minerals (layer silicates) are most common. In processing and formation the ceramic systems are inherent in coagulation set pattern of space-thixotropic nets of certain strength. Their rheological curves are the scientific base for optimization of constructive peculiarities of production equipment taking account of energetic expenditure, in technology. In this connection the curves of clay suspensions having different structure are obtained, the yield and viscosity points are calculated and peculiarities of the contact interactions within them are stated basing on realization power of dispersed structures.

TEMPERATURE DEPENDENCE OF ELECTRICAL RESISTIVITY AND DIELECTRIC CHARACTERISTICS OF POLED AND BaZrO_3 MODIFIED BaTiO_3 CERAMICS

Morsy M. Abou Sekkina, M.K. El-Nimr and E.W. ABD Allah

Samples of pure BaTiO_3 , pure BaZrO_3 and intermediates containing from 5 up to 30% BaZrO_3 were carefully prepared by the usual ceramic procedure followed by X-ray diffraction analysis to ensure the complete reaction. Well sintered and translucent ceramic bodies were obtained. Measurements of dielectric constant (ϵ), dielectric loss ($\tan \delta$) and a.c. resistivity (ρ) were undertaken as a function of temperature up to 250°C and at various frequencies of 10-50 Kc/s before and after polarization (800 V). The effect of poling field is discussed on the basis of the presence of spontaneous polarization in BaTiO_3 lattice. Finally, it was established that the introduction of Zr^{4+} ions in BaTiO_3 lattice occurs in three steps: firstly, filling of Ba^{2+} vacancies, secondly solid solution formation from BaZrO_3 in BaTiO_3 lattice and thirdly, occupying interstitial sites in BaTiO_3 lattice.

A HIGH TEMPERATURE TERNARY PHASE IN THE SYSTEM MgO - Al_2O_3 - ZrO_2

P. Reynen, A. Firatli, D. von Mallinckrodt, H. Boeß

Short communication.

STABLE AND METASTABLE PHASE EQUILIBRIA AND REACTIONS IN THE SiO_2 - $\alpha\text{Al}_2\text{O}_3$ SYSTEM

Joseph A. Pask

Procedures in the preparation of specimens in this system are critical due to the difficulty of nucleating $\alpha\text{Al}_2\text{O}_3$ when the silicate liquid is not saturated with Al_2O_3 even though it may be supersaturated relative to crystalline $\alpha\text{Al}_2\text{O}_3$, and the ease with which mullite growing from an alumino-silicate melt during cooling accommodates an excess of Al_2O_3 . Metastable phase compositions and microstructures occur commonly. As a result, misinterpretations of experimental data have occurred in published reports. Stable and metastable phase equilibria diagrams in the $\alpha\text{Al}_2\text{O}_3$ - SiO_2 system are presented.

ELEVATED TEMPERATURE INSTRUMENTED CHARPY IMPACT OF A SINTERED SILICON CARBIDE

H.C. Chandan, L. Hermansson, H. Abe and R.C. Bradt

A commercially available, densely sintered alpha silicon carbide was tested in air from room temperature to 1700°C using a modified instrumented pendulum unit and standard Charpy size test specimens. The resistance heated silicon carbide specimens exhibited only elastic behavior, even at 1700°C. A compliance analysis of the test revealed a linear elastic decrease of the absorbed impact energy and also a decrease of the fracture stress of the silicon carbide with increasing temperature.

INFLUENCE OF CERAMIC PROCESSING ON DIELECTRIC PROPERTIES OF PEROVSKITE TYPE COMPOUND: $\text{Pb}(\text{Mg}_{1/3}\text{Nb}_{2/3})\text{O}_3$

M. Lejeune and J.P. Boilot

$\text{Pb}(\text{Mg}_{1/3}\text{Nb}_{2/3})\text{O}_3$ perovskite type compound which can be sintered at low temperatures has a high dielectric permittivity and so can be used as multilayer ceramic capacitors. In this study we show that ceramic processes resulting in different mixtures of phases and different microstructures strongly influence the dielectric properties (dielectric permittivity, dissipation factor and resistivity). Only a careful characterization in each step of the process allow the optimization of ceramics.

PRE-EUTECTIC DENSIFICATION IN MgF_2 - CaF_2

S.C. Hu and L.C. De Jonghe

Increased densification rates were found as much as 200°C below the eutectic temperature (980°C) for MgF_2 containing small amounts of CaF_2 . Constant heating rate and constant temperature sintering data, as well as microstructural developments indicated that solid state grain boundary transport rates had been enhanced by the eutectic forming additive. The effect saturated at about 1 wt% CaF_2 . The results suggest that densification of ceramic powders could be favorably affected without a substantial increase in the grain growth rate, by the addition of small amounts of eutectic forming additives, and sintering below the eutectic temperature.

DEVELOPMENT OF PHOSPHATE GLASS-CERAMICS FOR BONE IMPLANTS

F. Pernot, P. Baldet, F. Bonnel, J. Zarzycki and P. Rabischong

Porous glass-ceramics were prepared by the controlled crystallization of various phosphate «foam» glasses. The crystalline phases were detected and the following properties of the materials were studied: — textural properties: porosity, interconnection pore size distribution; — mechanical properties: fracture bending stress, Young's modulus. It is shown that these properties depend not only on the composition of the base glasses, but also upon the grain size of the foaming agent.

MECHANICAL PROCESSING OF BENTONITES

Jiří Bulandř and Jaroslav Duda

Investigations into dry grinding and pneumatic processing of three bentonite types, aimed at improving their quality, were carried out. Grinding tests indicated that changes in bentonite grain size have little effect on its quality, unless it is complemented with rearrangements in smectite texture. Common nonclay admixtures of bentonite were shown to in-

erly dilute its properties. Pneumatic processing proved efficient in separating the nonclay fraction and thus substantially improving the bentonite quality. Mutual collisions of smectite particles in the course of pneumatic processing result in their mechanical activation which substantially enhances the quality of processed bentonite.

INTERFACE INTERACTION AND STRUCTURAL TRANSFORMATION IN PARTICLES OF CERAMIC AND CERMET COMPOSITE POWDERS IN FLAME SPRAYING

Yu. Borisov and A.L. Borisova

The behavior of particles of Al_2O_3 , TiO_2 , $\text{Al}_2\text{O}_3\text{-TiO}_2$, $\text{Al}_2\text{O}_3\text{-Ni}$, $\text{ZrO}_2\text{-Ni}$, $\text{Al}_2\text{O}_3\text{-Ni-Ti}$ powders in flame spraying has been studied. The interaction between the surface tension forces and the wetting forces has been found to produce either a melt shell around the particles core or drops of the second component on the surface of the core. Subsequently a total or partial capture of drops of the second component melt by the core melt or their separation during the movement within the plasma jet volume are possible. At high particle heating and cooling rates, polymorphous transformations, higher-to-lower oxide transformations and metastable phase fixations in the coating take place. These effects influence the conditions of ceramic powder plasma coating formation and also the properties of the coatings.

RAW MATERIALS FOR THE PRODUCTION OF PIGMENTS IN THE SYSTEM $\text{ZrO}_2\text{-SiO}_2\text{-Fe}_2\text{O}_3$

M.S. Bibilashvili, O.S. Grum-Grzhimailo, N.S. Belostotskaya

The authors show that (FeZr)-pigments may be obtained from coarse-sized materials ($\mu\text{-ZrO}_2$ and $\alpha\text{-SiO}_2$) having a lower degree of chemical purity. The quantity of $\alpha\text{-Fe}_2\text{O}_3$ introduced should not exceed 8% (by weight). Mixing of batch components in a ball mill lined with porcelain plates is an indispensable condition for obtaining high-quality (FeZr)-pigments from the said raw materials. Steel taper rollers should be used as the grinding media.

ELASTIC AND PLASTIC BEHAVIOUR OF WC - Co COMPOSITES

J. Dusza, Ľ. Parilák, J. Diblík and M. Šlesár

Tungsten carbide - cobalt composites with various mean sizes of carbide grains and different fractions of binder phase were tested in compression. The fracture stress, elastic limits and deformations up to fracture were determined. By microstructural analysis the change in the microstructure at different strain levels and the mechanisms of the crack initiation and propagation were explained.

OPTIMIZING THE DEFORMATION PROPERTIES OF CERAMIC PASTES BY EVALUATING RELEVANT PHYSICAL AND CHEMICAL MECHANISMS

N.N. Kruglitski

The peculiarities of the boundary layers in silicate dispersions are described as the factors that control the interactions between the solid particles, and thus determine the structural, mechanical and deformation properties. The importance of surfactants and regularities of the structure formation are also discussed. The usefulness of elastic-plastic-viscous constants for elaboration of the optimized technology in ceramic industry is shown and the preparation of ceramic dispersions (slips) with various contents of solids, plastic pastes, semidry masses, and highly concentrated powders are analyzed.

Vol. X, January/December, 1984

THE STRUCTURE AND PROPERTIES OF REFRactory ZIRCONIA CERAMICS I. FUNDAMENTAL INVESTIGATIONS

An Annotated Bibliography of Research Works Carried out in the USSR

E.K. Koehler

This paper is a review of the Soviet fundamental investigations on zirconium dioxide, ZrO_2 -based compounds and solid solutions as regards the tasks of high-temperature technics. The review covers a period of recent 20-30 years and is mainly based on publications in the Soviet magazines such as the «Proceedings of the Academy of Sciences of the USSR» (Doklady Akademii Nauk SSSR), «Journal of Applied Chemistry» (Zhurnal Prikladnoi Khimii), «Journal of Inorganic Chemistry» (Zhurnal Neorganicheskoi Khimii), «Inorganic Materials» (Izvestiya Akademii Nauk SSSR, Neorganicheskie Materialy) and «Refractories» (Ogneupory). The paper gives an account of research work including studies of the structure of zirconium dioxide, its polymorphic transformations, the influence of various impurities and other conditions on these transformations as well as investigations of the systems containing ZrO_2 and refractory oxides of elements of groups II, III, IV and V of the periodic system. It is also concerned with problems of the mechanism and kinetics of interaction between oxides in ZrO_2 -containing systems. The second part will be devoted to applied investigations directed towards the elaboration of the synthesis processes of zirconia materials, the preparation of ceramic materials from them, the study of the relations between composition, structure and physicochemical properties. The third, concluding part, will contain information about the elaboration of several concrete technical materials for various purposes and their properties.

FORMATION OF SILICON OXINITRIDE FROM Si_3N_4 AND SiO_2 IN THE PRESENCE OF Al_2O_3

Z.K. Huang, P. Greil and G. Petzow

The formation of $\text{Si}_2\text{N}_2\text{O}$ from SiO_2 and $\alpha\text{-Si}_3\text{N}_4$ powder mixtures with addition of 3 mol % Al_2O_3 was investigated. An eutectic at 98 mole % SiO_2 and 2 mole % Si_3N_4 was formed at 1863 K which is decreased by the Al_2O_3 , thus enabling the formation of $\text{Si}_2\text{N}_2\text{O}$ via the liquid phase. Microstructural analysis by TEM showed a strong orientation between $\text{Si}_2\text{N}_2\text{O}$ and $\alpha\text{-Si}_3\text{N}_4$ crystals. Oxidation resistance and bending strength were also measured.

INFLUENCE OF POWDER PROPERTIES AND PROCESSING CONDITIONS ON MICROSTRUCTURE AND MECHANICAL PROPERTIES OF SINTERED Si_3N_4

G. Wötting and G. Ziegler

The influence of powder properties and the amount and ratio of $\text{Y}_2\text{O}_3\text{-Al}_2\text{O}_3$ -additions on sintering behaviour, microstructural development and mechanical properties was investigated. The effect of applied pressure was studied by hot pressing and hot-isostatic-pressing experiments with powder compacts and sintered materials. The results show a strong dependence of the densification behaviour on powder properties (specific surface area, grain morphology, oxygen and carbon content), amount and composition of sintering aids, and applied pressure. It was found that microstructure, characterized quantitatively by the mean length and the aspect ratio of the elongated β -grains, is strongly dependent on the amount and viscosity of the secondary phase. The mechanical properties, fracture strength and fracture toughness, are mainly controlled by the aspect ratio and grain size.

PREPARATION AND PROPERTIES OF BINARY AND TERNARY COMPOSITE SOLIDS IN THE CLAY-MICA-GLASS SYSTEM

M.M.P. Low and P. Fazio

Binary and ternary composite solids in the clay-mica-glass system have been fabricated by combining both natural mica flakes of the phlogopite type and ground powders prepared from recycled waste glass, and clay grains and mixtures of clay-glass powders, employing a simple sintering process at temperatures in the range of 850-1050°C. Results of the study showed that these composites have very different physical appearance and material characteristics. In the glass-mica system, mixtures can be fabricated into composite solids which exhibit either a porous cellular structure or a densified ceramic structure. The mixtures can also be fabricated into multilayer structural products consisting of both the cellular structure layer and densified structure layer. In the clay-mica binary system and in the clay-mica-glass ternary system, mixtures can be readily fabricated into composite solids with low density and low thermal conductivity. All composite solids showed excellent insulation properties and would contribute to energy conservation when used for building envelope design applications.

KINETIC STUDY OF THE CRYSTALLIZATION OF AMORPHOUS - DERIVED $\text{CaO} \cdot 2\text{Al}_2\text{O}_3$

M. Vallino

An amorphous-solid with a high degree of homogeneity has been prepared which, upon heating for a few hours at 850°C, gives well crystallized monoclinic Ca_2 . The amorphous material transforms into monoclinic Ca_2 via a phase having a $\gamma\text{-Al}_2\text{O}_3$ type structure. Isotherms of transformation from the $\gamma\text{-Al}_2\text{O}_3$ phase to monoclinic Ca_2 , may be described by a first-order equation - $\ln(1-f) = kt$; the activation energy corresponding to this phase transformation is 112 ± 5 kcal/mol.

COUNTER CURRENT COMPENSATION OF DOUBLE DOPED $\text{Pb}(\text{Zr}_{1-x}, \text{Ti}_x)\text{O}_3$ PIEZOELECTRIC CERAMICS

M.M. Abou-Sekkina and Bd-El-Raouf F. Tawfik

Various compositions of pure $\text{Pb}(\text{Zr}/\text{Ti})\text{O}_3$ having Zr/Ti ratio ranging from 50/50 up to 58/42 were prepared by the usual ceramic technique and firing at 1400°C. The prepared materials were single doped with 0.1 wt.% lanthana and double doped with (0.1 wt.% lanthana + 0.1 wt.% neodymia). Measurements of dielectric properties (constant and anisotropy), piezoelectric properties and Young's modulus were conducted as a function of Zr/Ti ratio and type of doping. The obtained results were discussed on the bases of the effects of varying (Zr/Ti) ratio and single doping with lanthana on forcing of $\text{Pb}(\text{Zr}/\text{Ti})\text{O}_3$ normal lattice to a defective crystal lattice having high dielectric values. Further lattice strain and defects were induced by static stress causing a generation of high piezoelectric charges at the surface of the specimens. A conclusion had been attained that $\text{Pb}(\text{Zr}_{0.55}, \text{Ti}_{0.45})\text{O}_3$ doped with 0.1 wt.% La_2O_3 constitutes the optimum composition for attaining a better quality ceramic dielectric and piezoelectrics to be used in industry for converting mechanical energy (static stress) to electrical energy (piezoelectric charges). Thus, it was possible to make use of counter doping (compensation phenomenon) to control the desired properties and to get rid of the undesired impurities in ceramic bodies in industry which would be very profitable economically instead of chemical purification or other destructive means.

A COMMENT ON THE EQUILIBRIUM OF $\text{Si}_3\text{N}_4 + 3\text{C} \rightleftharpoons 3\text{SiC} + 2\text{N}_2$

A. Kato, H. Mizumoto and Y. Fukushige

Short communication.

STRUCTURE FORMATION IN HEATED CLAY DISPERSIONS

V.V. Minchenko and S.F. Mischenko

The results of an investigation of structure formation processes in mineral dispersions are given. It is shown that the thixotropic phenomenon has an important meaning in the strengthening of mineral systems without additional pressure. The conditions for achieving optimum structure under drying of mineral dispersions were revealed. The theological investigations of some minerals under high temperature was introduced, and the role of crystalline transformations of kaolinite and montmorillonite was shown affect the greatest plastic viscosity η_1 of their dispersions.

DISPERSION OF BaTiO_3 POWDERS (PART I)

S. Mizuta, M. Parish and H.K. Bowen

The fundamental properties of BaTiO_3 dispersions in pure organic liquids and water were studied by sediment volume and contact angle measurements. The liquid groups included alcohols, aldehydes, acids, esters, ketones, ethers, hydrocarbons, and water. Benzaldehyde was found to be the best dispersing medium for the commercial BaTiO_3 powders tested.

HOT-PRESSING OF BORON CARBIDE

R. Angers and M. Beauvy

Seven different boron carbide powders were hot-pressed between 1775 and 2575 K at pressures from 20.7 to 68.9 MPa during various times. The influence of temperature, pressure, time and heating and cooling rates on densification of these powders and on the microstructure of the hot-pressed specimen were studied. It was found that temperatures above 2400 K are necessary to obtain fully dense boron carbide and that densification is strongly influenced by the characteristics of the starting powder. The cooling rate has also an effect on the density of hot-pressed specimens.

PRESSURE SINTERING OF $\text{Al}_2\text{O}_3\text{-MgO}$ MIXTURES UNDER 10 KBARS

K. Kodaira, S. Teramoto, S. Shimada and T. Matsushita

Densification of $\text{Al}_2\text{O}_3\text{-MgO}$ mixtures was performed under 10 kbars. Theoretically dense translucent ceramics were obtained at 1000-1300°C for 15-60 wt% MgO and 75-40 wt% Al_2O_3 . Within this composition range, a uniform grain size of $\sim 0.5 \mu\text{m}$ was obtained with the absence of abnormal grain growth. Fragmentation and rearrangement of particles take place as operative mechanisms in the initial stage of sintering.

DEVELOPMENT OF LIGHT-WEIGHT INSULATING CLAY PRODUCTS FROM THE CLAY-SAWDUST-GLASS SYSTEM

N.M.P. Low, P. Fazio and P. Guite

Employing a simple dry-pressing and sintering process, lightweight clay products with various physical, mechanical and thermal properties have been fabricated from mixtures of maplewood sawdust and local gray burning clay and mixtures of sawdust, clay and soda-lime glass grains prepared from recycled waste glass. Studies showed that thermal conductivity, compressive strength, and cold water absorption of the sintered sawdust-clay products are significantly modified by the addition of sawdust particles to the clay mixes. Studies also showed that portions of the clay particles can be

VOI
11
1985

replaced with soda-lime glass grains of similar sizes. These light-weight composite clay products have compressive strength in excess of 31 MN/m², thermal conductivity value in the range 0.21-0.39 W/m, °C and water saturation coefficient of about 0.72. The fabricated clay products exhibit attractive characteristics as building materials and could contribute to energy conservation because of their high thermal insulation value.

THE STRUCTURE AND PROPERTIES OF REFRACTORY ZIRCONIA CERAMICS

II. APPLIED INVESTIGATIONS

A Review of Research Works Carried out in the USSR

E.K. Koehler

In a previous publication (Ceramics International 10, 1984, 3) we considered the fundamental investigations carried out in the USSR on the systems containing zirconium dioxide. The practical use of ZrO₂ - based materials required the elaboration of a number of applied problems important for refractory technology and use. These include: the synthesis methods of compounds and solid solutions; molding of wares; the influence of modifying additions and non-stoichiometry of oxides on the sintering temperature and crystal growth; measures for increasing thermal shock resistance. The works in the indicated directions were carried out mainly at the ceramic departments of higher technical educational schools and industrial research institutes. In reviewing each of the above problems we tried to follow the chronological order in the publication of papers.

NARROW SIZE DISTRIBUTION POWDERS FROM COMMERCIAL CERAMIC POWDERS

M. Parish and H.K. Bowen

Size classification of commercial ceramic powders to obtain powders possessing more nearly ideal characteristics (submicron size, equiaxed, and monodispersed) is presented. A powder-liquid dispersion sedimentation technique was used to acquire the narrow size distribution, submicron ceramic powders. This paper discusses the basic theory and methods of the classification techniques with an example and variations.

THE INFLUENCE OF RAW MATERIALS COMPOSITION ON THE PROPERTIES OF FIRED CLAY PRODUCTS

N.N. Kruglitsky, B.M. Datsenko and B.I. Moroz

One factor controlling formation of ceramic structures is the initial mineralogical composition which has a great influence on processing and fabrication stages and the properties of the product. This paper investigates the relationship between the mineral content of raw compositions and the product properties after thermal treatment. Optimum compositions have been established for binary and ternary systems of kaolinite, hydromica, montmorillonite and also their genetic varieties. The trends have been used to develop new ceramic compositions with improved properties.

DISPERSION OF BaTiO₃ POWDERS (Part II)

S. Mizuta, M. Parish and H.K. Bowen

Highly concentrated BaTiO₃ suspensions in benzaldehyde were investigated for adaptation toward tape casting. Effects of particle concentration, total particle mass, gravitational forces, and particle size distribution on sediment density were studied.

MODE OF TALC ADDITION AND ITS EFFECT ON THE PROPERTIES OF CERAMIC BODIES

E.H. Sallam, S.M. Naga and D.M. Ibrahim

Raw and precalcined talc were added to feldspar to produce low temperature firing mixes. The feldspar content was kept constant, 25%, while talc was added in the range from 5 to 15% at the expense of quartz. Mixes were fired between 1150° to 1400°C. The results show that there is no significant difference in the properties obtained for the fired bodies whether talc is added raw or in a precalcined state. The addition of raw talc favoured the formation of cordierite in low-addition (5-10%), while addition of precalcined talc favoured its formation in high-addition (15%). The mode of talc addition affected the form and shape of enstatite and cordierite grains developed.

SOME COLOR ASPECTS OF PARIAN BODIES

M. Hassanein, Wafa I. Abdel-Fattah, K. Nakhla and F.A. Nour

The two coloring oxides, CoO and NiO were included separately in a self-glazed parian body «highly feldspathic porcelain» in 5 different concentration between 1 and 10 wt%. The host body consisted of 75% feldspar and 25% kaolin. The mixes were pressed and matured between 1125°C and 1150°C. The produced colors were characterized visually as well as in reference to the CIE system. The densification of the blue and green bodies were slightly reduced, although higher density values were achieved. This was attributed to the effect of the Co²⁺ or Ni²⁺ dense aluminate or silicate. However, their influence was counter balanced by the enhanced leucite formation and higher porosity glassy phase. Various shades of blue were obtained by introducing Co²⁺. Maximum difference in color $\Delta E = 12.97$ Judds was obtained by incorporating 5 wt % and firing at 1125°C while a value of 11.69 Judds was obtained upon firing a specimen with only 1 wt % at 1150°C. The latter value is comparable to that obtained by incorporating 10% of blue stain. Ni²⁺ produced various shades of green with a maximum of $\Delta E = 5.44$ Judds upon firing a sample with 5 wt % at 1150°C. The results are discussed in view of the ligand field theory as well as X-ray diffraction analysis.

EFFECT OF PRECURSOR FREEZE-DRYING CONDITIONS ON THE SINTERABILITY OF HYDROXIDE-DERIVED Y₂O₃ POWDERS

M.D. Rasmussen, M. Akinc and M.F. Berard

The effect of a variety of precursor freeze-drying treatments on the sinterability of Y₂O₃ powders produced by calcination of reverse strike hydroxides were investigated. Attempts were made to separate the influences of the freezing step and the subsequent water removal step. Variations in both steps were found to affect ultimate sinterability. Freezing of the gelatinous precursor was found to be beneficial, regardless of the way in which water was later removed, although vacuum removal without remelting led to the most sinterable powders. A brief study was made of possible benefits to be derived by precipitation of the precursor at pH values above that corresponding to the isoelectric point.

MÖSSBAUER STUDIES OF THE CORROSION REACTIONS IN ARC-FURNACE REFRACTORIES - PART I

C. Saragovi-Badler and C. Puglisi

The purpose of this paper is to show the kind of information that can be obtained from the use of Mössbauer spectroscopy in the study of corrosion reaction taking place between refractories and metallurgical environments.

Mössbauer spectroscopy provides information concerning the local surroundings of iron ions in any solid material, and this can be useful in the study of the above mentioned reactions, considering the important role of iron in them. The present paper describes the wear mechanism of the high-alumina roof and the basic magnesia bricks at the slag line of an arc-furnace. The analysis of the high alumina bricks indicate that the chemical reactions taking place in service produced mainly calcium ferrite, some cordierite and anorthite. The iron oxide migrating into the brick was partially incorporated by the corundum grains as solid solution and partially remained as impurified magnetite and hematite. In the case of the slag-line magnesia bricks, the main identified products are magnesio-ferrite and magnesio-wüstite. The rest of the iron content is distributed in the silicate phase which was probably liquid at the service temperature, giving rise on cooling to glassy and crystalline silicates. From the peaks area of the Mössbauer spectra an estimation of the iron distribution among the different components can be calculated.

MÖSSBAUER STUDIES OF THE CORROSION REACTIONS IN ARC-FURNACE REFRactories - PART II

C. Puglisi, F. Labenski and C. Saragovi-Badler

Mössbauer spectroscopy has been used, together with conventional techniques, in the study of corrosion reactions taking place in service in co-clinkered chrome-magnesite bricks from the hot spots of an electric-arc furnace. Co-clinkered bricks present a better distribution of spinel phases than conventional bricks of similar composition. The Mössbauer data show that iron uptake took place in service, being incorporated only into the spinel structure. This structure accepts considerable substitutional ions, admitting in this case impurities from the slag. Experimental results confirm the relative stability of that phase in the presence of migrating components of the slag.

DENSIFICATION OF NONADDITIVE SnO_2 BY HOT ISOSTATIC PRESSING

S.J. Park, K. Hirota and H. Yamamura

Short communication.

THERMAL SPRAYING OF CERAMICS

P. Chagnon and P. Fauchais

In the last few years, the number of publications dealing with ceramic coatings has increased very rapidly. To present an overview of this field, a bibliographic review of the thermal sprayed ceramics is performed. Investigated and studied successively are the thermal spraying techniques (flame, plasma and detonation), the sprayed ceramics and the applications of these coatings. It appears that plasma spraying is the most common technique, that ceramic coatings are most often made of the metal oxides and their main application is for wear resistance.

INFLUENCE OF THE CO_2 BACK FLUX ON THE REACTION MECHANISMS OF BaTiO_3 FORMATION FROM HIGH TiO_2 CONTENT IN $\text{TiO}_2\text{-BaCO}_3$ MIXTURES

M. Gavoglio and D. Beruto

The solid state reactions between 18.2% mol BaCO_3 - 81.8% mol TiO_2 powders were investigated in the initial stage of the process where BaTiO_3 is the only solid products. In O_2 (g) environment BaTiO_3 formation occurs in two regimes. The first one is characterized by a total apparent activation enthalpy (ΔH^\ddagger) of 42 kJ/mol ± 20 kJ/mol. The second one is a more activated process with ΔH^\ddagger equal to 230 kJ/mol ± 25 kJ/mol. In CO_2 (g) environment and 'in vacuo' there was only one activated process with a ΔH^\ddagger respectively equal to 222 kJ/mol ± 25 kJ/mol and to 20 kJ/mol ± 10 kJ/mol. The low activated mechanism is consisted with a layered interphase model, while the high activated step requires a bulk phenomena such as needle-like crystals BaTiO_3 grown from TiO_2 particles.

The chemical composition of cristobalite, tridymite, glass, and accessory phases of different zones of used silica bricks taken from the roof of a glass tank was studied with a high resolution microprobe. Tridymite and cristobalite contain as impurities TiO_2 (≤ 0.36 wt%), Al_2O_3 (≤ 0.37 wt%), and Na_2O (≤ 0.27 wt%). Main constituents of the glass phase coexisting with crystalline silica are: SiO_2 (74 to 60 wt%), TiO_2 (0.4 to 9 wt%), Al_2O_3 (1 to 5 wt%), Fe_2O_3 (0.3 to 3 wt%), CaO (5 to 20 wt%), and Na_2O (8 to 17 wt%). Temperature curves within the bricks during operation of the glass tank have been estimated using direct temperature measurement at the hot front of the bricks, and the transition temperatures of cristobalite to tridymite (~1450°C), and of α - to β -wollastonite (~1200°C). Microchemical data and supposed temperatures were correlated with the Nernst distribution law. The applicability of the Nernst law shows that local equilibrium conditions were reached during the use of the bricks; they have been preserved during cooling of bricks. The results of the Nernst law cation distribution imply that structural saturation with Al_2O_3 , TiO_2 , and Na_2O was not reached in the investigated composition range. Al^{3+} is believed to substitute Si^{4+} at tetrahedral lattice sites. Al^{3+} substitution is favoured with decreasing temperature in relation to the Al_2O_3 content in the glass phase. $\text{Al}^{3+} \rightarrow \text{Si}^{4+}$ substitution produces charge deficiency, which is compensated by interstitial entry of Na^+ into structural channels and voids of tridymite and cristobalite. Ti^{4+} incorporation into the cristobalite and tridymite structures is favoured at higher temperatures with respect to the TiO_2 content of the glass phase. The close reciprocal dependence between Al^{3+} and Ti^{4+} in silica may indicate that Ti^{4+} is tetrahedrally incorporated as well.

SYNTHESIS, PROPERTIES AND APPLICATION OF HIGH CONDUCTIVE LaCrO_3 -BASED CERAMIC MATERIALS

S.T. Song, H.Y. Pan, Z. Wang and B. Yang

The synthesis of LaCrO_3 and LaCrO_3 -based materials by the hydrothermal method and in air has been investigated. In respect to the synthesized products, the structure and a number of physical properties, such as electrical and magnetic properties, are discussed. The authors utilized the doped LaCrO_3 material as various «conducting leads» for ZrO_2 -based heating elements to substitute the expensive Pt-Rh wire. The working temperature of these elements can be up to 2000-2100°C in oxidizing atmosphere.

ELASTIC/PLASTIC INDENTATION IN CERAMICS: A FRACTURE TOUGHNESS DETERMINATION METHOD

P. Miranzo and J.S. Moya

An extensive literature survey of the evolution of the indentation technique is made. The elastic/plastic solution for the spherical cavity expansion is used to obtain a physical explanation for the quantitative measurement of the radial cracks that occur at the indentation impression corners.

Finally an expression based on the mentioned theory is given. Experimental data from a serie of brittle materials are well fitted by this expression.

SOLID-STATE REACTION OF Cr_2O_3 AND SnO_2

P. Escribano, C. Guillen and J. Alarcon

Various mixtures of $\text{SnO}_2\text{-Cr}_2\text{O}_3$ and $\text{SnO}_2\text{-K}_2\text{Cr}_2\text{O}_7$, were subjected to different thermal treatments. The crystalline phases in the calcination products have been identified by X-ray diffraction. The non-formation of definite compounds was also proved by diffuse reflectance: The structural environment of the cation Cr(III) was also studied.

solution as starting reagents, respectively, produced an amorphous or crystalline oxalate regardless the reagent for Ba. The crystalline oxalate has a different structure from the one reported previously. It may be speculated that this originates from the deficiency of water of crystallization. Chemical formula of the oxalate obtained in the present study could correspond to $\text{BaTiO}(\text{C}_2\text{O}_4)_2\text{-3H}_2\text{O}$ as indicated by TGA experiments. The oxalate, which was prepared by use of $\text{Ba}(\text{NO}_3)_2$ and $\text{TiO}(\text{NO}_3)_2$ as starting reagents and by low reaction-temperature and rapid titration-rate of ethanol solution of oxalic acid to Ba-Ti mixed aqueous solution, converted to stoichiometric barium titanate having a perovskite-type structure with tetragonal symmetry. The barium titanate obtained consists of very fine particles of size around $0.3\ \mu\text{m}$ and shows translucency after hot pressing at 1150°C for 3 hr at $600\ \text{kg}/\text{cm}^2$.

Vol. XI, January/December, 1985

THE STRUCTURE AND PROPERTIES OF REFRACTORY ZIRCONIA CERAMICS

III. STUDIES OF TECHNICAL PROPERTIES OF MATERIALS AND TECHNOLOGICAL ELABORATIONS

A Review of Research Works Carried out in the USSR
E.K. Koehler

The use of zirconia and zirconia-containing materials in the various fields of engineering required a study of their appropriate properties. In the majority of cases the determination of these properties were made along with the general physical-chemical investigation of zirconia-containing oxide systems and related with the phase composition and structure of the material. For convenience of comparison of the results obtained, the papers have been grouped according to their main topics in the following subgroups: (1) thermal properties (refractoriness, thermal expansion coefficient, heat conduction, thermal shock resistance); (2) chemical properties (acid-and alkali resistance, wettability with various melts etc.); (3) mechanical properties at room and elevated temperatures; (4) electrical properties; (5) evaporation, high-temperature erosion; (6) optical, radiation properties, coatings etc. The list of references is given in the general chronological order of the publication of papers.

THE USE OF ELECTRICAL CONDUCTIVITY MEASUREMENTS TO STUDY SINTERING MECHANISMS

M. Haviar, Z. Pánek and P. ŠAJGALÍK

A new method for the determination of neck size and for assessing the contribution of nondensifying mechanisms to the total mass transport during sintering has been developed. The method is based on the simultaneous measurement of the conductivity and shrinkage of the sintering sample. From the conductivity value the instant neck size is calculated. The knowledge of the neck size and shrinkage enables us to determine the contribution of nondensifying mechanisms to the total mass transport during sintering.

PREPARATION OF BARIUM TITANATE BY OXALATE METHOD IN ETHANOL SOLUTION

H. Yamamura, A. Watanabe, S. Shirasaki, Y. Moriyoshi and M. Tanada

Barium titanate was prepared by addition of ethanol solution in oxalic acid to barium-titanium mixed aqueous solution at room temperature. The influence of various factors such as starting reagents, reaction temperature and titration rate were investigated. The use of TiCl_4 or $\text{TiO}(\text{NO}_3)_2$

PREPARATION OF PLZT BY OXALATE METHOD IN ETHANOL SOLUTION

H. Yamamura, M. Tanada, H. Haneda, S. Shirasaki and Y. Moriyoshi

PLZT oxalate was prepared by addition of an ethanol solution of oxalic acid to an aqueous solution with Pb, La, Zr, and Ti at 30°C . The resulting oxalate had very fine particle size, but was usually much agglomerated after filtration. The agglomerated powders were highly dispersed by washing with pure ethanol more than three times, whereby the crystalline oxalate was transformed to an amorphous due to the removal of water of crystallization by ethanol. This effect was confirmed by the TEM observation, and measurement of particle size distribution and surface area. The calcined particles in the «As-filtered» and the «Washed» oxalates at 800°C in air was found to be $25\ \text{nm}$ and $15\ \text{nm}$ respectively by TEM. The PLZT powder from the «Washed» sample, calcined at 800°C , gave transparent high-quality PLZT after hot pressing ($600\ \text{kg}/\text{cm}^2$, 10 hr at 1150°C).

SYNTHESIS, FORMATION MECHANISMS AND POLYMORPHISM OF IRON AND/OR ALKALI-SUBSTITUTED CORDIERITES

Y.H. Kim, J.P. Mercurio and C. Gault

Iron and/or alkali substituted cordierites with general formula $\text{X}_{2y}(\text{Mg}_{1-x}\text{Fe}_x)_2\text{Al}_{4+2y}\text{Si}_{5-2y}\text{O}_{18}$ where $\text{X} = \text{Li}, \text{Na}, \text{K}, \text{Rb}, \text{Cs}$ and $0 \leq x, y \leq 1$ have been synthesized either by solid state reaction or by glass crystallization. The mechanisms involved during the syntheses have been studied as a function of composition and experimental conditions. A semiquantitative test for the extent of the hexagonal \rightarrow orthorhombic transformation has been proposed.

A COMPARISON OF PLASTER CASTING AND PRESSURE CASTING OF SANITARYWARE WITH PARTICULAR REFERENCE TO CLAY PROPERTIES

C.S. Hogg

Sanitaryware body slips have been prepared using a range of ball clays and china clays, and the pressure casting and plaster casting properties of these slips were examined as a function of their state of deflocculation. Some properties of the resulting cast pieces were also investigated. Pressure casting was carried out at two pressures, 13.3 and 40 bar and at the higher pressure, slip temperatures of 20 and 40°C were used. It was confirmed that casting times can be substantially reduced by pressure casting compared with plaster casting. The ratio of pressure casting time to plaster casting time is independent of the ball clay or china clay type used in the body, confirming that the parameters controlling casting time are the same for both pressure and plaster casting. It was also shown that while plaster casting times

are significantly influenced by slip thixotropy, pressure casting times are almost independent of this parameter. Moisture contents of pressure cast pieces were lower than those of plaster cast pieces by up to 3 wt% and there was little variation with slip thixotropy. As a result of the decreased moisture contents, drying shrinkages of pressure cast pieces were reduced. Also as a result of their lower moisture contents, the stiffness of pressure cast pieces was equivalent to or higher than that of plaster cast pieces that had been dried for two or three hours, thus allowing the pieces to be demoulded immediately after forming.

OXYGEN PENETRATION INTO SILICON CARBIDE CERAMICS DURING OXIDATION

J.A. Costello and R.E. Tressler

The penetration of oxygen into polycrystalline silicon carbide ceramics, in advance of the oxide/substrate interface, during oxidation for 1-100 hrs at 1200-1400°C was studied using SIMS and TEM techniques. Fully dense hot pressed ceramics containing aluminum additives, with and without an oxide grain boundary phase and CVD silicon carbide exhibited sharp interfaces. Sintered silicon carbides with boron and carbon additives (~97% dense) and aluminium carbide additive (~90% dense) exhibited a region of oxygen penetration ~10-15 μm in depth beneath the oxides scale, the depth of which was insensitive to the time and temperature of oxidation. The amorphous oxide phase in this zone was located at three and four grain junctions but the two grain junctions were unaffected in this zone by oxidation. This oxygen affected region, which is responsible for the slow crack growth susceptibility of these ceramics after oxidation, results from gaseous oxygen penetration along interconnected or nearly interconnected pores and oxidation of impurity laden channels and SiC surfaces. The depth of penetration is presumably limited by closure of the channels by the oxidation products.

CONSTITUTION OF CALCINED REFRACRYORY-GRADE BAUXITES: AN INTERPRETATION

A. Caballero, F.J. Valle, S. De Aza and S. Castillo

Four calcined refractory bauxites were studied by ICP, EDX, X-ray and optical microscopy. Results were interpreted by considering the systems $\text{Al}_2\text{O}_3\text{-SiO}_2\text{-TiO}_2$ and $\text{Al}_2\text{O}_3\text{-SiO}_2\text{-TiO}_2\text{-Fe}_2\text{O}_3$. An equilibrium index was established as a measure of degree of calcination. Influence of microheterogeneity on calcined microstructure is discussed.

PROCESSING OF YTTRIA POWDERS DERIVED FROM HYDROXIDE PRECURSORS

M.D. Rasmussen, M. Akinc and O. Hunter Jr.

Roles of calcination and sintering schedules on the final sintered density and microstructure of Y_2O_3 compacts were studied. Optimum calcination procedure appeared to be at 1000°C and for one hour in air atmosphere. Final sintered density of 95% theoretical was achieved around 1450° and nearly pore free (>99% theoretical) pellets were obtained at 1650°C for one hour sintering in vacuum. High heating/cooling rates when coupled with high sintering temperature caused discontinuous grain growth and large internal cracks.

HfO₂-BASED REFRACRYORY COMPOUNDS AND SOLID SOLUTIONS

1. Phase Diagrams of the Systems $\text{HfO}_2\text{-M}_2\text{O}_3$ and $\text{HfO}_2\text{-MO}$

V.B. Glushkova and M.V. Kravchinskaya

This paper is a review of works performed mainly in the USSR. The purpose of many of these works was the finding of new refractory compounds which could create the basis of

high-refractory materials. The objects of the investigations were hafnium dioxide (HfO_2) and oxides of alkali-earth and rare-earth elements. The phase diagrams for the systems $\text{HfO}_2\text{-Ln}_2\text{O}_3$ and $\text{HfO}_2\text{-MO}$ are given as well as the structures of the compounds and solid solutions formed in the systems.

MICROSTRUCTURAL CHANGES IN HOT-PRESSED SALT-LIME BODIES DURING HEATING

J. Zborowski

Processes occurring in the ternary $\text{CaO-CaCl}_2\text{-CaCO}_3$ on heating and their effects on microstructure of salt-lime bodies are discussed. Volume and density changes in investigated bodies accompanying CaCO_3 decomposition and CaCl_2 high-temperature transformation were followed to 1770 K and the distribution of the products of those processes in the microstructure was determined. The behaviour of dense, hot-pressed salt-lime bodies on heating is not similar to that of pure oxide nor to the previously described cold formed salt-lime briquettes. Marked expansion was noticed within the range of 870-1170 K in connection with CO_2 evolution. Further disturbance of the sintering process was observed at higher temperatures as the result of the CaCl_2 high-temperature transformation. Rather rare SEM pictures of secondary CaO which crystallize as the results of the forementioned processes are presented. Some remarks on the possibilities of modification of the observed salt-lime bodies behaviour are presented.

CORROSION STUDY ON CERAMICS FOR CONDUCTANCE MEASUREMENTS OF MOLTEN CARBONATES

S. Tanase, Y. Miyazaki, M. Yanagida and T. Kodama

In order to find corrosion-resistant materials applicable to a conductance cell used in a conductance measurement apparatus for molten carbonates, several ceramics were examined for durability in both hydrochloric acid solution and carbonate melt. It was found that beryllia-based ceramics and alumina ceramics of high purity exhibited high corrosion-resistance against those agents, and could be applied in conductance cells. This article gives valuable criteria for the application of potential ceramic materials in carbonate melts.

MECHANICAL PROPERTIES OF $(\text{Pb,Ca})\text{TiO}_3$ FAMILY CERAMICS WITH ZERO PLANAR COUPLING FACTOR

T. Yamamoto, H. Igarashi and K. Okazaki

Mechanical properties of $(\text{Pb,Ca})\text{TiO}_3$ family ceramics were measured using a micro-indentation technique and a three point bending test. The internal stress was calculated from the fracture toughness measurement and the grain size dependence of the internal stress was found. In addition, it was shown that internal stresses induced by poling were compressive and tensile in the directions perpendicular and parallel to the poling field, respectively. The magnitude of anisotropy in internal stresses was estimated by 110 MN/m². From three point bending test, it was revealed that the average failure stress for the poled samples became weaker compared to that for the unpoled sample, because of the fracture surface by the DC field application.

HfO₂-BASED REFRACRYORY COMPOUNDS AND SOLID SOLUTIONS

2. Kinetics and Mechanism of Compound Formation in the Systems $\text{HfO}_2\text{-M}_2\text{O}_3\text{-MO}$

V.B. Glushkova and V.A. Krzhizhanovskaya

In a previous communication we considered the papers published in the USSR on studies of phase diagrams for the

systems hafnia-alkali-earth oxides and hafnia-rare-earth oxides. The purpose of many investigations was the preparation of new refractory compounds and solid solutions which could create the basis for high-refractory materials. In addition to the great analogy between binary systems with hafnia and zirconia, our interest in hafnium-containing compounds was promoted by their higher melting temperatures compared with those of zirconia-based compounds and by several peculiar physico-chemical properties characteristic of hafnia-based compounds and solid solutions. It has been shown in the HfO_2 -MO systems, strontium forms the greatest number of compounds: SrHfO_3 , Sr_2HfO_4 , $\text{Sr}_3\text{Hf}_2\text{O}_7$ and $\text{Sr}_4\text{Hf}_3\text{O}_{10}$; calcium forms two compounds: CaHfO_3 and CaHf_4O_9 ; barium and magnesium each produce one compound: BaHfO_3 and $\text{Mg}_2\text{Hf}_2\text{O}_{12}$, respectively. Rare earth oxides with large ionic radii usually form pyrochlore-type (P) compounds of composition $\text{Ln}_2\text{Hf}_2\text{O}_7$, whereas rare-earth oxides with small ionic radii combine with hafnia to form wide regions of fluorite-like solid solutions. In the region of compositions corresponding to the pyrochlore-type compounds rare-earths with the smallest ionic radii (Sc, Yb) form compounds with rhombohedral structures (R) of the composition $\text{M}_4\text{Hf}_3\text{O}_{12}(\text{M}_7\text{O}_{12})$. Together with the latter, compounds $\text{M}_7\text{O}_{11.5}$ and M_7O_{11} were found for gadolinium and erbium and M_9O_{17} and M_7O_{13} for scandium. Most of these compounds are stable only over a certain temperature range and transform into disordered F-type cubic solid solutions at elevated temperatures. In addition, there exist limited regions of solid solution based on the monoclinic (M) and tetragonal (T) modifications of HfO_2 as well as on various structural modifications (C, B, A, H, X) of rare-earth oxides.

SOL-GEL DERIVED ALUMINA SUBSTRATES

J.J. Lannutti and D.E. Clark

Sol-gel processing may provide an alternative to the current tape cast powder method manufacturing alumina substrates. The two methods are compared and advantages/disadvantages are discussed. One potential disadvantage of the sol-gel derived alumina substrates has been their brittleness after drying. The use of glycerol improves the flexibility of the

prefired dried gels, making it possible to fabricate a variety of shapes through punching, cutting and laminating.

MICROINDENTATION BEHAVIOUR K_{IC} FACTOR DETERMINATION AND MICROSTRUCTURE ANALYSES OF SOME $\text{Li}_2\text{O}-\text{SiO}_2$ GLASS-CERAMIC MATERIALS

J.Ma Rincon and F. Capel

Knoop and Vickers microhardnesses as well as K_{IC} values obtained from microindentation methods for some $\text{Li}_2\text{O}-\text{SiO}_2$ glasses and glass-ceramic materials (26-36 mol% Li_2O) have been determined. The microhardness values and the indentation textures as observed by SEM have been discussed and related to the microstructure and the percentage of crystalline phases present as determined by XRD.

MAGNESIUM-COBALT (II) - ALUMINIUM SPINELS FOR PIGMENTS

H. Warachim, J. Rzechula and A. Pielak

Magnesium, cobalt (II) and aluminium hydroxides coprecipitated from a single solution have been sintered at 400-1200°C for 0.5 to 8 hours. A series of spinels of a general formula $\text{Mg}_{1-n}\text{Co}_n\text{Al}_2\text{O}_4$ have been obtained. Within the entire range of compositions the colour of the products sintered above 900°C varied from white to dark blue. The formation of these spinels and variation of their colours were analyzed in the trichromatic system.

FORMATION OF YAlO_3 WITH GARNET STRUCTURE

O. Yamaguchi, K. Matui and K. Shimizu

Amorphous material, which yields a YAlO_3 powder, has been prepared by the simultaneous hydrolysis of yttrium and aluminum alkoxides. A phase with a garnet structure is formed as an intermediate product. The formation process of YAlO_3 is described.